

Teneurins in Development and Disease

Inauguraldissertation

zur

Erlangung der Würde eines Doktors der Philosophie
vorgelegt der
Philosophisch-Naturwissenschaftlichen Fakultät
der Universität Basel

von

Daniela Kenzelmann Brož

aus Zeneggen (VS), Schweiz

Basel, 2008

Genehmigt von der Philosophisch-Naturwissenschaftlichen Fakultät
auf Antrag von:

Prof. Dr. Ruth Chiquet-Ehrismann

Prof. Dr. Markus Rüegg

Prof. Dr. Nancy Hynes

Basel, den 9.12.2008

Prof. Dr. Eberhard Parlow
Dekan

TABLE OF CONTENTS

1. SUMMARY	- 5 -
2. INTRODUCTION	- 6 -
2.1 Cell-cell and cell-extracellular matrix adhesion	- 6 -
2.1.1 Cell-cell adhesion	- 8 -
2.1.2 Cell-ECM adhesion	- 9 -
2.2 Limb development	- 10 -
2.3 Neuronal development and axon guidance	- 15 -
2.3.1 Early neuronal development	- 15 -
2.3.2 Development of the visual system and axon guidance	- 18 -
2.4 Regulated intramembrane proteolysis	- 22 -
2.5 X-linked mental retardation	- 25 -
2.5.1 Definition and classification	- 25 -
2.5.2 How many XLMR genes?	- 26 -
2.5.3 Biological functions of MR genes	- 28 -
2.6.4 Teneurin-1 is a promising XLMR candidate gene	- 31 -
2.6 Biology of brain tumors	- 32 -
2.6.1 Glioma	- 32 -
2.6.2 Medulloblastoma	- 36 -
2.7 Teneurin – an emerging family of transmembrane proteins	- 38 -
2.7.1 Invertebrate Teneurins	- 38 -
2.7.2 Vertebrate Teneurins	- 40 -
3. AIM OF MY WORK	- 46 -
4. MATERIALS AND METHODS	- 47 -
4.1 Production of antibodies against chicken teneurin-4	- 47 -
4.1.1 ICD antibody	- 47 -
4.1.2 ECD antibody	- 47 -
4.2 IHC of developing chick embryos	- 48 -
4.3 WB analysis of developing chick embryos	- 49 -
4.4 Sequencing of human teneurin-1	- 50 -
4.4.1 Patient samples	- 50 -
4.4.2 PCR and sequencing primers	- 51 -
4.4.3 Sequence analysis	- 51 -
4.5 Production of antibodies against human teneurin-4	- 53 -
4.5.1 ICD antibody	- 53 -
4.5.2 ECD antibody	- 53 -
4.7 IHC of brain tumors	- 54 -
4.8 Microarray analysis of brain tumors (performed in the Hemmings lab)	- 55 -

5. RESULTS	- 56 -
<i>Part I – Teneurins in Development</i>	- 56 -
5.1 Teneurin-1 is expressed in interconnected regions of the developing brain and is processed in vivo.	- 56 -
5.2 Expression of teneurin-4 in the developing chick embryo	- 71 -
5.2.1 Expression of teneurin-4 in the visual system	- 71 -
5.2.2 Expression of teneurin-4 in the CNS (outside of visual system)	- 73 -
5.2.3 Expression of teneurin-4 in non-neuronal tissues	- 74 -
5.2.4 Expression of teneurin-4 in the limb	- 75 -
5.2.5 WB analysis of teneurin-4 expression during chick development	- 76 -
<i>Part II – Teneurins in Disease</i>	- 78 -
5.3 Teneurin-1 as an X-linked mental retardation candidate gene	- 78 -
5.3.1 Analysis of the human teneurin-1 genomic locus	- 78 -
5.3.2 Summary of SNPs in the analyzed sequence	- 79 -
5.3.2 Summary of XLMR patient sequencing results	- 81 -
5.3.3 SNPs in the 5' upstream region	- 83 -
5.4 Teneurin-4 overexpression in brain tumors	- 85 -
5.4.1 Microarray data of brain tumors	- 85 -
5.4.2 WB analysis of brain tumors	- 88 -
5.4.3 IHC of brain tumors	- 91 -
5.4.4 Comparison between WB analysis and IHC	- 93 -
6. DISCUSSION	- 95 -
6.1 Teneurins in neuronal development and the teneurin signaling hypothesis	- 95 -
6.2 Teneurin-4 expression during chick CNS and limb development	- 100 -
6.3 Is teneurin-1 a candidate gene for XLMR?	- 101 -
6.4 Is teneurin-4 a marker for cancer?	- 104 -
6.5 Final conclusions	- 110 -
7. APPENDIX	- 111 -
7.1 Abbreviations	- 111 -
7.2 List of Figures and Tables	- 113 -
7.3 References	- 113 -
7.4 Acknowledgement	- 118 -
7.5 Curriculum Vitae	- 119 -

1. SUMMARY

The teneurins are a novel type II transmembrane protein family originally discovered in *Drosophila* and highly conserved between invertebrates and vertebrates. Studies in invertebrates suggest important functions for the teneurins in many processes during development. However, still very little is known about the biological function and mechanism of action of the vertebrate teneurin family, which consists of four paralogs called teneurin-1 to -4.

In the first part of my thesis, I analyzed the expression pattern and signaling mechanism of teneurin-1 during chick development. Teneurin-1 was prominently expressed in specific regions of the brain, and often complementary to teneurin-2. The presence of teneurin-1 and -2 in interconnected regions of the brain implies a role for teneurins in the establishment of appropriate neuronal connectivity. Using a novel antibody recognizing the teneurin-1 intracellular domain (ICD), N-terminal processing products were detected and nuclear staining was observed in specific neurons and tissues. This provides evidence for our working hypothesis, according to which teneurins can be processed by a mechanism called regulated intramembrane proteolysis, resulting in the release and nuclear translocation of the ICD. Similar results were obtained for teneurin-4 during chick development.

In the second part of my thesis, I investigated the implication of teneurins in two human diseases.

X-linked mental retardation: Teneurin-1 was analyzed as an X-linked mental retardation (XLMR) candidate gene in 23 XLMR patients. No mutation that is likely to cause the disease was found the coding region or splice sites of the teneurin-1 gene in these patients.

Brain tumors: Teneurin-4 was found to be upregulated in a microarray analysis of human brain tumors including astrocytomas, oligodendrogliomas and glioblastomas (GBMs). The overexpression of teneurin-4 was confirmed on protein level in brain tumor lysates. Immunohistochemistry (IHC) revealed strong staining around tumors cells in some brain tumors whereas in others teneurin-4 restricted to blood vessels.

2. INTRODUCTION

Teneurins are a family of transmembrane proteins which are thought to be involved in cell adhesion, which is important in many processes during development. Therefore, the main principles of cell adhesion will be introduced first. Subsequently, I will give an overview of limb and central nervous system (CNS) development, during both of which patterns are formed and teneurins are prominently expressed. Since our working hypothesis is that the teneurins are a substrate of regulated intramembrane proteolysis (RIP), I will dedicate one chapter to this signaling mechanism. In the second part of the introduction, I will give a background on the XLMR and on brain tumors, because I investigated the implication of human teneurins in these diseases. The introduction will be concluded by a comprehensive review of the teneurin literature.

2.1 Cell-cell and cell-extracellular matrix adhesion

In multicellular organisms, cells do not exist individually, but are organized in tissues and organs. To establish and maintain tissue architecture, cells need to adhere to each other as well as to the surrounding extracellular matrix (ECM). Before mature cell anchoring junctions (desmosome, hemidesmosome, focal adhesion, adherens junction) can be assembled, cells must first adhere to each other through cell adhesion molecules (CAMs), as summarized in Figure 1. This dynamic cell adhesion is particularly important during development, when cells need to migrate and adhere to the appropriate cells to form organs and tissues. Changes in cell adhesion are also characteristic for pathologic conditions such as cancer and inflammatory diseases. CAMs bind their ligands with much lower affinity than other cell surface receptors, but they are present in high concentrations. Therefore, cell adhesion depends on a large number of weak adhesions, which allows more dynamic regulation of cell adhesion. The most important families of CAMs are introduced below.

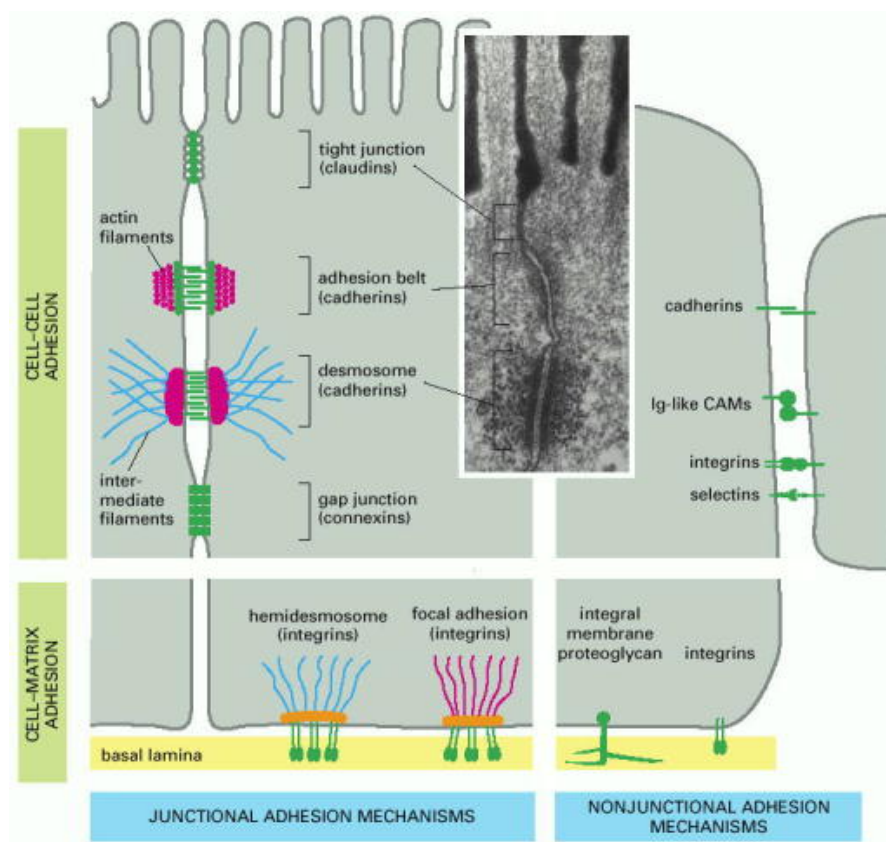


Figure 1: Overview Cell-Cell and Cell-ECM adhesion.

Stable forms of cell-cell adhesion include tight junctions, the adhesion belt, desmosomes and gap junctions, and hemidesmosomes and focal adhesions in the case of cell-ECM adhesion. The major CAM families involved in dynamic are the cadherins, the selectins and the Ig-like CAMs mediating cell-cell adhesion, whereas the integrins and transmembrane proteoglycans mediate cell-ECM adhesion¹.

2.1.1 Cell-cell adhesion

The cadherins are the major CAMs responsible for holding cells together through Ca^{2+} -dependent homophilic interaction. The most extensively studied cadherins include E-Cadherin expressed on epithelial cells and N-Cadherin present on nerve, muscle and lens cells, both have important functions during development. The classical and nonclassical cadherins, which include the desmosomal cadherins and the protocadherins form together the cadherin superfamily. All classical and some nonclassical cadherins have highly conserved ICDs which mediate interaction with the actin cytoskeleton through catenins, or with intermediate filaments in the case of desmosomal cadherins. The connection to the cytoskeleton is essential for the adhesive function of cadherins. Particularly in the central nervous system there are many different cadherins, each expressed in a distinct but overlapping pattern. Since they are concentrated on synapses, they are thought to be involved in synapse formation and stabilization. Some Protocadherins are also thought to contribute to the establishment of synaptic connectivity, because of their distinct expression patterns in the brain. Additional complexity is achieved by alternative splicing, which generates many isoforms varying in the extracellular domain (ECD).

Selectins are cell-surface carbohydrate binding proteins that mediate transient Ca^{2+} -dependent cell-cell adhesion in the bloodstream. They bind to mucins and thus mediate heterophilic interactions. L-selectin is present on white blood cells, P-selectin on blood platelets and on locally activated endothelial cells, and E-selectin on activated endothelial cells. They play important roles in recruitment of white blood cells to sites of inflammation.

Immunoglobulin-like CAMs (Ig-CAMs) are a large family of Ca^{2+} -independent cell adhesion molecules containing Ig-like domains. The best studied example is neuronal cell adhesion molecule N-CAM, which is expressed in many cell types including most neurons. At least 20 isoforms of N-CAM are generated by alternative splicing, some having a high content of negatively charged sialic acid, which serves to prevent rather than promoting cell adhesion. Some Ig-CAMs like N-CAM mediate cell adhesion by a homophilic mechanism, whereas others like intercellular adhesion molecules (ICAMs) on endothelial cell

mediate heterophilic interactions by binding to integrins on blood cells. Since Ig-CAM mediated adhesion is much weaker than cadherin-dependent adhesion, they are more involved in the fine tuning of adhesive interactions during development and regeneration.

2.1.2 Cell-ECM adhesion

The integrins are a family of transmembrane glycoproteins that form non-covalently linked heterodimers. There are genes for 18 α - and 8 β -subunits, which can combine to form 24 $\alpha\beta$ -integrin receptors. Integrins are the principal ECM receptor on cells, since they can bind most ECM proteins including collagens, fibronectin and laminins. On the intracellular side, integrins interact with anchor proteins connecting them to the actin cytoskeleton with the exception of $\alpha6\beta4$ integrin, which is found in hemidesmosomes and binds to intermediate filaments. Clustering of integrins mediates stronger adhesion through increased integrin concentration and higher ligand binding affinity. In addition to promoting adhesion integrins activate signaling pathways leading to proliferation, survival and migration. Moreover, there is crosstalk between integrins and growth factor receptors. Conversely, signals from inside the cell can modulate the ligand binding affinity of integrins and thus the ability of cells to adhere to the ECM.

The major transmembrane proteoglycan family that mediates cell adhesion is the syndecan family (Syndecan-1 to -4), which are composed of a protein core with covalently attached heparin sulphate and chondroitin sulphate glycosaminoglycan sugar chains. Like integrins, syndecans can bind to many ECM proteins, which often have binding sites for both integrins and syndecans. Moreover, with their large flexible glycosaminoglycan chains, they are ideal receptors for growth factors that are dilute or distant from the cell membrane. For full spreading of cells on the ECM, both integrins and syndecans need to be engaged.

2.2 Limb development

The formation of complex three-dimensional structures during development is achieved through a process called pattern formation. The limb buds are an excellent model to study this process, as they are not required for survival and can be molecularly and experimentally manipulated. Moreover, many key genes that control limb formation are also important in other developmental contexts when patterns are formed. To form a limb bud, cell proliferation, death and movement have to be coordinated with the assignment and interpretation of positional information. Cells have to be determined and signaling centers have to be established to provide positional information. This information has to be recorded by the cells, and the cells have to differentiate in response to additional cues. To form early limb buds, cells start to proliferate in specific regions of the flank. They consist of homogenous mesenchyme cells that are enveloped by a layer of ectoderm. The mesenchymal cells will subsequently differentiate into skeletogenic mesenchyme, cartilage and tendons. Cells from the lateral edges of nearby somites migrate into the limb and will later generate the limb musculature. The apical ectodermal ridge (AER) at the distal tip is an important signaling center inducing proliferation of the underlying mesenchymal cells during limb outgrowth. To initiate AER formation, the mesenchyme signals to the ectoderm. Wnt signaling activates FGF10 in the mesenchyme, which induces AER precursors in both dorsal and ventral ectoderm to express Fgf8. Subsequently, the AER precursor cells migrate to the dorsal-ventral boundary at the distal tip of the limb bud where they undergo compaction. A second important signaling center is the zone of polarizing activity (ZPA) located in the dorsal mesenchyme of the limb bud, which is responsible for anterior/posterior specification. To generate a limb bud, positional information needs to be specified on three axes:

1. *Proximal-distal.* Several fibroblast growth factors (FGFs) are specifically expressed in the AER and maintain the underlying mesenchymal cells in an undifferentiated, proliferative state (Figure 2). As the limb bud is growing, mesenchymal cells start to condense and differentiate first into

cartilage and later into bone. The limb is divided in three parts, the proximal stylopod, the intermediate zeugopod and the distal autopod (Figure 2). Originally, the progress zone model was postulated, in which the time the mesenchymal cells spend in the progress zone under influence of the AER determines their proximal-distal specification. Thus, cells that leave the progress zone early become the stylopod, and those who leave later become the zeugopod and autopod. This model explains the fact that removal of the AER at earlier timepoints during development results in more severe truncation of the limb, which can be rescued by FGFs^{2,3}. Alternatively, the early specification model predicts that all the proximal-distal segments (stylopod, zeugopod and autopod) are specified early in limb development and these progenitor pools are subsequently expanded as the limb bud grows out. After AER removal, the 200µm distal-most cells undergo apoptosis; this affects a proportionally bigger portion of the early limb bud, this also explains a more severe truncation if the AER is removed early. A comparison of both models is depicted in Figure 3. In the past few years mouse genetics experiments have produced results that cannot be explained by either model; therefore neither of these models is entirely true.

2. *Anterior-Posterior*. The ZPA in the posterior limb mesenchyme secretes the morphogen sonic hedgehog (SHH) which determines anterior-posterior patterning (Figure 2). Cells receiving high doses of SHH adopt posterior fates, whereas cells further away from the ZPA adopt anterior fates. In the chick, transplantation of ZPA cells to the anterior limb mesenchyme or expression of SHH results in additional digits in a mirror-like duplication of the normal digits⁴. Genetic removal of SHH in mice leads to a dramatic loss of skeletal elements along the anterior-posterior axis^{5,6}.

3. *Dorsal-Ventral*. The information for dorsal-ventral limb patterning is already contained in the mesenchyme before specification of the limb bud and is transferred to the ectoderm as the limb bud forms. However, the molecular nature of this interaction is not known. When the ectoderm is rotated 180° relative to the mesenchyme, the mesenchymal structures become inverted and correspond to the polarity of the ectoderm⁷. Wnt7a secreted by the dorsal ectoderm induces Lmx1b, a transcription factor required for dorsal specification

of cells, in the dorsal mesenchyme. In the ventral ectoderm, the transcription factor Engrailed1 (En1) is induced by bone morphogenic protein (BMP) signaling and represses Wnt7a, which remains confined to the dorsal ectoderm (Figure 2). In the absence of Wnt7a dorsal patterns are not established and the limbs appear bi-ventral. Conversely if En1 is missing Wnt7a is misexpressed in the ventral ectoderm and the limb develops with bi-dorsal character⁸.

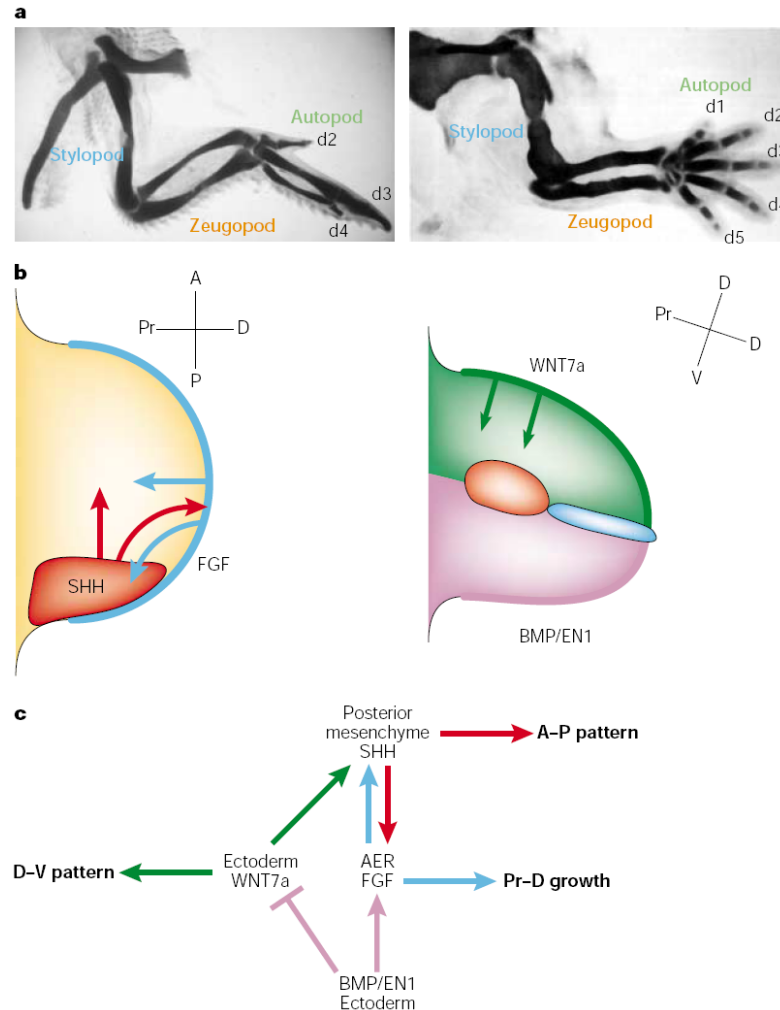


Figure 2: Signaling pathways in vertebrate limb development.

Chick (left) and mouse (right) skeletons showing the proximal-distal and anterior-posterior parts of the limbs. (B) Molecular interactions that coordinate the proximal-distal axis under the control of FGFs and the anterior-posterior axis regulated by Shh. The dorsal-ventral axis is defined by BMPs and En1 in the ventral ectoderm and Wnt7a in the dorsal ectoderm. (C) Schematic view of the interactions between the molecules regulating the three axes in the limb bud⁹.

Three-dimensional growth and patterning of the limb requires coordinated interactions between the molecules that specify each axis. The AER is required for SHH expression in the ZPA, which is rapidly downregulated after AER removal^{10,11} and is absent in FGF4/FGF8 knockout mice¹². Conversely, Shh maintains Fgf4 expression in the AER by inducing Formin, which maintains expression of gremlin, a BMP antagonist. Inhibition of BMP signaling by gremlin allows expression of FGF4 in the AER^{13,14}. Similarly, removal of the dorsal ectoderm or loss of Wnt7a reduces Shh expression^{15,16}.

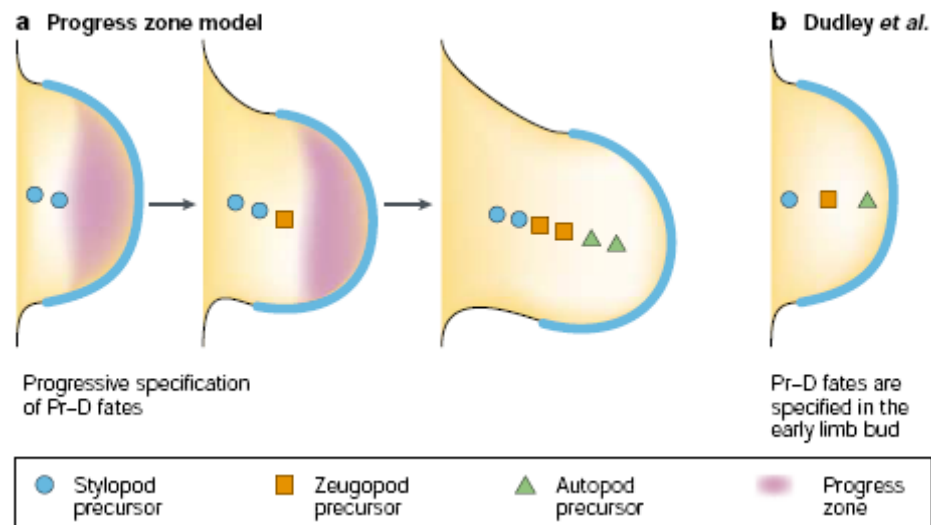


Figure 3: Comparison of the progress zone and early specification model.

A) The progress zone model predicts that specification depends on the AER which proceeds from proximal to distal. B) The early specification model by Dudley et al. suggests that all fates are specified in the early limb bud, and progenitor pools are expanded during limb outgrowth⁹.

Once the positional cues are provided by the established signaling centers, key regulatory genes must be activated in the cells to execute the patterning program, in particular genes of the Hox cluster. It has been shown that HoxD genes (Hoxd9 to Hoxd13) which are expressed at the posterior limb bud can be induced by combined influence of SHH and FGFs. This led to the suggestion that this may occur *in-vivo*¹⁷. However, the expression of the HoxD as well as HoxA genes is very dynamic during limb bud development and does not correlate with the anterior-posterior or proximal-distal axes. Analysis of Hox gene gain and loss of function suggests that the primary role of Hox genes is to regulate the rate and timing of cartilage proliferation and differentiation. Additionally, Hox genes function also at earlier stages of limb development as well, such as during the proliferation of undifferentiated mesenchyme, the condensation of mesenchyme into blastemal primordia, and the organization of the cartilage cells within the skeletal elements^{18,19,20}. It is still unknown which genes regulated by Hox genes exert these cellular effects.

2.3 Neuronal development and axon guidance

2.3.1 Early neuronal development

Neuronal development begins with the specification of cells in the dorsal ectoderm to become the neural plate. During neurulation these cells form the neural tube which develops into the CNS. The anterior part will become the brain and the posterior part the spinal cord. Neural crest cells then appear and start to migrate out of the dorsal neural tube. Later they will differentiate into the cells of the peripheral nervous system (PNS), among others. Therefore, the entire nervous system is derived from the ectoderm as shown in Figure 4. The three primary brain vesicles at the anterior end are further subdivided into five secondary brain vesicles (Telencephalon, Diencephalon, Mesencephalon, Metencephalon and Myelencephalon). The adult brain structures derived from each part are listed in Figure 4. This anterior-posterior patterning is directed by a set of genes, that includes the hox genes. The dorsal-ventral polarity of the neural tube is induced by signals coming from its environment. SHH secreted by the notochord induces ventral cell types and BMPs secreted by the dorsal ectoderm induces dorsal structures. Depending on the concentration and exposure time to these paracrine factors, different transcription factors are induced in the neural tube, which specify cellular identity. The original neuronal tube is composed of a germinal neuroepithelium, which is a layer of rapidly dividing neuronal cells. Their nuclei move between the luminal and external surface of the neural tube as they go through the cell cycle, with mitosis occurring at the luminal surface. Cells exit the cell cycle at a specific time point and begin to migrate and differentiate; this timepoint is called the birth of a neuron. Neurons that are born earlier migrate the shortest distance, whereas neurons that are born later have to migrate through the first layers to more superficial layers. Finally, as proliferation and differentiation proceed several layers of neurons are generated, forming the ventricular, intermediate and marginal zones. Later in development, this basic organization is maintained with specific modifications in the spinal cord or medulla, cerebellum and cerebral cortex, depicted schematically in Figure 4.

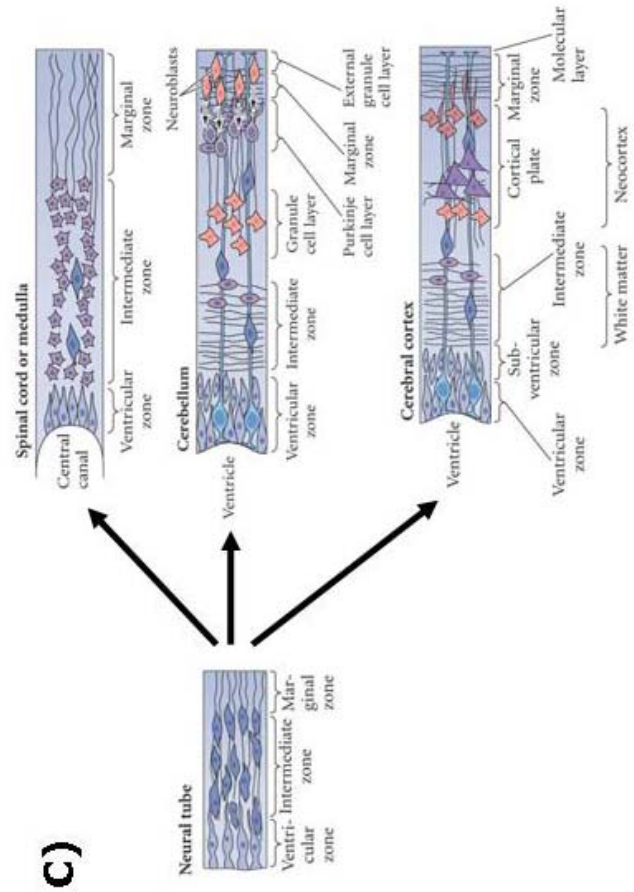
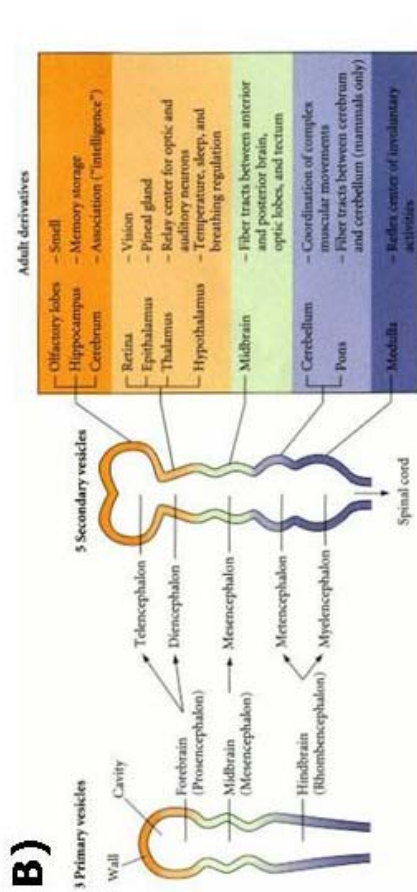
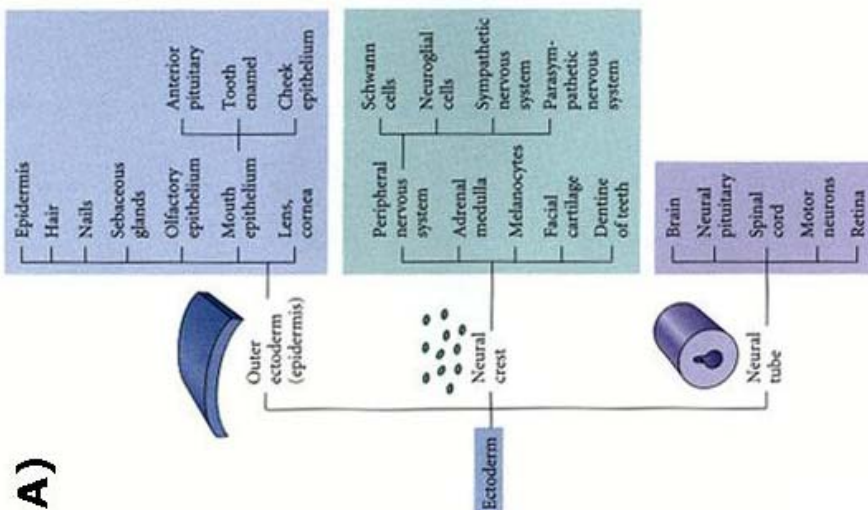


Figure 4: Early development of the CNS.

(A) *Ectodermal Derivatives.* The ectoderm is divided into three major domains, the surface ectoderm (primarily epidermis), the neural crest (peripheral neurons, pigment cells and facial cartilage) and the neural tube (brain and spinal cord). The cell types that are derived from each domain are listed. (B) *Early human brain development.* The three primary brain vesicles are subdivided as development continues. The list on the right side indicates from which regions structures in the adult brain originate. (C) *Differentiation of the walls of the neuronal tube.* In the differentiating neural tube, three zones can be distinguished: the ventricular, the intermediate and the marginal zone. The spinal cord and medulla contains one source of neurons and glial cells, the ventricular zone. In the cerebellum, a second germinal zone forms within the marginal zone, from which neuroblasts migrate inwards to generate the internal granule cell layer. In the cerebral cortex, migrating neuroblasts and glioblasts form a cortical plate containing six layers²¹.

2.3.2 Development of the visual system and axon guidance

The optic vesicle extends from the diencephalon and induces the lens placode, which invaginates to form the lens. The optic vesicle also invaginates and becomes the two-layered optic cup. The outer layer starts to produce melanin pigment and becomes the pigmented retina, and the inner layer containing the retinal precursor cells generates the neural retina. One retinal precursor cell can give rise to the six neuronal and one glial cell types, which are generated in an orderly manner²². First, the retinal progenitor cells expand through proliferation, then exit the cell cycle, commit to a particular cell fate and differentiate. Finally, the neural retina is organized in three nuclear layers, retinal ganglion cells (RGCs) reside in the ganglion cell layer (GCL), horizontal, amacrine, bipolar and Müller glial cells in the inner nuclear layer (INL) and rod and cone photoreceptors in the outer nuclear layer (ONL). Between these nuclear layers, there are the inner and outer plexiform layers (IPL and OPL), which contain axons and dendrites of the neuronal cells in the retina. The axons of the RGCs exit the retina together through the optic nerve and project primarily to the optic tectum (OT) in chicken, or to the superior colliculus (SC) and dorsal lateral geniculate nucleus (dLGN) in mammals.

The ability of developing axons to navigate to the appropriate target is mediated by a specialized structure on their distal tip, the growth cone. Neuronal growth cones are highly motile, sensory structures that constantly extend and retract two types of processes: thin, finger-like filopodia and flat, veil-like lamellipodia. By responding to cues in the extracellular environment, growth cones control the rate and direction of axon extension. The guidance cues can be either attractive and promote growth towards a specific region, or repulsive and prevent growth in a particular direction. Both type of cues can be associated with cell surfaces or the extracellular matrix, or be diffusible and act at a distance from their source. Growth cones respond to extrinsic guidance cues through receptors on their surface, which activate downstream signaling pathways that induce changes in cytoskeletal organization. Several ligands and corresponding receptors have been identified as key axon guidance cues. They include Ephrins/Ephs, netrin/Dcc, Slits/Robos and Semaphorins/Neuropilins/Plexins²³. In addition, secreted factors known as

morphogens have additional roles in axon guidance, such as SHH, FGFs, BMPs and Wnts²⁴. In addition, the cell adhesion molecules N-CAM, Nr-CAM, L1 and cadherins are involved in guiding axons. Finally, ECM proteins such as laminin, heparin sulphate proteoglycans (HSPGs), chondroitin sulphate proteoglycans (CSPGs) and metalloproteases are either directly involved in axon guidance, or modulate the activity of axon guidance molecules. As described in more detail in the next section, a small set of molecules is used at several points along the pathway to serve different functions.

Shortly after its final cell division, an axon arises from the basal surface of each RGC and extends directly into the optic fiber layer (OFL), where it grows towards the optic disc/nerve head. The initiation of axon extension is regulated by integrins and cadherins^{25,26}. As they extend to the optic disc, RGC axons are restricted to the OFL at the inner surface of the retina. This is regulated by growth promoting molecules such as NCAM present in the OFL²⁷ as well as inhibitory guidance cues localized in the outer retinal layers, like Slits/Robos²⁸. CSPGs present in the peripheral neuroepithelium inhibit RGC axon extension²⁹. Several cell adhesion molecules, including L1, Neurolin/DM-GRASP/BEN and NrCAM direct growth of RGC axons towards the optic disc^{30,31,32,33}. Additionally, SHH mediates disc-directed growth³⁴. The ligand Netrin-1 is expressed by glial cells surrounding the optic disc and its receptor deleted in colorectal cancer (DCC) on RGCs; both are required for RGC axons to exit the retina³⁵. Other factors contribute to targeting the RGC axons to the optic disc and mediate subsequent exit, such as EphBs (reverse signaling), BMP receptor 1B and NrCAM^{36,37,38,33}.

After leaving the eye, RGC axons grow within the developing optic stalk, to which they are restricted by inhibitory Semaphorin5A signaling³⁹. In the ventral diencephalon, the optic nerves from both eyes meet to form the optic chiasm, the position of which is specified by downregulation of SHH signaling⁴⁰. After arriving at the optic chiasm, RGC axons face the decision to cross to the contralateral side or to remain on the ipsilateral side. The proportion of axons that remain on the ipsilateral side is species-dependent and correlates with the extent of binocular vision. The axons that are not destined to cross the midline at the optic chiasm are prevented to do so by repulsion. The transcription factor

ZIC2 is exclusively expressed in uncrossed RGCs and correlates with EphB1 levels, which mediates repulsion by EphrinB2 present in the midline⁴¹. Isl2, another transcription factor, is expressed in a distinct subset of contralaterally projecting RGCs and appears to be a negative regulator of ZIC2 and EphB1⁴². The cell adhesion molecule NrCAM is expressed by RGCs that project contralaterally and at the midline and promotes axon outgrowth. Similarly, the secreted guidance molecule Semaphorin3D is expressed in the chiasm and guides RGC axons to the contralateral optic tract⁴³. Clearly, crossing the midline is not a default mechanism, but an active process.

Expression of growth associated protein 43 (GAP-43) is required for the RGCs to overcome inhibitory signals and grow from the optic chiasm into the optic tracts. Several molecules are involved in keeping the axons within the optic tract, including Slits/Robos, CSPGs, N-Cadherin, tenascin-R, secreted frizzled related protein 1 (SFRP1) and β 1-integrin. FGF signaling is required for entry into the optic tectum⁴⁴. As the axons reach the end of the laminin-lined optic tract, they spread out and find their specific targets in the optic tectum or superior colliculus, and a topographic map of the retina is established. Axons that arise from RGCs in the nasal retina project to targets at the posterior end of the OT/SC and dLGN, whereas axons from the temporal region of the retina project to the anterior end, and the same is true for the dorsal-ventral axis. The generation of this topographic map is mainly achieved by graded expression of ligands and receptors of the Ephrin/Eph family in the retina and in the OT/SC and dLGN, which act as chemical labels to mediate synaptic connectivity as proposed by Sperry⁴⁵. Ephrins are membrane-bound ligands for the Eph receptor tyrosine kinases; therefore this signaling interaction requires cell-cell contact and reverse signaling can occur in the cell expressing the Ephrin ligands⁴⁶. EphA/EphrinA signaling is required for proper mapping along the anterior-posterior axis, whereas EphB/ephrinB signaling patterns the medial-lateral axis of the tectum/SC. Additionally, Ephs/Ephrins appear to be involved in the formation of eye-specific layers: neuronal activity segregates the axons from the two eyes, and EphAs/ephrinAs regulate the shape, position and size of the eye-specific territories⁴⁷.

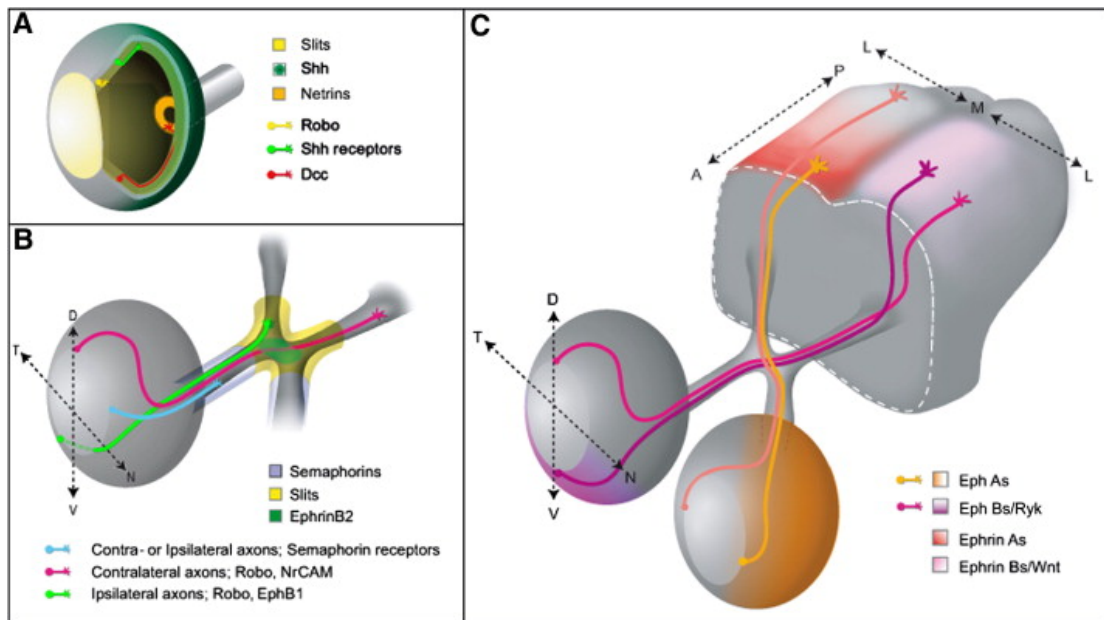


Figure 5: Key guidance cues acting in the mouse optic pathway.

(A) Guidance within the retina towards the optic disc involves Slit/Robo, Shh and cell adhesion molecules, whereas Netrin/DCC is needed to exit the retina through the optic disc. (B) Guidance at the chiasm. Semaphorins and Slit/Robo confine the axons to the optic nerve. At the midline of the optic chiasm, EphrinB2 repels EphB1 expressing RGC axons from the ventral-temporal region of the retina, which project ipsilaterally. Nr-CAM present at the midline facilitates crossing of contralateral RGC axons. (C) Topographic mapping in the SC is achieved by gradients of Eph/Ephrin expression, which is counteracted by Wnt and Ryk signaling⁴⁸.

D, dorsal, L, lateral, M, medial, N, nasal, T, temporal, V, ventral.

2.4 Regulated Intramembrane Proteolysis

Proteases are classified into four general types based on their catalytic residues and mechanism of action, which are conserved from archaea to humans: Serine/Threonine proteases, Cysteine proteases, Aspartyl proteases and Metalloproteases. Until about ten years ago, all proteases were functioning in an aqueous environment, which is required for the hydrolysis of peptide bonds to occur. The discovery of intramembrane proteases was puzzling, since they act in a hydrophobic environment and their substrates are transmembrane domains of proteins, which are typically folded into an α -helix. Therefore, intramembrane proteases must create a microenvironment for water and the hydrophilic residues needed for catalysis, and bend or unwind their substrate to access the peptide bonds for hydrolysis. It is an area of intense investigation how these proteases achieve this, especially since the essential catalytic residues are the same as those found in conventional proteases.

Four protease families are known to date to catalyze intramembrane proteolysis, the Presenilins, the Site-2 Protease (S2P) family, the Rhomboids and the Signal-Peptide Peptidase (SPP) family (Figure 6). All of them are multispan transmembrane proteins with the catalytic residues located on different transmembrane domains, which together form the active site. Both Presenilins and SPPs are aspartic proteases, but their catalytic sites are oriented in opposite directions in the membrane and cleave accordingly oriented substrates. Presenilins cleave type-I transmembrane proteins, whereas SPP cleaves type-II transmembrane proteins. Presenilin is unique since it is processed into a C-terminal and N-terminal part that remain physically associated and contribute each one essential aspartate. In addition, Presenilin does not act alone but forms the γ -secretase complex together with nicastrin, PEN2 and APOE2, whereas the other transmembrane proteases function alone. S2P is a metalloprotease which uses two conserved histidine and one aspartate to coordinate a zinc ion and cleaves type-II transmembrane proteins. Rhomboid is a serine protease containing the catalytic triad aspartate, histidine and serine, which are connected by hydrogen bonds. It cleaves type-I transmembrane

proteins and is the only intramembrane protease that releases extracellular factors instead of ICDs⁴⁹.

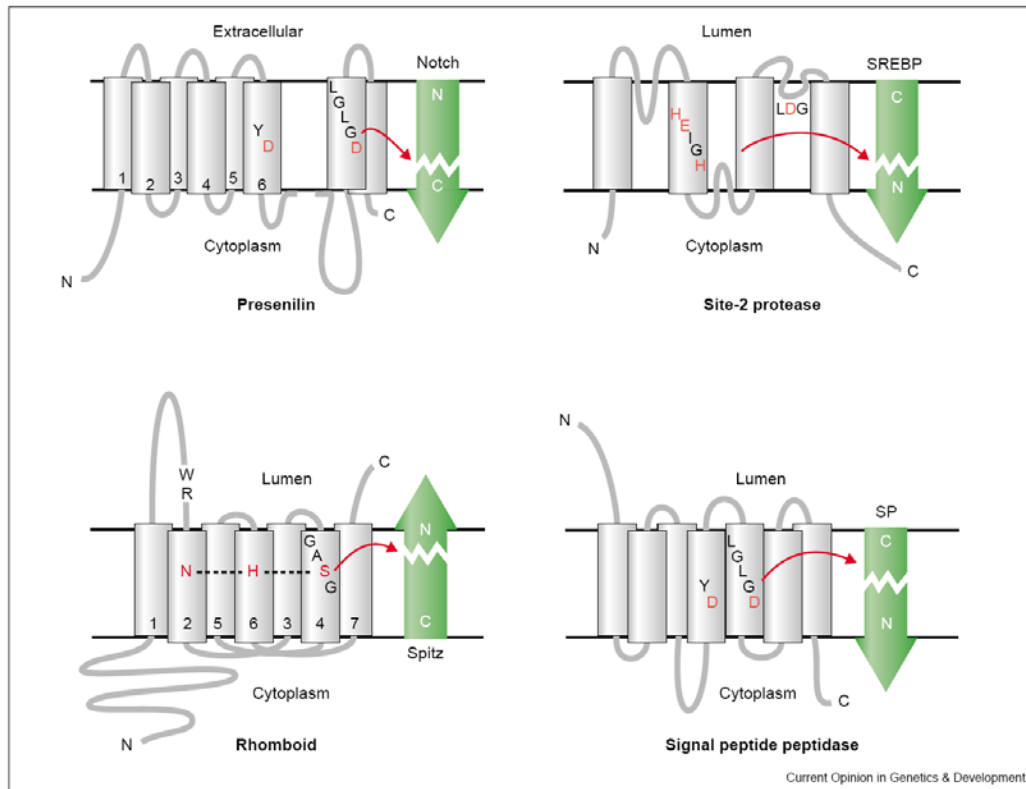


Figure 6: The four intramembrane protease families.

Presenilin and Rhomboid cleave type-I transmembrane proteins, whereas S2P and signal peptide peptidase cleave type-II transmembrane proteins. Presenilin and SPP are both aspartic proteases, however their catalytic domain is oriented in the opposite direction and accordingly they cleave type-I and type-II transmembrane proteins, respectively. S2P is a metalloprotease using a zinc ion coordinated between two conserved histidines and an aspartate. Rhomboid is a serine protease containing a typical catalytic triad, and is mainly involved in the release of extracellular factors in contrast to the other transmembrane proteases which release intracellular signaling domains⁴⁹.

Red = catalytic residues, black = conserved motifs, green arrow = direction of substrate domain release.

To date, most of the substrates known to be processed by intramembrane proteolysis are type-I transmembrane proteins cleaved by γ -secretase, including APP, Notch and the Notch ligands Delta and Jagged, ErbB4, CD44, E-Cadherin, N-Cadherin, Ephrins, DCC and p75^{NTR}⁵⁰. Only ATF6 and SREBP are type-II transmembrane proteins cleaved by S2P in the Golgi apparatus. SPP also acts in the Golgi, where it clears remnant signal peptides from the membrane after their cleavage by signal peptidase. Therefore, type-II cell surface proteins have not been associated with intramembrane proteolysis, although it has been speculated that some may also transmit signals through RIP, e.g. the reverse-signaling of transmembrane forms of tumor necrosis factor (TNF) ligands⁵¹. The recently described SPP-like (SPPL) proteases are strong candidates for the cleavage of type-II plasma membrane receptors, particularly since members of the SPPL-family have been shown to be sorted to different subcellular compartments, including the plasma membrane⁵². Indeed, human SPPL2a and SPPL2b have been shown to promote intramembrane proteolysis of TNF α in activated dendritic cells, which leads to induction of IL-12 expression. Additionally, a novel splice variant of mouse SPP lacking the ER-retention signal was described, which localizes to the cell surface⁵³.

2.5 X-linked mental retardation

2.5.1 Definition and classification

Mental retardation (MR) is a complex phenotype, defined by significant limitations both in intellectual functioning and in adaptive behavior as expressed in conceptual, social and practical adaptive skills, which originate before 18 years of age and are not degenerative⁵⁴. Recent estimates suggest that of the population in developed countries, 0.3% - 0.5% are affected by moderate and severe MR (IQ < 50), and 1-3% for mild MR (IQ 50-70)⁵⁵. MR can be caused by both environmental and genetic factors, the former include maternal intoxication, prematurity, fetal infection, peri- and postnatal traumata, vascular accidents, asphyxia, and postnatal infections. Genetic causes comprise chromosomal abnormalities such as aneuploidies and microdeletions affecting multiple genes or mutations in a single gene. Whereas mild MR is thought to represent the lower end of normal IQ distribution resulting from the interactions of many genes and non-genetic influences, severe MR is more likely to be caused by specific genetic factors. XLMR is the most frequent cause of monogenic MR. It is inherited recessively and therefore affects mostly males, who are hemizygous for the mutation and inevitably affected by the disease. Females are usually non-manifesting carriers, but sometimes exhibit milder symptoms, possibly due to skewed X-inactivation. The concentration of genes causing MR is suggested to be twice as high on the X-chromosome compared to autosomes, but this might be biased by the fact that the localization of MR conditions to the X-Chromosome is easier due to the hemizyosity of affected males⁵⁶. Traditionally, syndromic or specific XLMR was distinguished from non-syndromic or non-specific XLMR based on the presence of additional abnormalities other than MR. This had mostly practical reasons, as in the former case, families affected by the same syndrome can be recognized without the knowledge of the causative gene, which is not possible for nonspecific MR families. There is however no molecular basis for this distinction, as several genes were found to cause both syndromic and non-syndromic forms of XLMR (e.g. *XNP*, *RSK2*, *MECP2*, *SLC6A8*, *FLNA*, *ARX*, *PQBP1* and *JARIDIC*).

Furthermore, with the improvement of diagnostic technologies, such as molecular studies or brain imaging, it is likely that many non-syndromic will turn out to be syndromic⁵⁷.

2.5.2 How many XLMR genes?

When the genetic defects of XLMR families were mapped by linkage analysis or using cytogenetic markers, it became evident that XLMR is a genetically very heterogenous disease, as the candidate intervals were non-overlapping and distributed along the entire X-Chromosome⁵⁸. Fragile-X syndrome accounts for 25% of the XLMR cases and results from a CGG trinucleotide expansion in the 5'UTR of the Fragile X mental retardation-1 (*FMR1*) gene causing aberrant methylation of the promoter and loss of *FMR1* expression. The FMR1 protein associates with polyribosomes and binds to and regulates translation of specific mRNA's involved in dendrite development and synapse function. Further, the *ARX* gene commonly mutated (10% of XLMR cases), causing several distinct XLMR syndromes as well non-syndromic XLMR, depending on the type of mutation. Other relatively common XLMR genes are *JARID1C*, *SLC6A8* and *MECP2*, but the remainder of the XLMR genes is only rarely mutated, that is in the family where they were identified. The progress in identifying XLMR genes has been rapid in the past years, only 33 were known in 2000, 45 in 2004, and to date they are 82. Figure 7 summarizes the 82 genes causing XLMR have been identified until 2008, indicating their position on the X-chromosome. For 133 XLMR families, the genetic cause is still unknown⁵⁹.

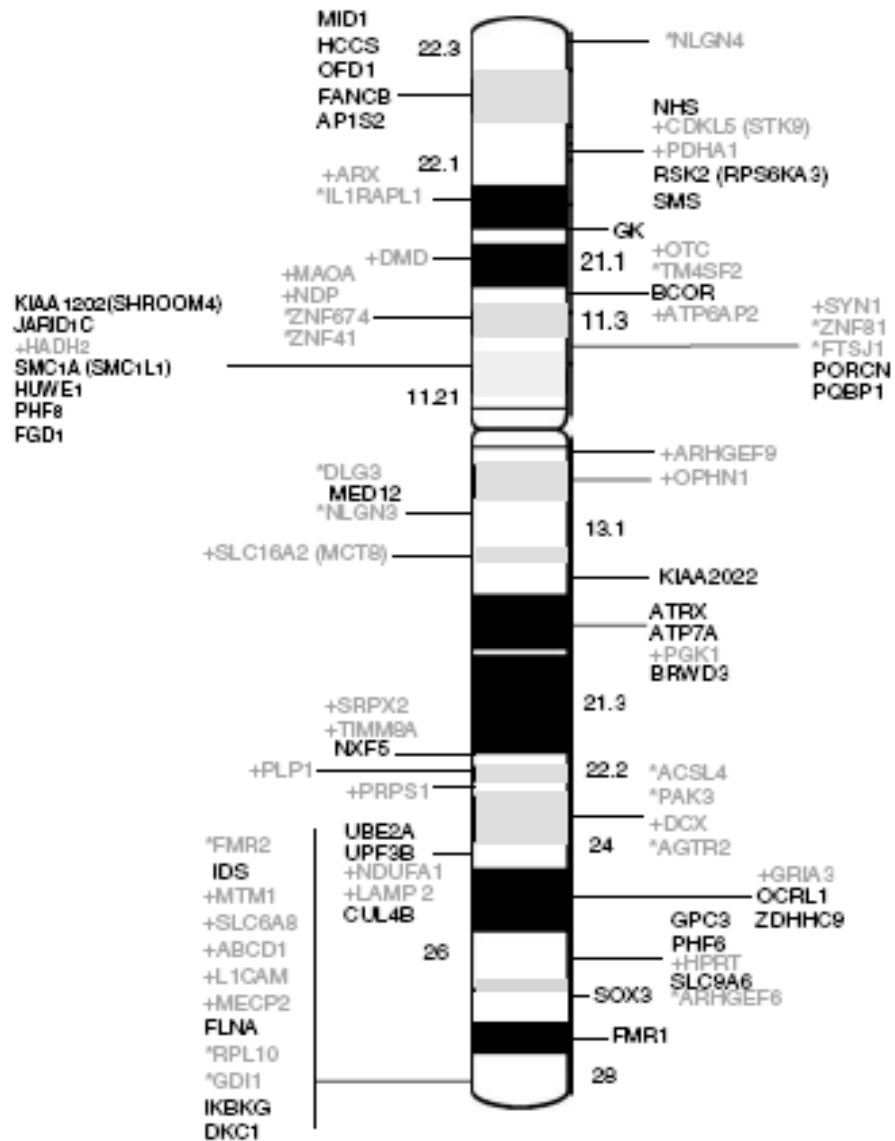


Figure 7: Known XLMR genes to date (XLMR update 2007).

Schematic representation of the X-Chromosome indicating the positions of the 82 known XLMR genes. Genes in black cause syndromes, genes in gray preceded by a + cause neuromuscular syndromes, while genes in gray preceded by a * cause nonspecific XLMR conditions⁵⁹. Two genes that were identified in the meantime are not represented on the scheme: IAP/MAGT1 at Xq21.1⁶⁰ and PCDH19 at Xq22.2⁶¹. Source: GGC XLMR Update⁶².

The interesting question is how many XLMR genes are still to be discovered. There are more than 900 protein-coding genes listed in the ENSEMBL database on the X-chromosome, of which about 40% are expressed in the brain⁶³, suggesting that the actual number of XLMR genes could possibly be over 200. Several strategies are used to identify new XLMR genes; the most comprehensive approach is high-throughput genomic DNA resequencing of all genes on the X-chromosome. Such studies are performed at the Sanger institute with a cohort of 250 XLMR families⁶⁴, or by the Euro-MRX consortium in a mutational screening of genes within a 7.4 Mb region in Xp11⁶⁵. Both projects resulted in the discovery of several new XLMR genes; however it is unlikely that all XLMR genes will be found because certain types of mutations (e.g. duplications) and mutations outside the coding regions are not detected by these methods. A different approach is focused on candidate genes, for example genes that are highly expressed in the brain, paralogues of known XLMR genes, and genes that interact with known XLMR genes. In some cases, chromosomal abnormalities such as reciprocal translocations, subtelomeric translocations, and cryptic deletions or duplications are extremely useful to localize candidate genes. Recently, comparative genome hybridization technology (array-CGH) has been established to analyze XLMR patients. With a resolution of > 100 kb, this technique allows identification of cryptic deletions which were previously missed by standard karyotyping and subtelomeric fluorescence in-situ hybridization (FISH)⁶⁶. Additionally, the development of a cDNA array with ~1700 expressed sequence tags (ESTs) corresponding to most of the protein-coding regions of the X-chromosome will permit the analysis of gene expression levels to find mutations affecting the regulatory region of the candidate gene⁶⁷. Finally, microRNAs (miRNAs) and noncoding RNAs (ncRNAs) transcribed from the X-chromosome could also be mutated and contribute to XLMR or other X-linked inherited disorders.

2.5.3 Biological functions of MR genes

It is important to keep in mind that MR is in many cases part of a complex syndrome comprising developmental brain abnormalities such as microcephaly, lissencephaly, neuronal heterotopia, agenesis, polymicrogyria

and schizencephaly. In these cases, the cerebral cortex lacks its normal pattern of organization because the responsible gene is required for normal brain development, and MR is a secondary symptom. In other MR conditions however, the brain structure and architecture appears normal and subtle defects in neuronal or glial cell function, morphology or interactions are responsible for the disease. It is suggested that in these cases, defects in synaptogenesis and synaptic function as well as plasticity are responsible for cognitive impairment.

Figure 8 gives an overview of the broad range of molecular functions in which MR genes (including those on autosomal chromosomes) are implicated. This suggests that disruption of many biological processes can impair brain function. Surprisingly, many of the MR genes are not specifically expressed in the brain. This can be explained by the fact that the brain is more sensitive to damage because of its higher energy requirement and its susceptibility to toxic metabolites, therefore fundamental cellular defects that affects many tissues may result in MR. In contrast, other XLMR genes are expressed or function mainly in the brain, resulting in impairment of unique features of brain development or physiology⁶⁸. Many XLMR genes affect gene expression, including genes involved in chromatin remodeling (e.g. *MECP2*), transcription factors (e.g. *ARX*, *SOX3*, *ZNF* genes) and RNA processing (*FTSJ1*) and regulation of translation (*FMR1*, *RPL10*). Some MR genes are implicated in crucial cellular processes such as DNA repair (e.g. *FANCB*), cell cycle regulation (e.g. *JARID1C*, *DKC1*), cell division (e.g. *OFD1*, *SMC1A*) and degradation of macromolecules through the lysosomal (e.g. *ATP6AP2*) or ubiquitin (e.g. *UBE3A*, *MID1*, *CUL4B*) pathway. A striking number of XLMR genes belong to metabolic pathways, such as glycolysis (e.g. *PDHA1*), urea cycle (e.g. *OTC*), lipid synthesis (e.g. *HDH2*, *ACSL4*, *FACL4*). Cytoskeletal components (e.g. *DMD*, *DCX*), actin binding (e.g. *FLNA*, *SHROOM4*) and RhoGTPase signaling genes (e.g. *FGD1*, *ARHGEF9*, *OPHN1*, *AGTR*, *GDI1*) are also affected by XLMR mutations. Several XLMR genes are implicated transmembrane transport (e.g. *AP1S2*, *ATP6AP2*, *SYN1*, *SLC16A2*, *ATP7A*, *TIMM8A*, *SLC9A6*, *SLC6A8*, *ABCD1*) and in signal transduction (e.g. *RSK2*, *ILRAPL1*, *PORCN*, *DLG3*, *PAK3*, *MTM1*), and some XLMR genes function in cell adhesion (e.g. *NLGN2*, *NLGN4*, *L1CAM*, *PCDH19*). A complete list of the 82 XLMR genes and their subcellular localization and function can be found in XLMR update 2007⁵⁹. An emerging hypothesis proposes that defects in synaptogenesis, synaptic activities and plasticity are the

underlying causes for MR, especially when gross brain abnormalities are absent⁶⁹. Indeed, the protein products of 20 of the 82 XLMR genes (that include also nuclear proteins like transcription factors) localize to synapses⁵⁹. Neuronal and synaptic remodeling occur throughout life, and abnormalities of dendritic spine morphology and density have been observed post mortem in MR patients⁶⁹.

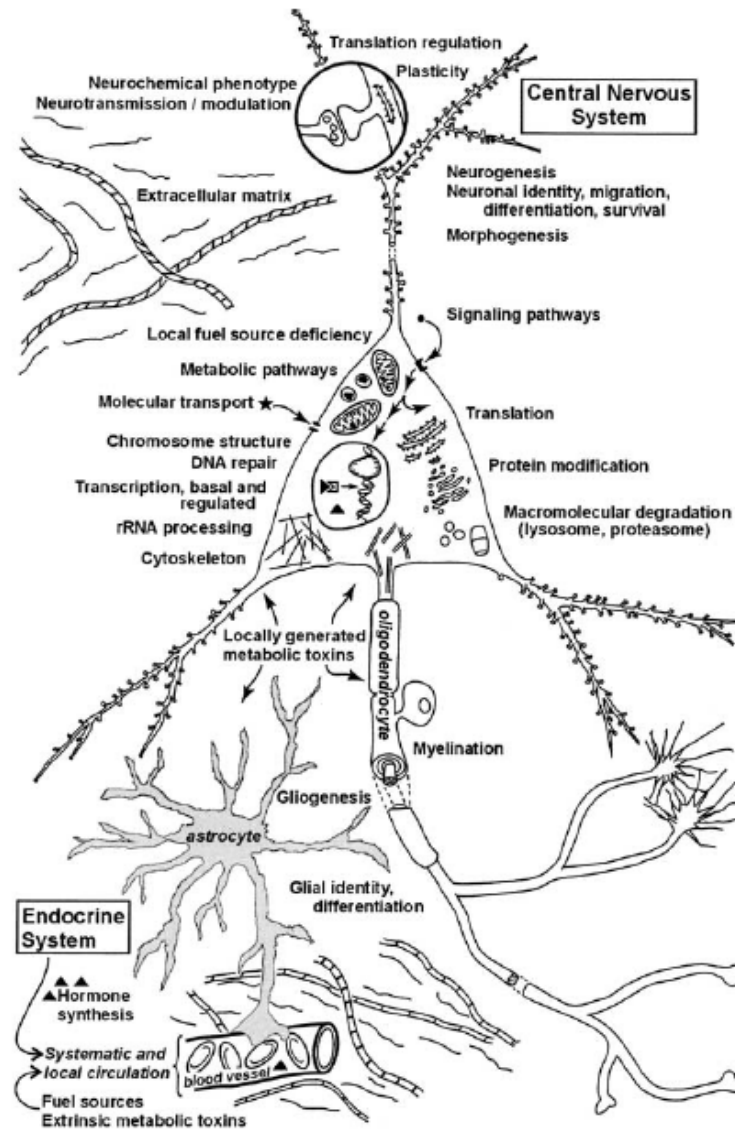


Figure 8: Biological functions that underlie mental retardation.

Drawing of a mammalian cortical neuron including associated structures (oligodendrocytes, astrocytes, blood vessels and the thyroid gland). Sizes are not to scale. Each of the terms in bold script represents a biological function that is affected by mutation of one or several MR genes⁶⁸.

2.6.4 Teneurin-1 is a promising XLMR candidate gene

We hypothesize that teneurin-1/odz1 is a promising candidate gene for XLMR, because it resides in Xq25, a locus of very low gene density that is comprised in the linkage intervals of several XLMR families. The *OCRL1* gene in Xq25 was known to be mutated in Lowe-Syndrome⁷⁰ for more than a decade; and since our analysis was started, two more XLMR genes in Xq25 have been identified: *ZDHHC9*⁷¹, which is near *OCRL1*; and *GRIA3*⁷², which is very close to teneurin-1 (*ODZ1*). Moreover, the teneurins are predominantly expressed in the developing CNS, and proposed to have a function in axon guidance and establishment of neuronal connectivity. *SYN1* was recently identified as an XLMR gene⁷³, and we found that the teneurin-1 ICD interacts with the Synapsin-1 protein (unpublished observation). Additionally, since *MECP2* is frequently mutated in XLMR and causes Rett syndrome⁷⁴, the entire family of methyl-CpG binding proteins was analyzed and a nonsense mutation in *MBD1* in one autistic and mentally retarded patient was revealed⁷⁵. The MBD1 protein was shown to interact and colocalize in the nucleus with the teneurin-1 ICD⁷⁶. Li et al suggest that the teneurins might be regulated by Emx2⁷⁷, mutations in *EMX2* causes schizencephaly in humans because of abnormal neuronal migration in the rostral forebrain leading to gross morphogenetic as well as more subtle lamination defects^{78,79}. Mutation of the transcriptional repressor gene *ZIC2* causes MR due to holoprosencephaly⁸⁰ (failure of right and left hemispheres to form distinct hemispheres), and the teneurin-2 ICD was shown to repress transcription mediated by another ZIC family member, ZIC1⁸¹. Thus, several proteins that interact with teneurins are XLMR genes and therefore it is likely that teneurins are also implicated in pathways required for proper brain development.

2.6 Biology of brain tumors

The most frequent types of brain tumors are glioma (astrocytoma, oligodendroglioma and oligoastrocytoma, both of which are composed of glial cells and occur predominantly in adults. Medulloblastoma (MB) is the most frequent neuronal brain tumor, which mainly affect humans early in their life (Figure 9).

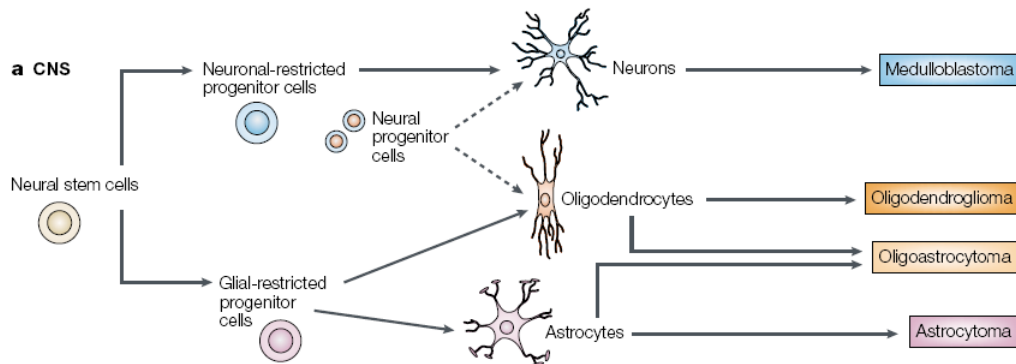


Figure 9: Developmental paths in the CNS and classification of CNS tumors.

Multipotent neuronal stem cells residing in the ventricular (VZ) and subventricular zones (SVZ) of the embryonic neural tube give rise to the three major cell types in the mature CNS: Neurons, oligodendrocytes and astrocytes. Neuronal progenitor cells differentiate first into restricted progenitor cells that are competent to generate neurons or glia, respectively. Neuronal progenitor cells might also give rise to oligodendrocytes (dotted arrow). CNS tumors are classified according the cell type they resemble based on morphological criteria and expression of markers. Astrocytoma and Oligodendroglioma are both glial tumors, whereas medulloblastoma is a neuronal tumor⁸².

2.6.1 Glioma

Malignant gliomas are the most common primary brain tumor in adults. Because of diffusely infiltrative growth, they are generally not curable despite rigorous therapy including surgery, chemotherapy and irradiation. Gliomas are subdivided in astrocytomas, oligodendrocytomas and mixed oligoastrocytoma

based on histological appearance and expression of protein markers. Oligodendrogliomas tend to have better prognoses and response to chemotherapy than astrocytomas⁸³. In addition, malignant gliomas are classified in three degrees of malignancy by the WHO: grade II, grade III (anaplastic) and grade IV (glioblastoma, the most aggressive form of astrocytoma). Glioblastomas (GBM) are very aggressively invading tumors with extremely poor prognosis and survival of approximately one year only. Primary GBM occurs de novo in the absence of pre-existing low grade lesion, mostly in older patients. In contrast secondary GBM evolves from lower grade astrocytoma over a period of 5-10 years and is more frequent in younger patients⁸⁴. Phenotypically, primary and secondary GBMs are indistinguishable, but they have distinct underlying genetic alterations⁸⁵ (Figure 10).

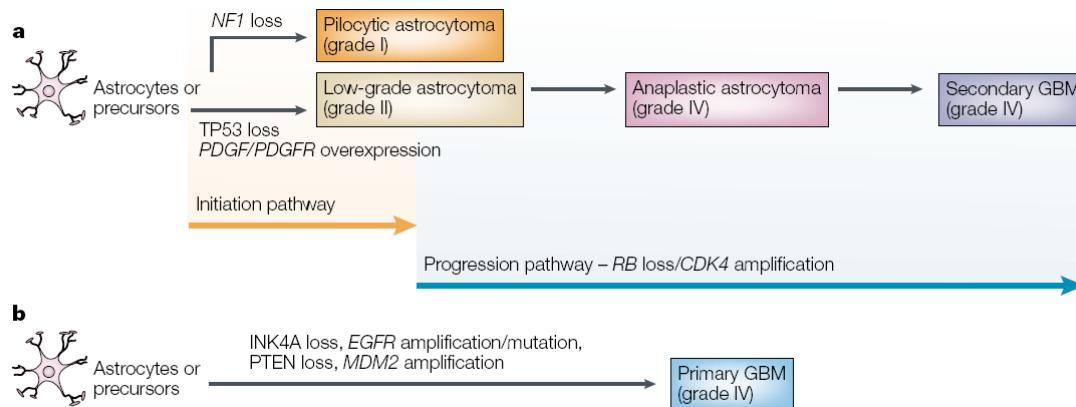


Figure 10: Genetic pathways in the development of primary and secondary GBM. Primary and secondary GBMs appear clinically and histologically indistinguishable, but their molecular profiles are different. A) Genetic changes in secondary astrocytoma include those required for tumor initiation (*TP53* loss, *PDGF* autocrine loop) and those involved in tumor progression (mutations in the *Rb* pathway: eg. loss of *Rb*, *CDK4* amplification). B) Deletion *INK4A* locus is very common in primary GBM, which results in the simultaneous loss of *p16* (an effector of the *Rb* pathway inducing cell cycle arrest) and *ARF* (which stabilizes *p53* by sequestering *mdm2*). The disruption of both crucial tumor suppressor pathways at the same time is thought to be a reason for the rapid development of primary GBM. Additionally, mutation or amplification of the *EGFR* and loss of *PTEN* are more frequent in primary GBM⁸².

For a long time, it was postulated that astrocytoma arises from astrocytes and oligodendroglioma from oligodendrocytes, however most cells in the brain do not normally undergo cell division which is a prerequisite for transformation, except during reactive proliferation after trauma^{83,86}. Therefore, the idea of a “window of neoplastic vulnerability” was described, in which oncogenic events may occur in still proliferating fetal cells. This is in accordance with the fact that neuronal tumors are uncommon and occur early in life, when neuronal cells are still dividing. Glioma in contrast is more common and occurs in adults, because glial cell proliferation occurs later in development and for a more prolonged period. Alternatively, recent work in animal models and primary glioma suggests that malignant glioma arises from neural progenitor cells. These cells reside in the ventricular zone of the adult brain and share important characteristics with glioma cells: Proliferative potential, migratory capacity, and competence to differentiate into different cell types. Mouse models expressing activated RAS and AKT in specific cell types revealed that glial progenitors are more sensitive to transformation than more mature astrocytic cells⁸². Alternatively, it was demonstrated that loss of *CDNK2A/p16* can confer a more progenitor-like phenotype to astrocytic cells⁸⁷. The cancer stem cell hypothesis suggests that tumors are maintained only by a rare fraction of cells with stem cell properties, as it has been shown in hematologic malignancies and several solid tumors. Likewise, gliomas contain a subpopulation of cells which are CD133+ and have the capacity to self-renew and undergo lineage-specific differentiation. Orthotopic injection of CD133+ cells results in tumors displaying the same cellular heterogeneity as the original tumor, but CD133- cells fail to form tumors⁸⁸.

The p53 pathway is commonly disrupted in astrocytoma; p53 itself is mutated in 50% of the tumors, and in most others p53 activity is downregulated by amplification of *MDM2* or *MDM4* or loss of *ARF* (which sequesters MDM2). In addition, many growth factors are overexpressed in early stage astrocytomas, including epidermal growth factor (EGF), FGFs, vascular endothelial growth factor (VEGF) and platelet derived growth factor (PDGF). In the case of PDGF both the ligand and receptor are overexpressed resulting in an autocrine loop. Oligodendrogliomas exhibit coordinated loss of chromosomes 1p and 19q in 40-80% of the cases, however the identity of the tumor suppressor genes located

there is unknown. Although oligoastrocytomas exhibit mixed phenotypic appearance, their genetic background resembles either oligodendrogliomas (loss of 1p and 19q), or astrocytomas (*TP53* mutations). Either the type of oncogenic alteration can dictate the tumor phenotype, as in the glioma mouse model where overexpression of Ras and Akt in progenitor cells results in astrocytic tumors, but overexpression of PDGF-B in the same cells generates oligodendrogliomas⁸⁹. Alternatively, the phenotypic repertoire of the cells undergoing transformation and the cerebral environment may also influence tumor differentiation. During progression from grade II to grade III, gliomas acquire genetic lesions affecting cell cycle control, such as loss of p16 or pRb, or alternatively by overexpression of CDK4, CDK6 or cyclin D1. In about 50% of anaplastic astrocytomas and glioblastomas, deletions in chromosome 9p encompassing the *CDKN2A* locus result in the loss of p16 and ARF proteins, or the *CDKN2A* gene is inactivated by point mutations or hypermethylation⁹⁰. Deletions of 13q affecting the *RB* gene is detected in 30-50% of high-grade astrocytomas, and rarely occurs together with loss of *CDKN2A* in the same tumor⁹¹. Loss of *PTEN* due to deletions of chromosome 10 or inactivating mutations (20%) lead to downstream activation of the AKT pathway, as it is observed in almost all glioblastomas⁹². In addition, upregulation of the RAS pathway by EGFR overexpression mediated by Shc and Grb2 is crucial for glioma progression facilitating proliferation, survival and angiogenesis.

The main reason for poor prognosis for glioma patients is the invasiveness of glioma cells, which is already acquired early in tumorigenesis and requires a dynamic interplay between cell-cell adhesion, ECM remodeling and cell motility. Secretion of extracellular proteases by glioma cells not only clears the path for migration, but also releases growth factors that are sequestered in the ECM and generates growth-promoting ECM fragments⁹³. Several integrin have been implicated in glioma migration, including $\alpha 2\beta 1$, $\alpha 5\beta 1$, $\alpha 6\beta 1$, $\alpha 5\beta 3$, which interact with tenascin, fibronectin, laminin and vitronectin, some of which are also produced by the tumor cells⁹⁴. Both EGFR and integrins signaling activates focal adhesion kinase (FAK), which stimulates pathways leading to proliferation, survival and migration⁹⁵. In addition, FGF, EGF and VEGF expressed by astrocytic gliomas likewise stimulate migration. In particular, clusters of tumor cells with EGFR amplification were preferentially

localized to infiltrating edges of glioblastomas⁹⁶, and some gliomas express a constitutively active EGFR mutant (vIII EGFR)⁹⁷. The ECM in the brain is rather scarce, and basement membranes are only around blood vessels and the pial surface. Therefore glioma migration exhibits specific characteristics: Cells preferentially invade along white matter tracts, often cross the corpus callosum to form “butterfly lesions” affecting both brain hemispheres, and some gliomas stop growing abruptly at the border between white and grey matter junction. In the grey matter, glioma cells prefer to grow either around neurons, blood vessels or underneath the pial surface. Necrosis is a prominent feature of high-grade gliomas and predicts poor outcome. Small areas of necrosis can develop in areas where the metabolic demands of rapidly growing tumor cells exceed nutrient supply, and larger necroses arise from vascular thrombosis, possibly caused by the tumor secreted tissue factor, which acts as a local coagulant. It is suggested that hypoxia promotes acquisition of molecular changes which result in more active migration, and necrotic cells may release growth factors. Importantly, hypoxia may select for very malignant cells that are resistant to apoptosis⁹⁸. Two different types of vascular proliferation are observed in glioblastoma, microvascular proliferation and a diffuse increase in vascular density consisting of more densely arranged small vessels. Glomeruloid vessels are a characteristic form of microvascular proliferation consisting of proliferating endothelial and smooth muscle cells and often surround regions of necrosis. Tumor cells release VEGF and PDGF, which stimulate proliferation of VEGFR1, VEGFR2 and PDGF β -receptor expressing endothelial cells. VEGF is the major factor for glioblastoma angiogenesis, downstream of both crucial signaling pathways activated in glioblastomas, EGFR and AKT, and may also induced by hypoxia⁹⁹. Additionally, VEGF enhances vascular permeability, resulting in leakage of the blood-brain barrier and tumor edema.

2.6.2 Medulloblastoma

Medulloblastoma, the most common pediatric brain tumor, is a malignant invasive neoplasm of the cerebellum composed of primitive neuroectodermal cells, but often contain glial cells as well¹⁰⁰. As with glial tumors, there is a lot of debate about the cell of origin. The cerebellum contains two distinct germinal

zones, the VZ which generates both neurons and glia, and the external germinal layer (EGL) which generates primarily neuronally restricted granule cell precursors. It is not clear from which layer MB's arise, there is evidence for both and human MBs express either VZ or EGL markers. There are two major subclasses of MB's described as either "desmoplastic" or "classic". Desmoplastic tumors occur in 15-20% of patients, more often in adults, and are located in the cerebellar hemispheres, display relatively favorable prognosis. 75-80% of MBs are classic MB's, which are located at the center of the cerebellum and grow in relatively uniform sheets of cells with high nuclear/cytoplasmic ration, and have a tendency to invade adjacent brain and leptomeninges¹⁰¹. Like gliomas, MB's contain cells expressing the stem cell marker CD133, which can form neurospheres, undergo self-renewal, can be induced to differentiate into both neurons and glia, and can generate tumors after transplantation into immunocompromised mice.

Two signaling pathways are crucial for MD development, SHH and Wnt signaling. Patients with the Gorlin syndrome have activating mutations in the SHH receptor patched, and exhibit recurrent basal cell carcinomas of the skin, craniofacial abnormalities, and increased incidence of MB¹⁰². Additionally, 20-30% of sporadic MBs harbor activating mutations of the SHH pathway, and mice with activating patched mutations develop MB¹⁰³. SHH signaling is known to control proliferation of granule cell precursors (GCPs)¹⁰⁴ and influence multipotent neuronal stem cell growth¹⁰⁵. Humans with the Turcot's syndrome caused by a germline mutation in the adenomatous polyposis coli gene (APC) have a high incidence of colon cancer and brain tumors, which are mostly MBs¹⁰⁶. Sporadic MBs rarely carry mutations in APC, but 5 to 15% of tumors have mutations β -catenin and axin, which also lead to activation of the Wnt pathway¹⁰⁷. Unlike the SHH pathway, the WNT pathway was not implicated in the growth or survival of GCPs. However it is critical for the specification of the midbrain-hindbrain boundary from which the entire cerebellum develops, and therefore may be important for the growth and survival of multipotent progenitors¹⁰⁸.

2.7 The teneurins – an emerging family of transmembrane proteins

The teneurin protein family is highly conserved from invertebrates to vertebrates, both regarding domain architecture and amino acid sequence. Moreover, the teneurin expression patterns are conserved across phyla, suggesting that this is also the case for their function. Since most of the data available for vertebrate teneurins are limited to expression patterns and in-vitro studies, I will first describe the expression pattern and the phenotypes of teneurin mutants in invertebrates.

2.7.1 Invertebrate Teneurins

The Teneurins were initially discovered in *Drosophila melanogaster* by two independent groups, one searching for orthologs of the vertebrate tenascin protein family¹⁰⁹, and one performing a screen for tyrosine phosphorylated proteins¹¹⁰. Both groups reported expression of *ten-m/odz* or *odz* in alternating parasegments during the blastoderm stage, and loss of function resulted in a pair-rule phenotype with missing alternative parasegments and fused denticle belts. This was surprising for a gene causing a pair-rule phenotype as all other known pair-rule genes encode transcription factors. In *Drosophila*, segmentation along the anterior-posterior axis is initiated by maternal genes, which then activate zygotic genes which act in a stepwise, hierarchical manner. Gap genes activate pair rule genes, which subsequently activate segment polarity genes. Baumgartner et al. suggested that *ten-m/odz* acts as a secondary pair rule gene downstream of the pair-rule genes *ftz* and *eve*, and upstream of the segment polarity genes *prd* (paired), *slp1* (sloppy paired 1), *gsb* (gooseberry), *en* (engrailed) and *wg* (wingless). Levine et al. describe *ten-m/odz* as a late acting pair-rule gene, which is expressed just as the syncytial blastoderm becomes transformed into the cellular blastoderm in which cell-cell communication can take place. Many genes involved in pattern formation during embryogenesis are also important in morphogenetic processes

occurring at later stages in development, this appears to be true also for the teneurins. During embryonic development, *ten-m/odz* is expressed in cardiac cells, in the lymph gland, and in the tracheal system as well as in all segmental furrows that fold during gastrulation (cephalic furrow, anterior and posterior transverse fold and posterior midgut plate). After hatching and during larval development, *ten-m/odz* is present in the ventral nerve cord, in the brain, in pioneering commissural axons, in cardiac cells, in lymph glands, in the tracheal system, around muscle attachment sites and in the visceral mesoderm. *Ten-m/odz* is particularly strongly expressed in the developing eye during pupal stages. A very distinct *ten-m/odz* expression pattern has been described in all imaginal discs of *Drosophila* larvae. In the eye imaginal disc, *ten-m/odz* is present in the morphogenetic furrow which implies a function in differentiation of imaginal disc cells. As ommatidia mature, *ten-m/odz* is expressed in the photoreceptor R7 and may be involved in specification of this cell. Mutations in *ten-m/odz* result in R7 photoreceptor and visible light photoreceptor loss and defects in ommatidial size, shape and rotation, ommatidial disorder and fusion, and interommatidial bristle defects¹¹¹. Expression of the *ten-m* and its paralog *ten-a* are largely overlapping, suggesting that both proteins may act cooperatively. Although *ten-a* mutants alone do not show a pair-rule phenotype, the phenotype of *ten-m/odz* mutants is enhanced and they exhibit very similar defects in eye patterning¹¹².

In *Caenorhabditis elegans*, there is only one gene named *ten-1*, from which two isoforms are generated by the use of alternative promoters. The long form *Ten-1L* corresponds to the full length protein, whereas the short form *Ten-1S* is missing most of the N-terminal ICD. Both isoforms have distinct expression patterns: *Ten-1L* is mainly found in the mesoderm, including pharynx, somatic gonad, various muscles and in neurons, whereas *Ten-1S* is predominantly expressed in some hypodermal cells and in a subset of neurons. The *in-vivo* function of *ten-1* was analyzed using deletion mutant and siRNA, which resulted in a pleiotropic phenotype including gonad disorganization, nerve cord defasciculation and defects in distal tip cell migration and axonal pathfinding¹¹³. More detailed analyses gonad rupture and germ cell leakage phenotype revealed that it is caused by a defect in the integrity of the basement membrane (BM) surrounding the gonad. Moreover, *ten-1* was shown to

genetically interact with the genes for the BM proteins nid-1 (nidogen) and epi-1 (laminin α -chain) as well as with the cell-surface BM receptors ina-1 (integrin α) and dgn-1 (dystroglyan)¹¹⁴.

2.7.2 Vertebrate Teneurins

Vertebrate teneurins are between 30-40% conserved compared to both fly and worm teneurins. In vertebrates, four teneurin paralogs called teneurin-1 to -4 (or ten_m1 to ten_m4 in the mouse) exist, which share a conserved domain architecture and amino acid identity of 60-70%. The teneurins are type II transmembrane proteins with a molecular weight of more than 300kDa containing an N-terminal ICD, a single span transmembrane domain (TM) and a large C-terminal ECD which is particularly well conserved. The ICD contains two EF-hand like motifs, two polyproline motifs and several conserved tyrosines which are predicted to be phosphorylated. On the extracellular side, there are eight tenascin-type EGF-like repeats followed by a region of highly conserved cysteines and the unique YD-repeats which do not occur in any other eukaryotic protein (Figure 11).

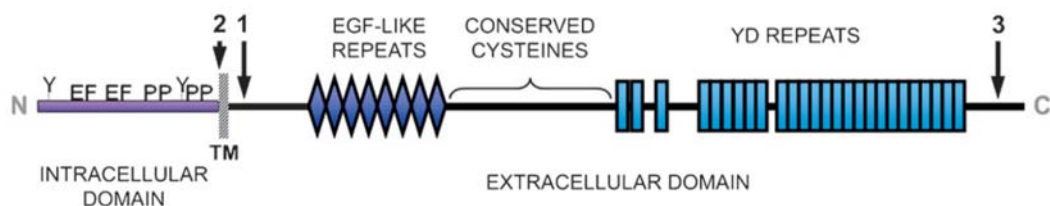


Figure 11: Domain architecture of vertebrate teneurins.

Teneurins have an N-terminal ICD, a single-span transmembrane domain TM and a large ECD. The ICD contains two EF-hand like motifs (EF), two polyproline motifs (PP) and several conserved tyrosines (Y) that are predicted to be phosphorylated. The ECD consists of eight tenascin-type EGF-like repeats, a region of conserved cysteines, and the unique YD repeats. Arrows with numbers indicate postulated cleavage sites: 1. Cleavage site for ectodomain shedding, 2. Transmembrane cleavage site resulting in the release of the ICD, and 3. C-terminal cleavage site resulting in the release of the TCAP¹¹⁵.

Several postulated cleavage sites are present in teneurins: There is a conserved furin cleavage site between the TM domain and EGF-like repeats, which was shown to be functional in teneurin-2¹¹⁶. The resulting ectodomain shedding appears to take place in vivo, since an antibody recognizing the teneurin-2 EGF-like repeats labels both the cell surface and the extracellular matrix in the chick embryo¹¹⁷. This cleavage site is conserved in invertebrate teneurins, suggesting that ectodomain shedding is important for the function of teneurins. A putative cleavage site within or near the TM domain serves to release the teneurin ICD. Finally, there is a conserved furin cleavage site near the C-terminus, which was proposed to release the teneurin C-terminal associated peptide (TCAP), with neuromodulatory activity¹¹⁸. Many ECM proteins are built by a combination of domain modules, for example Tenascin-C for which individual domains have distinct functions¹¹⁹. The modular domain composition of the teneurins and the evidence for proteolytic processing suggest that different domain of the teneurins could act separately to mediate distinct teneurin functions. The teneurins are posttranslationally modified by glycosylation, as treatment with N-glycosidase F alters their electrophoretic mobility¹²⁰. The Teneurin EGF-like repeats are most closely related to those of Tenascin-C and Notch; which in the case of Notch are glycosylated by Fringe. This posttranslational modification is required for proper ligand interaction and Notch signaling^{121,122,123}. In a database search, the EGF-repeats of all four Teneurins and Tenascin-C were found to contain a protein-O-fucosyltransferase-1 (POFUT1) consensus site and therefore are predicted to be O-fucosylated¹²⁴. Additionally, the YD-repeats are predicted to be glycosylated, and recombinantly expressed YD-repeats have been shown to bind the glycosaminoglycan heparin¹²⁵.

All studies investigating the expression of vertebrate teneurins performed in mice, chicken and zebrafish agree that the teneurins are prominently expressed in the developing central nervous system, but are also present at other sites of morphogenesis. The expression pattern of vertebrate teneurins is strikingly similar to teneurin expression in *Drosophila*; particularly remarkable examples include the expression during invertebrate and vertebrate eye development and the expression in fly leg imaginal discs and the limb buds of

chicken and mice. A summary of teneurin expression profiles described to date is provided in Table 1.

zebrafish

teneurin-1	ND
teneurin-2	ND
teneurin-3	developing brain ⁷ , somites ⁷ , notochord ⁷ , pharyngeal arches ⁷
teneurin-4	developing brain ⁷ , spinal cord ⁷

chicken

teneurin-1	developing CNS ^{2,8,10} , visual system ^{2,8,10}
teneurin-2	developing CNS ^{10,12} , visual system ¹⁰ , AER of limb buds ¹² , tendon primordia ¹² , pharyngeal arches ¹² , heart ¹² , somites ¹² , neural tube ¹² , craniofacial mesenchyme ¹²
teneurin-3	ND
teneurin-4	developing CNS ¹¹ , ZPA of limb buds ¹¹ , pharyngeal arches ¹¹

mouse

teneurin-1	developing and adult CNS ^{5,9,14} , visual system ^{5,9} , smooth muscle cells in lungs ⁹ , kidney glomeruli ⁹ , adult testes ⁹
teneurin-2	developing and adult CNS ¹⁴ , visual system ⁵
teneurin-3	developing and adult CNS ^{1,2,3,5,13,14} , visual system ^{1,5} , spinal cord ^{1,14} , notochord ¹⁴ , craniofacial mesenchyme ¹ , tongue ¹ , dermis ¹ , sacculle ¹ , developing limb ¹ , periosteum ¹
teneurin-4	developing and adult CNS ^{1,5,6,14} , visual system ⁵ , somites ¹⁴ , spinal cord ¹ , trachea ¹ , nasal epithelium ¹ , sacculle ¹ , joints ¹ , adipose tissue ¹ , tail bud and limbs ⁶

Table 1: Summary teneurin expression in vertebrates

¹Ben-Zur et al. 2000¹²⁶, ²Kenzelmann et al. 2008¹²⁷, ³Leamey et al. 2007a¹²⁸, ⁴Leamey et al. 2007b¹²⁹, ⁵Li et al. 2006⁷⁷, ⁶Lossie et al. 2004¹³⁰, ⁷Mieda et al. 1999, ⁸Minet et al. 1999¹³¹, ⁹Oohashi et al. 1999¹³², ¹⁰Rubin et al. 1999¹¹⁶, ¹¹Tucker et al. 2000¹³³, ¹²Tucker et al. 2001¹¹⁷, ¹³Zhou et al. 2003¹³⁴.

An early study of neurestin (rat teneurin-2) called shows expression in the developing olfactory bulb, which persists in the continuously regenerating granule cells. Since expression in tufted cells is re-induced during olfactory bulb regeneration after injury, the authors speculate that neurestin is involved in neuronal development and regeneration. Neurestin expression also persisted in hippocampal granule cells, which are known to be generated throughout life¹³⁵. In a microarray study, teneurin-4 was also shown to be expressed in the regenerating olfactory bulb, suggesting that the teneurins might not only be important during neuronal development, but also during neuronal regeneration¹³⁶.

A few studies have addressed the function of teneurins using cell culture or biochemical assays. Explanted chick dorsal root ganglia were induced to grow neurites which tended to fasciculate when plated on teneurin-1 YD-repeats¹²⁵. In transfected Nb2a cells, full-length teneurin-2 induced an increased number of filopodia and enlarged growth cones¹¹⁶, and this effect was shown to be dependent on the presence of the ICD¹³⁷. The ICD of teneurin-1 was shown to interact with the adaptor protein CAP/Ponsin, which could represent a possible link to the actin cytoskeleton⁷⁶. Moving filopodia left a trace of teneurin-2 behind, suggesting that the ECD is cleaved and deposited on the substrate. The induction of neurite outgrowth was enhanced on laminin compared to polylysine, suggesting that teneurin-2 interacts with laminin¹¹⁶. This idea is further substantiated by the colocalization of ten-2 ECD with laminin in the basement membrane of some tissues¹¹⁷. Several experiments suggest that the teneurins promote homophilic interactions between cells. Overexpression of a teneurin-2 construct missing the ICD in HT1080 cells resulted in cell aggregation, and if the cells were grown in a monolayer they exhibited epithelial morphology and teneurin-2 was highly enriched at sites of cell-cell contact¹³⁷. Recombinant proteins consisting of the ten_m1 EGF-like repeats were shown to dimerize, possibly mediated by the odd number of cysteines present in the EGF-like repeat, which allows for the formation of intramolecular disulfide bonds. Additionally, a recombinant ten_m1 ECD fused to Alkaline Phosphatase was used to detect teneurin binding activity on tissue sections, which largely overlapped with the ten_m1 expression domain, suggesting that homophilic interaction takes place. The homophilic binding of ten_m1 could be confirmed

on a far western blot (WB)¹³². Electron microscopy analysis of purified and rotatory shadowed teneurin ECDs revealed dimers with a C-terminal globular domain for all four mouse teneurins. Furthermore, co-expression of different teneurin paralogs in cell culture suggests heterophilic interaction. However if this occurs at physiological expression levels remains to be shown¹²⁰.

Some experiments suggest that the Teneurin ICD may have transcriptional activity: Transfected teneurin-2 ICD colocalized with PML bodies in the nucleus, and cotransfection of ZIC2 led to a proteasome-dependent decrease of teneurin-2 ICD protein levels. Conversely, expression of teneurin-2 ICD inhibited the transcriptional activation of ZIC2 as determined by a reporter assay⁸¹. When a recombinant protein with a transcriptional activator domain fused to the teneurin-2 ICD was expressed in cells, transcription of a luciferase reporter can be detected, indicating that the ICD is released from the membrane. Luciferase activity was enhanced 6.5 fold by cotransfection of a teneurin-2 construct containing only the TM domain and ECD, which simulates homophilic interaction⁸¹. The availability of antibodies recognizing the N-terminus of teneurin-1 enabled detection of ICD in the nucleus of cells that overexpressed full-length teneurin-1 by subcellular fractionation and WB analysis. Moreover, the ICD was found to interact with the methyl-CpG-binding protein MBD1, which could mediate teneurin-dependent modulation of gene expression⁷⁶.

Recently, two studies of mouse *ten_m3* in mice shed light on the in-vivo function of vertebrate teneurins. In a microarray study comparing the gene expression between the visual and somatosensory cortex at time of establishment of neuronal connectivity, several teneurins (*ten_m2*, *ten_m3* and *ten_m4*) were found to be specific for the visual cortex. Further experiments demonstrated that the cell bodies of neurons transfected in utero with GFP-*ten_m3* tend to aggregate and exhibit increased neurite outgrowth that persists during development¹²⁸. The same group published the first analysis of a teneurin knock-out mouse. In the visual pathway, most of the axons of the RGCs cross the midline of the optic chiasm and project to the contralateral dLGN, with the exception of a subset of RGCs that does not cross the midline and projects to the ipsilateral dLGN. The proportion of uncrossed projections varies among

species and correlates with the extent of binocular vision. Ten_m3 knockout mice do not exhibit an overt phenotype, and their brain and visual system appear normal on anatomical and histological level. However, the mice lacking teneurin-3 have defects in RGC axon targeting of the ipsilateral projections, resulting in an impairment of binocular vision. The authors conclude that ten_m3 is the first molecule that was shown to affect only ipsilateral, but not contralateral RGC axon guidance^{129,138}.

3. AIM OF MY WORK

Teneurins are a unique transmembrane protein family, conserved from flies and worms to vertebrates. Analysis of teneurin expression and function in invertebrates suggests important functions in many processes during development. However, still very little is known about the biological function and mechanism of action of the vertebrate teneurin family, which consists of four paralogs called teneurin-1 to -4.

The goal of the first part of this thesis was to gain insights in the function and signaling mechanism of the vertebrate teneurins using the chick embryo and cultured cells as a model system.

In the second part, the aim was to investigate the implication of teneurins in human disease. Teneurin-1 is localized on the X-chromosome, and I analyzed it as a candidate gene for XLMR. Additionally, a microarray study suggested that teneurin-4 was overexpressed in brain tumors, and therefore I generated the tools to analyze teneurin-4 in brain tumor samples.

4. MATERIALS AND METHODS

4.1 Production of antibodies against chicken teneurin-4

RT-PCR was performed on chick brain RNA using the Superscript RT-PCR kit (Invitrogen) and oligodT primers. The obtained cDNA was subsequently used as a template for PCR amplification of chick teneurin-4 sequences.

4.1.1 ICD antibody

A fragment corresponding to the first two exons of chick teneurin-4 was amplified using the Hi-Fi Expand Kit (Roche), standard PCR conditions ($T_a = 55^\circ\text{C}$ and $T_e = 45\text{s}$) and the primers cten4 fw SphI: ACTAGCATGCGATGTAAAAGAAAGGAAACCG and cten4 rev KpnI: TAGTGGTACCAGTTTCGGTATTCTCGTGCTC. The resulting PCR fragment was cloned SphI-KpnI into the PQE30 vector (Qiagen) containing a C-terminal HIS-tag for protein expression and purification in bacteria. M15 Prep4 bacteria were transformed with the cten-4 ICD construct, and protein expression was verified by SDS-PAGE (Acrylamid (BioRad), APS (Sigma), TEMED (Sigma) followed by Coomassie staining (Pierce). The cten-4 recombinant protein was found in the soluble fraction and therefore purified under native conditions. 50 ml of bacterial culture in 2YT medium were induced for protein production, and the lysate was prepared. The HIS-tagged recombinant protein was bound on a ProBond Nickel-Column (Invitrogen) and eluted with increasing concentrations of Imidazole (Fluka) according to the Qiagen Expressionist protocol. The purified protein was sent for injection into rabbits (RCC) to generate polyclonal antibodies, and the resulting antibodies were tested on recombinant protein.

4.1.2 ECD antibody

A recombinant fusion protein between the Tenascin-C signal peptide and the chick teneurin-4 EGF-like repeats was generated by splicing by overlap

extension. The TNC fragment was produced from the pCTN-230 plasmid using the primers KS fw: CGAGGTCGACGGTATCG and TNC/cten4 EGF rev: ACAATTATCCACTGATTCATTGAGCCCAGTCTCCCG and the cten4 EGF fragment using the primers TNC/cten4 EGF fw: CGGGAGACTGGGCTCAATGAATCAGTGGAT AATTGT and cten4 EGF rev: TAGTCTGGAGTTAGTGATGGTGATGGTGATGTCCATC GTTGCCTTCCCGTC containing a HIS tag and XhoI site. To obtain the fusion protein, a second PCR was performed using both fragments as template and the KS fw and EGF rev primers. The resulting PCR fragment was cloned into the pCEP-Pu vector using the restriction enzymes NotI and XhoI and sequenced. Expression and secretion of the recombinant protein in 293T-EBNA cells was verified by WB analysis of cell lysates and cell culture medium using the penta-HIS antibody (Qiagen). Cells stably expressing the TNC/hTEN4 EGF protein were selected with G418 for the EBNA-plasmid (Promega) and Puromycin for the pCEP plasmid (Sigma). These cells were finally grown in 0.3% FCS in triple flasks (Nunc) to produce and secrete the TNC/cten4 EGF protein. Subsequently, the recombinant protein was purified from the tissue culture medium and sent for injection into rabbits to generate polyclonal antibodies. The antibodies were first tested on recombinant protein, and subsequently on cell and tissue lysates.

4.2 IHC of developing chick embryos

Chicken embryos were incubated and sacrificed on the appropriate day of development to prepare tissue sections as previously described¹²⁷. The sections were rinsed in PBS, blocked with BSA (Sigma) and stained with the cten4 NA (1:500), cten4 EGFA (1:500) and cten4 EGFB (1:500) antibodies overnight. Secondary FITC-labeled antibodies (Alexa) were used at a concentration of 1:1000 and the nuclei counterstained with Hoechst 33342 (Sigma) used 1:1000. As control, the preimmune serum or the secondary antibody alone were used to stain the sections. The sections were viewed on a Zeiss Z1 and images were acquired using the Image Access software.

4.3 WB analysis of developing chick embryos

Chicken embryos were sacrificed and the brains, eyes, limb buds and organs were dissected out. RIPA buffer (50mM Tris (Fluka), 150mM NaCl (Fluka), 0.1% SDS (BioRad), 0.5% Na-Deoxycholate (Merck), 1% Triton-X (Fluka)) was added and the tissues were homogenized with a small pestle. The lysates were clarified by centrifugation and the protein concentration determined by a Bradford Assay (BioRad). The samples were analyzed on a 7.5% Polyacrylamid-gel, blotted for 2h at 45 mA per minigel using a semi-dry blotting system (Millipore). The blots were stained with amidoblack to check the amount of protein on the membrane, and blocked with 5% milk (Fluka). The membranes were incubated overnight with cten4 Ab's at the following concentrations: cten4 NA (1:500), cten4 EGFA (1:1000) and cten4 EGFB (1:1000). Blots were washed in TBS-T (TBS containing 0.1% Tween (Fluka)) and incubated with HRP-labeled secondary antibody (Cappel) diluted 1:1000 and washed again. Chicken teneurin-4 was detected by Super Signal (Pierce) and recorded on a Hyperfilm™ (Amersham). As a loading control, human β -actin antibodies (Sigma) were used that crossreacted with chicken β -actin.

4.4 Sequencing of human teneurin-1

4.4.1 Patient samples

Literature search was performed to identify XLMR families with a linkage interval containing Xq25, and the European MRX-consortium and the Greenwood Genetic Center were contacted to ask for DNA samples of XLMR families linked to Xq25 with unknown cause of the disease. Three healthy control samples were obtained from the blood of volunteers after purification of genomic DNA from white blood cells using the QiAamp DNA Blood Mini Kit (Qiagen). All patients that were sequenced are listed in Table 2.

Euro-MRX	Consortium No	DNA No
a	D004	12318
b	L022	22317
c	L025	23402
d	L041	15363
e	N005	5309
f	N043	4235
g	P003	10644
h	P004	10651
i	P014	10655
j	T013	22408
k	T019	10963
l	T048	21236
GGC		
m	K8245	5897
n	K8310	8038
o	K8895	cms1438
p	K8917	cms2497
q	K8923	cms2605
r	K8941	cms3181
s	K8943	cms3235
t	K9033	cms6176
other source		
u	Italian patient	
v	English patient	
w	Brazilian patient	

Table 2: List of samples from XLMR families.

Samples from the Euro-MRX consortium were obtained from Arjan de Brouwer, samples from the Greenwood Genetic Center (GGC) were obtained from Dr. Charles Schwartz and Dr. Anand Sristava. The Italian patient was obtained from Dr. Alessandra Renieri, the English patient from Dr. Deirdre Cilliers¹³⁹ and the Brazilian patient from Dr. Fernando Kok¹⁴⁰.

4.4.2 PCR and sequencing primers

All exons according to transcript number NM_014253 were analyzed. A list of the PCR and sequencing primers used is provided in Table 3. If possible, different primers were used for PCR and sequencing, however in cases where it was difficult to find a primer that works, the PCR primer was reused for sequencing. Several sequencing primers had to be used for exon 1 including the putative promoter region, exon 27 and exon 31 including the 3'UTR several sequencing primers due to their size. Genomic DNA from XLMR patients and controls was used as the template. Standard PCR conditions were applied if not otherwise indicated, using the HiFi PCR kit, T_a of 55°C, t_e of 45s and 25 cycles of PCR. In some cases, the Expand Long Template kit (Roche) was used with the according DNA polymerase and the ELT-buffer mentioned. The PCR conditions for each exon were first set up using the control samples before PCR on XLMR patient samples were performed. PCR reactions were purified using the PCR purification Kit (Qiagen). For sequencing, an appropriate amount of PCR product (depending on its size) was combined with 10nM of primer and submitted to the sequencing facility at the FMI.

4.4.3 Sequence analysis

DNA sequencing was carried out at the FMI sequencing facility on an ABI PRISM 3700 DNA Analyzer and both the sequence in text format and the chromatogram were obtained. The irregular sequence in the beginning and after the end of the PCR product for each was cropped and all the exons of one patient were composed to one sequence for each patient. Subsequently the sequences of the 23 patients and 3 controls were aligned using the ClustalW program¹⁴¹ to find alterations. To exclude misinterpretation of the chromatogram by the sequence analysis program, the chromatograms of all deviations from the reference sequence were inspected carefully. If the deviation persisted, the PCR and sequencing was repeated to exclude PCR errors. All confirmed alterations were analyzed for a potential effect on teneurin-1 gene expression or amino acid sequence, and were labeled in the alignment and summarized (Table 6).

exon	PCR size	fw primer	rev primer	seq primer
exon 1 ^{b)}	2845	gagggttagtgcagctagggtac	gcacacaagcattctctaagagaa	gagggttagtgcagctagggtac ttgatattcaaagttgtggc ccagcacttgggaggccgag agttaatggttctaactac ctttattccatgagctctc gaatctgccagatgcatttcc cacgtaattactaccaatgg ttgaagttgaggaattgcag gccaagttgggagagtaagtctc cttggtatagcatgattgtttg gtgcaaaaggatgacctggctt atttgatatactgttcttg gaagttaggatgtttatcag aggctcagagttcctgcaact tcaatgagaattgctctttgg tcaatgtaatcctcgtttatc gcttggttaaccagcaagac gctacccttcttctacatgca gcaaatacatcattgttggcc tagaatttctccattatgta gactgtttccaagttctac ggaaggggactgaaataacc ctgttaagctctcctttgg gtagccaagtgatccacag caggccaaagctcctcctgc ggaagataaatgaaatcactc cagagcttagtcaaatgtgg ctgtccatggaagacatggt gtctgtggtatgttcatgaaatg attttgcaaaagctctgtatc gcttatccccaaactgcctc ggattcatgattgtcagtgctc tttagtgcctcaacttag aacactagaccttctgactc ttcatgaaatcagatgctgag accttaccacccataagag gcaacagagtgcagactgtc tccttccacaatcacaag cctggtgctcatcggttaacac gttttctagatcagaactctg tctgtctaccatgcttccctg caagtaaatccttccaaccg tgctgtcttgcgatgacag
exon 2	498	gcacagagtcctagctaccatg	ggaaggagaacaaagcaaaagg	
exon 3 ^{a)}	237	gcaccactagatgaagggttaaggg	cagagaagcaggggtccattttg	
exon 4	385	ctgaaatcctggtaagctctgc	accatcctctgccaactactaa	
exon 5 ^{a)}	431	ctgagctccatccagttctcttg	ccattcccaccacaagcaaaac	
exon 6	351	aaactccagttacttggcctaac	tcccagctacagttctaagacc	
exon 7	402	ggcaaggcctgaaagacagatg	gttcaaccatcacctcttg	
exon 8	358	gcaaaagaagtaagaaatagggcag	tgtctttctaggggtgaactgtca	
exon 9 ^{a)}	346	agcagtaagtgtccacaacacgc	ctgttgctgtcaccactactaatg	
exon 10 ^{a)}	436	ctgtttgtaatcatgaacatgtgcc	ttgcatcttactaggagaacag	
exon 11	420	ggacagagtggttgcacatgctca	ggaaggaacagttagaatttaagag	
exon 12	607	gctagagatcttctgacatcttg	tcccactccaacctcaaaa	
exon 13	187	gcaacagatggtaaccattagctac	catattgtatagctttagctc	
exon 14	289	atggttagatgcttccctatagg	tagaggctgggctattcctt	
exon 15	431	gtgaatttaacaaattctgaact	gaaatgaacgtggattatgtgg	
exon 16	327	cctcccagaatgttattagtagtt	cctggctagaagtcagtaattgg	
exon 17	445	acaatacaagtgatataagttgag	cactgttgaccatccatgatatta	
exon 18	551	taaagcaatccttaaggttgg	tctgttctgtcatgtaactgc	
exon 19	385	caactctaatacagaattcagtag	tgcggtcatctctaagtagtattc	
exon 20	474	tcactctcaggttctctatgcc	gcttctactggcagtgctttgctc	
exon 21	467	tccatctccttggtacttaagaag	gtggcaacagctcgggattttg	
exon 22	295	tgcttccattgctatggctt	ccatgatgccaatgacaataatc	
exon 23	628	cactttccgagacatcaccaatg	gctcataccaatgtttgcaagtaac	
exon 24 ^{a)}	694	aatgattcttgatgcacagagct	caacactcagcaattactaaggcat	
exon 25	325	gttaaactgtattagctgccaagtg	aagggtgaggttgacataggg	
exon 26 ^{a)}	545	cagataggaccacagcacc	cggccattagcatcctcttttg	
exon 27 ^{c)}	459	ggattcatgattgtcagtgctc	tgcaggtcctcaccaagatggac	
exon 28	609	atccactagggttgcccacagtg	tctatctcacactgtggtcagtaaa	
exon 29	1442	gcatttgatcagagatcagctc	caaaggcattgagattctgtga	
exon 30	542	gcaacagagtgcagactatgctc	taccttctcattaattgtgcacg	
exon 31 ^{d)}	2406	cactcactgacaaattaaagagag	gtggttaacttacaattacacagc	

Table 3: List of PCR and sequencing primers to analyze the human teneurin-1 gene.

31 exons including some flanking sequence were amplified and sequenced. In most cases, a separate primer was used for sequencing, but in some instances the PCR forward primer was used. For the larger exons (exon 1 including 5'UTR, exon 29 and exon 31 including 3'UTR), several sequencing primers were used. The PCR size includes the flanking region and is therefore larger than the size of the exons alone. Standard PCR conditions were used, unless otherwise noted: a) $T_a = 60^\circ\text{C}$, b) ELT buffer 1, c) ELT buffer 2, d) ELT buffer 3, $t_e = 3\text{min}$.

4.5 Production of antibodies against human teneurin-4

RT-PCR was performed on human brain RNA using the Superscript RT-PCR kit (Invitrogen) and oligodT primers. The obtained cDNA was subsequently used as a template for PCR amplification of human teneurin-4 sequences.

4.5.1 ICD antibody

A recombinant protein corresponding to the first exons of human teneurin-4 was produced using the same strategy as described in 2.1.1 and purified from bacterial lysates using the HIS-tag. Primers used for cloning were hten4 fw SphI: ACTAGCATGCTATCCATATGACGTCCCAGAC and hten4 rev KpnI: TAGTGGTACCTGTGCGGCAGAATTCCTCGGC. The resulting PCR fragment was cloned SphI and KpnI into pQE30 for production of recombinant protein in bacteria. In addition to the generation of polyclonal antibodies, the purified protein was also submitted for the generation of monoclonal antibodies to the FMI monoclonal antibody facility.

4.5.2 ECD antibody

A recombinant fusion protein between the Tenascin-C signal peptide and the human teneurin-4 EGF-like repeats was generated using the same strategy as described in 2.1.2. The following primers were used:

TNC/hten4 EGF fw: CGGCAGACTGGGCTCAATGAGTCGGTGGATAACTGC,

TNC/hten4 EGF rev: GCAGTTATCCACCGACTCATTGAGCCCAGTCTCCCG and

hten4 EGF rev: TAGTGCGGCCGCTTAGTGATGGTGATGGTGATGATCATTGTCTTTGC

TGTCACC containing a HIS tag and NotI site. The resulting PCR fragment was cloned using HindIII and NotI, sequenced and transfected into 293T EBNA cells to test expression and secretion and finally to produce the recombinant protein. In addition to the generation of polyclonal antibodies, the purified protein was also submitted for the generation of monoclonal antibodies to the FMI monoclonal antibody facility.

4.6 WB analysis of brain tumors

Protein lysates were prepared from pieces of frozen tumor material that was obtained from the Merlo lab at the University hospital, Basel. RIPA-buffer was added to the tumor pieces and they were homogenized by using a small pestle. The lysates were clarified by centrifugation and the protein concentration determined by a Bradford Assay. Normal brain protein samples were purchased from BioChain, including one sample of total brain (P1234035, age 71 Lot No A908046), cerebral cortex (P1234042, age 77, Lot No B107064) and cerebellum (P1234040, age 66, Lot No B109120). The samples were analyzed on a 7.5% Polyacrylamid-gel, blotted for 2h using a semi-dry system and stained with amidoblack to verify the amount of protein on the membrane. HRP-labeled secondary antibody was used at a dilution of 1:10'000 and the signal detected by Super Signal. As a loading control, β -actin or vinculin antibodies were used.

4.7 IHC of brain tumors

Frozen sections of brain tumors were obtained by the Merlo lab at the University Hospital, Basel. The sections were stained with the Ventana Automated Staining module using the standard IHC protocol with the following parameters: No pretreatment, 4 min AB-block, primary antibody incubation 60 min, secondary anti-rabbit incubation 32 min, Hematoxylin counterstain. Both hten4 ECDA and hten4 ECDB antibodies were used 1:1000 and resulted in similar staining, and subsequently only hten4 ECDA was used. A control using the preimmune serum was performed in parallel, and if enough sections were available also H&E staining. H&E Staining Procedure: Thaw 20' at RT, 30'' dH₂O, 1 x 2' Hematoxylin, rinse dH₂O, 5' tap water, 12 x dip in acid ethanol, 2 x 1' tap water, 2' H₂O, 30' Eosin, 2 x 2'' 95% EtOH, 2 x 2'' 100% EtOH, 2 x 5' HistoClear. Stained sections were coverslipped using the HistoClear kit, dried for at least 30 min and viewed on an Olympus Eclipse E600 microscope. Images were acquired using the Image Access software.

4.8 Microarray analysis of brain tumors (performed in the Hemmings lab)

Total RNA was extracted from the primary tumor samples using Trizol reagent, according to manufacturer's instructions, and resuspended in diethylpyrocarbonate (DEPC) treated water. Total RNA was further purified using the RNeasy kit and following the protocol for Total RNA cleanup. RNA was then amplified and labelled using the Affymetrix 2-cycle amplification protocol as per manufacturer's instructions (Affymetrix). Samples were hybridized to Affymetrix U133v2.0 GeneChips and scanned using an Affymetrix GeneChip scanner as per manufacturer's instructions. Expression values were estimated using the GC-RMA implementation found in Genedata's Refiner 4.1 (Genedata, Basel, Switzerland) package. Data-mining and visualization was performed using Genedata's Analyst 4.1 package. All samples were quantile normalized and median scaled to correct for minor variations in their expression distributions.

5. RESULTS

Part I – Teneurins in Development

5.1 Teneurin-1 is expressed in interconnected regions of the developing brain and is processed in vivo.

Research article

Open Access

Teneurin-1 is expressed in interconnected regions of the developing brain and is processed in vivo

Daniela Kenzelmann^{†1}, Ruth Chiquet-Ehrismann¹, Nathaniel T Leachman² and Richard P Tucker^{*2}

Address: ¹Friedrich Miescher Institute, Novartis Research Foundation, Maulbeerstr. 66, 4057 Basel, Switzerland and ²School of Medicine, 1 Shields Avenue, University of California at Davis, Davis, CA 95616-8643, USA

Email: Daniela Kenzelmann - daniela.kenzelmann@fmi.ch; Ruth Chiquet-Ehrismann - ruth.chiquet@fmi.ch; Nathaniel T Leachman - ntleachman@ucdavis.edu; Richard P Tucker* - rptucker@ucdavis.edu

* Corresponding author †Equal contributors

Published: 25 March 2008

Received: 30 August 2007

BMC Developmental Biology 2008, 8:30 doi:10.1186/1471-213X-8-30

Accepted: 25 March 2008

This article is available from: <http://www.biomedcentral.com/1471-213X/8/30>

© 2008 Kenzelmann et al; licensee BioMed Central Ltd.

This is an Open Access article distributed under the terms of the Creative Commons Attribution License (<http://creativecommons.org/licenses/by/2.0>), which permits unrestricted use, distribution, and reproduction in any medium, provided the original work is properly cited.

Abstract

Background: Teneurins are a unique family of transmembrane proteins conserved from *C. elegans* and *D. melanogaster* to mammals. In vertebrates there are four paralogs (teneurin-1 to -4), all of which are expressed prominently in the developing central nervous system.

Results: Analysis of teneurin-1 expression in the developing chick brain by in situ hybridization and immunohistochemistry defined a unique, distinct expression pattern in interconnected regions of the brain. Moreover we found complementary patterns of teneurin-1 and -2 expression in many parts of the brain, including the retina, optic tectum, olfactory bulb, and cerebellum as well as in brain nuclei involved in processing of sensory information. Based on these expression patterns, we suspect a role for teneurins in neuronal connectivity.

In contrast to the cell-surface staining of the antibody against the extracellular domain, an antibody recognizing the intracellular domain revealed nuclear staining in subpopulations of neurons and in undifferentiated mesenchyme. Western blot analysis of brain lysates showed the presence of N-terminal fragments of teneurin-1 containing the intracellular domain indicating that proteolytic processing occurs. Finally, the teneurin-1 intracellular domain was found to contain a nuclear localization signal, which is required for nuclear localization in transfected cells.

Conclusion: Teneurin-1 and -2 are expressed by distinct interconnected populations of neurons in the developing central nervous system. Our data support the hypothesis that teneurins can be proteolytically processed leading to the release of the intracellular domain and its translocation to the nucleus.

Background

Teneurins are a family of type II transmembrane proteins originally discovered as pair-rule gene products in *Drosophila* [1,2] and [3]. Homologs have been identified in

chicken, mouse and humans called teneurin-1 to -4 (for reviews see [4] and [5]).

Teneurin domain architecture is highly conserved across phyla. All teneurins described to date have an extracellular

domain (ECD) with eight tenascin-type EGF-like repeats followed by a region of conserved cysteines and YD-repeats [6]. The N-terminal intracellular domain (ICD) of vertebrate teneurins has a conserved and unique domain architecture, containing two polyproline motifs, EF-hand-like metal ion binding domains and several putative phosphorylation sites.

The expression of vertebrate teneurins has been studied most extensively in mouse and chicken. All of these reports are in agreement that the primary site of teneurin expression is the developing central nervous system ([7-13]), although teneurins are also expressed outside the nervous system at sites of pattern formation like the limb bud [14,15]. The expression of teneurins in specific subsets of neurons is conserved from *Drosophila* and *C. elegans* to vertebrates. For example, in the chicken visual system teneurin-1 transcripts are concentrated in the neurons of the tectofugal pathway, whereas mRNA encoding teneurin-2 is concentrated in the neurons of the thalamofugal pathway [16]. The pattern and timing of expression led to speculation that teneurins might have a role in synaptic connectivity. Further evidence for such a function is provided by the observation that teneurin-1 and -2 promote neurite outgrowth in vitro [7,8], (see also [17]) and in vivo [18], and by the fact that teneurins can homo- and heterodimerize through their EGF-like repeats [19]. Recently, the teneurin-4 gene was found in a screen for genes differentially regulated in *emx*^{-/-} mice, and because of its intriguing expression pattern, in situ hybridization was performed for all four teneurin paralogs revealing gradients of expression and striking complementary expression in the mouse forebrain [13]. Interestingly, the human teneurin-1 gene is located on the X-chromosome in a region to which several X-linked mental retardation (XLMR) syndromes have been mapped [7]. The predominant neuronal expression and suggested function in brain development make teneurin-1 a promising candidate gene for XLMR.

The discovery of teneurins in *Drosophila* as the only pair-rule gene that is not a transcription factor suggested that teneurins – although transmembrane proteins – could also have a nuclear function [3]. Transfection of a full-length teneurin-2 reporter construct with a transcriptional activator attached to its N-terminus resulted in transcription of a reporter gene particularly in response to homotypic interactions, indicating that the ICD is released upon specific stimuli [20]. In vitro the teneurin-2 ICD localizes to PML-bodies in the nucleus and affects zic-1 mediated transcription [20]. Similarly, the teneurin-1 ICD colocalizes in the nucleus with MBD1, a methyl CpG binding protein, after co-transfection of cells in culture [21]. Western blot analysis of cells transfected with full-length teneurin-1 show several N-terminal peptides which could

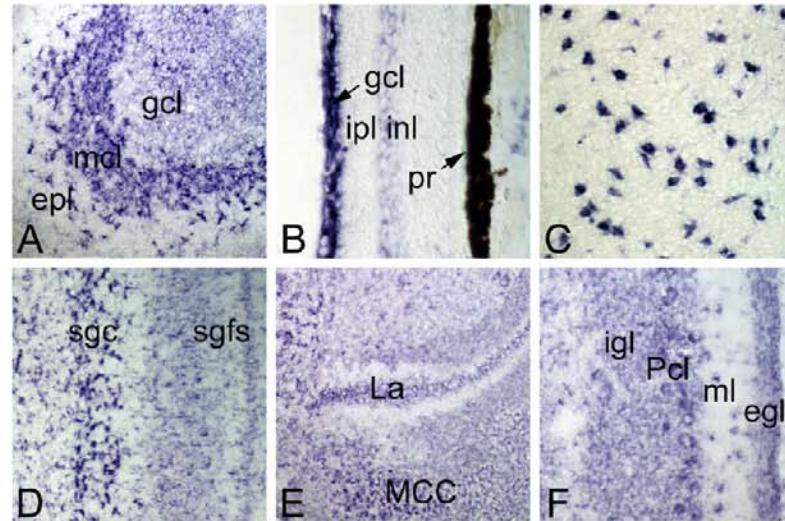
correspond to intermediate processing products and the ICD, but it was not possible to visualize the ICD in the nucleus by immunofluorescence [21]. Assuming that the released intracellular domain has an important signalling function, it is likely that such a cleavage is tightly regulated during development and that it would not occur spontaneously in cell culture, or only to a very small extent.

The aim of this work was to analyze teneurin-1 expression in detail and to determine if teneurins can be processed in the vertebrate embryo as they appear to be processed in vitro. We have studied the expression pattern and processing of teneurin-1 in the developing chicken embryo using in situ hybridization, immunohistochemistry and immunoblotting, and have compared the patterns of teneurin-1 expression with those of teneurin-2. As antisera to teneurin-1 were raised against both the ICD and ECD of the protein, we were able to show for the first time the nuclear localization of the ICD in neurons and mesenchymal tissues in situ. The processing of teneurin-1 in developing tissues was confirmed by immunoblot analysis. Finally, we show that the teneurin-1 ICD contains a specific nuclear localization signal that is required for translocation into the nucleus.

Results

In situ localization of teneurin-1 transcripts

Teneurin-1 was widely expressed in the chick nervous system at embryonic day (E) 17. The strongest hybridization signals seen with the teneurin-1 antisense probe were in the mitral cells of the olfactory bulb (Fig. 1A), subpopulations of neurons in the hippocampus and piriform cortex (not shown, but see immunohistochemistry), retinal ganglion cells and cells found in the inner nuclear layer adjacent to the inner plexiform layer (Fig. 1B), the large neurons found within the rotund nucleus (Fig. 1C), and the neurons of the stratum griseum centrale of the optic tectum (Fig. 1D). In the hindbrain teneurin-1 mRNAs were found in the nucleus laminaris and nucleus magnocellularis (Fig. 1E) and throughout the cerebellum (Fig. 1F). Adjacent sections processed with a sense probe were unlabelled. Thus, the expression of teneurin-1 in the chicken embryo is more widespread than suggested by our earlier studies using a less sensitive radiolabeled probe that only detected the most abundant sites of expression in the visual system. In addition to the strong expression in interconnected subset of neurons in the tectofugal portions of the visual system (e.g., retinal ganglion cells, the stratum griseum centrale of the optic tectum and the rotund nucleus), teneurin-1 transcripts were also present in diverse brain regions involved in general sensation, olfaction, the processing of auditory information, and the coordination of complex motor behavior.

**Figure 1**

Teneurin-1 is expressed in many parts of the developing CNS. In situ hybridization at E17 with a teneurin-1 antisense probe (sense controls were negative). In the olfactory bulb (A), there is a strong hybridization signal in the mitral cell layer (mcl). The ganglion cell layer (gcl) is also positive, but the external plexiform layer (epf) is not. In the retina (B), the ganglion cell layer (gcl) is labelled intensely, and there is a faint signal in neurons of the inner nuclear layer (inl) adjacent to the inner plexiform layer (ipl). The pigment retina (pr) has dark melanosomes. The nucleus rotundus (C) contains large, scattered neurons that are positive for teneurin-1 mRNA. In the optic tectum (D) teneurin-1 mRNA is widespread, but is seen most clearly in the large neurons of the stratum griseum centrale (sgc). In the hindbrain (E) the nucleus laminaris (La) and nucleus magnocellularis (MCC) are labelled, as are Purkinje cells (Pcl) and other neurons in the cerebellum (F).

Immunolocalization of teneurin-1 and teneurin-2

Polyclonal antibodies raised against recombinant fragments of teneurin-1 were used to study the distribution of teneurin-1 protein in the developing avian nervous system. Our results are summarized in Figure 2 and are briefly described here starting in the rostral forebrain and ending in the hindbrain, emphasizing regions also illustrated in Figure 1. At E17 the anti-teneurin-1 serum labelled the glomerular layer and mitral cell layer of the olfactory bulb (Fig. 2A). This pattern is consistent with the expression of teneurin-1 by mitral cells shown in Figure 1A and the transportation of the protein to the dendrites of mitral cells in the glomerular layer. In the retina teneurin-1 immunolabelling was observed in retinal ganglion cells, neurons within the inner nuclear layer adjacent to the inner plexiform layer, and within distinctive laminae (especially 2 and 5) within the inner plexiform layer (Fig. 2C). As predicted by in situ hybridization, teneurin-1 immunoreactivity was particularly strong throughout the rotund nucleus (Fig. 2E) and in the large neurons of the stratum griseum centrale of the optic tectum (Fig. 2G), two interconnected populations of neurons that make up part of the tectofugal visual pathway. Finally, the anti-teneurin-1 labelled the dendritic field of

the external portion of the nucleus laminaris (Fig. 2I), the large neurons of the nucleus magnocellularis (Fig. 2I), and in the cerebellum labelled Purkinje cells and the portion of the molecular layer adjacent to the external granular layer (Fig. 2K). Note that the teneurin-1 expression pattern observed with the antibody is more extensive in most brain regions than observed by in situ hybridization. For example, neurons in the outer portion of the inner nuclear layer of the E17 retina are stained with the antibody (Fig. 2C), but are not positive for teneurin-1 transcripts (Fig. 1B). Since these cells were not stained with preimmune serum or secondary antibody only controls (not shown), a possible explanation for this discrepancy is that teneurin-1 transcripts are present below the level of detection of our in situ hybridization protocol in some regions, but nevertheless at levels sufficient to generate enough protein to be recognized, albeit faintly, by immunohistochemistry.

In situ hybridization has previously suggested that the patterns of expression of teneurin-1 and teneurin-2 are largely complimentary with the possible exception of the retina, where transcripts encoding these proteins appeared to co-localize in retinal ganglion cells and in

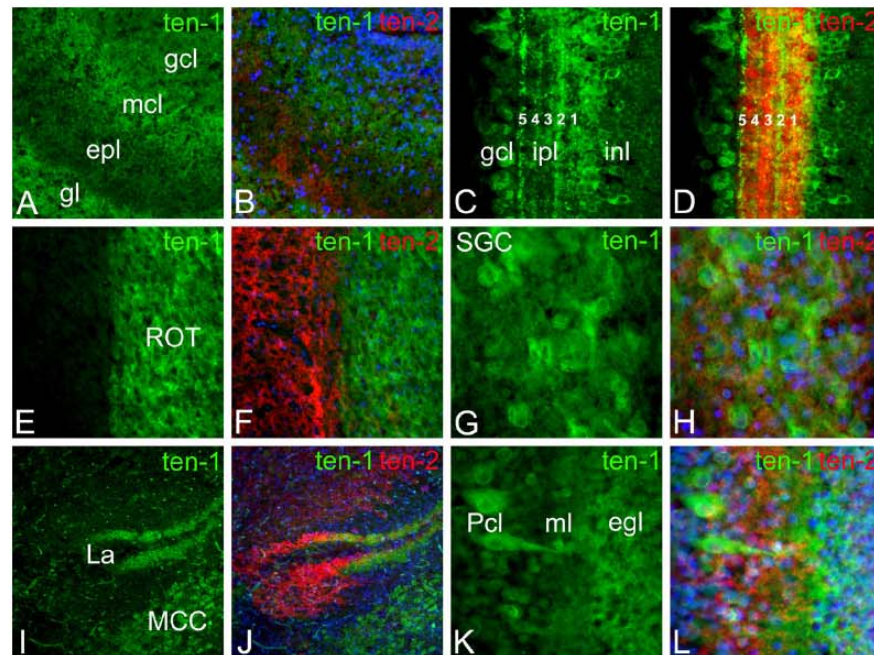


Figure 2
Teneurin-1 is expressed in interconnected regions of the brain and is complementary to teneurin-2 expression.
 Immunostaining of teneurin-1 and teneurin-2 in E17 brain. Green, teneurin-1; red, teneurin-2, blue (Hoechst), nuclei. In the olfactory bulb (A, B) the teneurin-1 antibody labels the mitral cell layer (mcl) and the glomerular layer. The external plexiform layer (epi) is positive for teneurin-2. In the temporal retina (C, D) subsets of neurons within the ganglion cell layer (gcl) and inner portion of the internal nuclear layer (inl) are positive for teneurin-1, as are laminae 2 and 5 within the inner plexiform layer (ipl). Teneurin-2 immunoreactivity is concentrated in laminae 1 and 3 of the ipl. The nucleus rotundus (E, ROT) is intensely labelled with teneurin-1 antibody, but not with anti-teneurin-2 (F). In the optic tectum (G, H) large neurons in the stratum griseum centrale (SGC) are positive for teneurin-1, but not teneurin-2. In the hindbrain (I, J), the nucleus laminaris (La) and nucleus mesencephalicus profundus (MCP) are labelled with the teneurin-1 antibody. Teneurin-1 and teneurin-2 immunoreactivity are found in distinctive dendritic fields within the La. In the cerebellum (K, L) teneurin-1 is found in Purkinje cells (Pcl) and in the molecular layer (ml) adjacent to the external granular layer (egl). In contrast, the anti-teneurin-2 labels the internal portion of the ml.

cells near the developing inner plexiform layer, which may be amacrine cells. Here we were able to compare the distribution of teneurin-1 and teneurin-2 by superimposing the patterns of expression found on adjacent frozen sections stained with antisera specific for each protein. In each region examined, there was very little overlap in the expression of the two proteins. For example, in the olfactory bulb teneurin-2 immunoreactivity was seen in the external plexiform layer sandwiched between the layers of teneurin-1 expression (Fig. 2B). In the retina both teneurin-1 and teneurin-2 were found in the inner plexiform layer, but they are concentrated in different laminae: teneurin-1 is found primarily in laminae 2 and 5, while teneurin-2 is most prominently expressed in laminae 1 and 3 (Fig. 2D). In the thalamus teneurin-2 immunoreactivity

was seen in the pretectal region and was completely excluded from the adjacent rotund nucleus (Fig. 2F). In the optic tectum anti-teneurin-2 immunolabelled puncta surrounding the large neurons of the stratum griseum centrale, but did not label the neuronal cell bodies themselves (Fig. 2H). The complementary expression of the two teneurins was particularly evident in the nucleus laminaris, where teneurin-2 immunoreactivity was seen in the thick dendritic field of the internal portion of the lamina and teneurin-1 was found in the thinner external portion (Fig. 2I). Finally, while teneurin-1 and teneurin-2 are both found in the molecular layer of the developing cerebellum, teneurin-1 was found in the younger, external portion of this layer whereas teneurin-2 was found in the more mature, internal portion (Fig. 2L). A summary of

teneurin-1 and -2 expression in the developing chick brain is provided in Table 1.

Nuclear localization of the intracellular domain *in situ*

Antibodies detecting the ICD (anti-ICD) or the ECD (anti-EGF and anti-ECD, see Fig. 3A) of teneurin-1 were used to detect teneurin-1 expression in brain homogenates harvested from chicken embryos.

The ICD antibody was used to determine if the ICD of teneurin-1 can be detected in the nucleus *in situ* with immunohistochemistry. We found nuclear teneurin-1 ICD in a few regions of the developing brain. One region where the majority of neurons expressing teneurin-1 showed

nuclear localization with the anti-ICD was the E17 piriform cortex (Fig. 3B, C). Here the anti-ICD stained fine puncta within nuclei as determined by co-staining with the Hoechst nuclear stain. The same fine puncta were labelled in the nuclei of neurons within the retinal ganglion cell layer at E12 (Fig. 3D, E). However, unlike the labelling of the piriform cortex the labelling pattern within the retinal ganglion cell layer was diverse: the nuclei of some cells are labelled (arrow, Fig. 3E), in some cells only the cytoplasm or cell membrane was labelled (arrowhead, Fig. 3E), and other cells were completely unlabelled (asterisks, Fig. 3E). All of these cells were identified as neurons by double labelling with the neuronal marker TuJ1 (not shown). The appearance of the ICD of teneurin-1 in the nuclei of retinal neurons is temporally and spatially regulated, as nuclear localization in the retinal ganglion cell layer was not observed at E7 or E17 (not shown), nor was it observed in neurons in the inner nuclear layer at any of the time points used in this study. The most dramatic examples of nuclear localization of the ICD of teneurin-1 were seen in non-neuronal tissues. In patches of head mesenchyme of E7 and E12 embryos the anti-ICD labelled the nuclei of fibroblasts intensely (Fig. 3H, I), in contrast to the antibody raised against the EGF-like repeats found in the ECD (Fig. 3F, G). The nuclear staining was specific, as it was abolished by preabsorbing the antibody with the ICD-peptide (not shown). Note that these two antibodies (anti-ICD and anti-EGF) stained the same regions of the fore, mid and hindbrain identically except for the occasional staining of some cell nuclei by the former and not the latter. Also, the anti-ICD stained some endothelial cells and the anti-EGF did not (e.g., note the endothelial cell labelling in Fig. 2I, which was stained with anti-ICD).

Teneurin-1 appears to be proteolytically processed

Western blot analysis using the ICD antibody showed a prominent band at 65 kDa (Fig. 4A, arrowhead), which is much smaller than expected for the full length protein (> 300 kDa). The specificity was confirmed by competition with the ICD peptide which completely abrogates detection of this band (not shown). However, 65 kDa is larger than we would expect for the teneurin-1 ICD, because an N-terminal fragment containing the amino acids up to the transmembrane domain (ICD construct) migrates at 45 kDa [21]. Therefore, this fragment may still contain the transmembrane domain. Such an N-terminal fragment would be expected to occur after ectodomain shedding (Fig. 4C, cleavage 1). The full-length protein was barely detectable (Fig. 4A, arrow), indicating that ectodomain shedding may take place constitutively. The faint bands observed below the 65 kDa band (Fig. 4A, asterisks) at approximately 50 and 35 kDa might be the released ICD generated after the second cleavage (Fig. 4C, cleavage 2), which occurs only in a specific subset of cells. These data

Table 1: The expression of teneurin-1 and teneurin-2 in the E17 avian central nervous system

Region	Teneurin-1 Intensity*	Teneurin-2 Intensity
Olfactory bulb: Glomerular layer	++	-
Olfactory bulb: External plexiform layer	-	+
Hippocampus	+/-	+++
Hyperstriatum accessorium	-	++
Hyperstriatum ventrale	-	++
Nucleus septalis lateralis	-	++
Nucleus taeniae	-	++
Posteromedial cortex piriformis	+/-	+++
Nucleus dorsolateral anterior thalami	-	++
Nucleus geniculatus lateralis	-	++
Nucleus pretectalis	-	++
Nucleus rotundus	+++	-
Nucleus spiriformis	-	++
Nucleus triangularis	-	++
Retina: Ganglion cell layer	+/-	-
Retina: Inner plexiform layer 5	+	-
Retina: Inner plexiform layer 4	-	+/-
Retina: Inner plexiform layer 3	-	++
Retina: Inner plexiform layer 2	+	-
Retina: Inner plexiform layer 1	-	+
Retina: Inner nuclear layer	+/-	-
Retina: Outer plexiform layer	-	+/-
Nucleus isthmi, pars magnocellularis	-	++
Nucleus isthmi, pars parvocellularis	-	++
Nucleus isthmo-opticus	-	++
Nucleus lentiformis mesencephali	-	++
Nucleus of Edinger-Westphal	-	++
Stratum griseum centrale	++	-
Stratum griseum et fibrosum superficiale	+/-	+
Stratum griseum periventriculare	-	+
Nucleus laminaris	++	+/-
Nucleus magnocellularis	++	-
Cerebellum: Molecular layer	+/-	+/-
Cerebellum: Purkinje cell layer	+	-
Cerebellum: Granule cell layer	-	+/-

*+ + +, intense signal, visible at low magnification; ++, strong signal, visible at intermediate magnification; +, weak signal, visible at high magnification; +/-, weak and sometimes missing; -, no signal

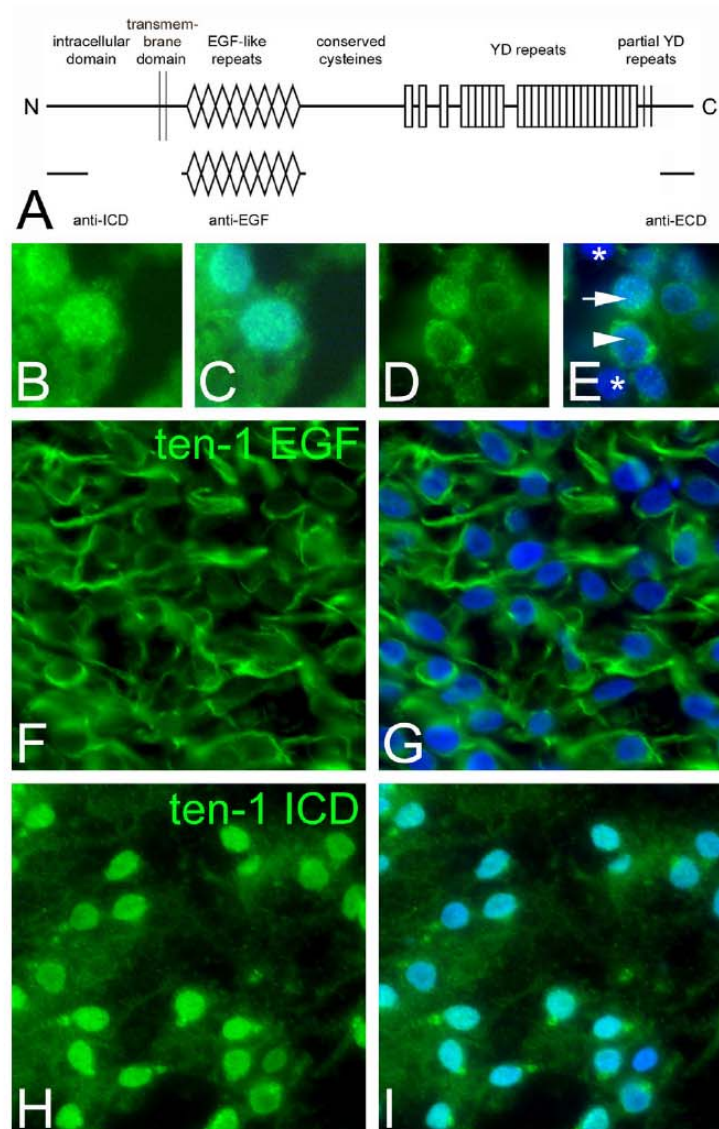


Figure 3
Nuclear teneurin-1 intracellular domain is observed in subsets of neurons and in specific tissues. Schematic diagram of teneurin domain architecture and antibodies used in this study (A). Comparison of immunostaining with antibodies to the extracellular and intracellular domains in sections and in vitro (B to I). Neurons of the piriform cortex at E17 (B, C) and neurons found in the retinal ganglion cell layer at E12 (D, E) stained with anti-ICD. The anti-ICD labels nuclei in the piriform cortex and labels a subset of retinal ganglion cells (arrow), but other TuJ1-positive neurons (label not shown) in the retinal ganglion cell layer are labeled with anti-ICD teneurin-1 but do not exhibit nuclear staining (arrowhead). There are also TuJ1-positive neurons in the retinal ganglion cell layer that are negative for teneurin-1 (asterisk). Head mesenchyme at E7 stained with anti-EGF (F, G) and anti-ICD (H, I). In the head mesenchyme, the anti-ICD labels the nucleus of most cells, whereas the anti-EGF exhibits cell-surface staining. Green, teneurin-1; blue (Hoechst), nuclei.

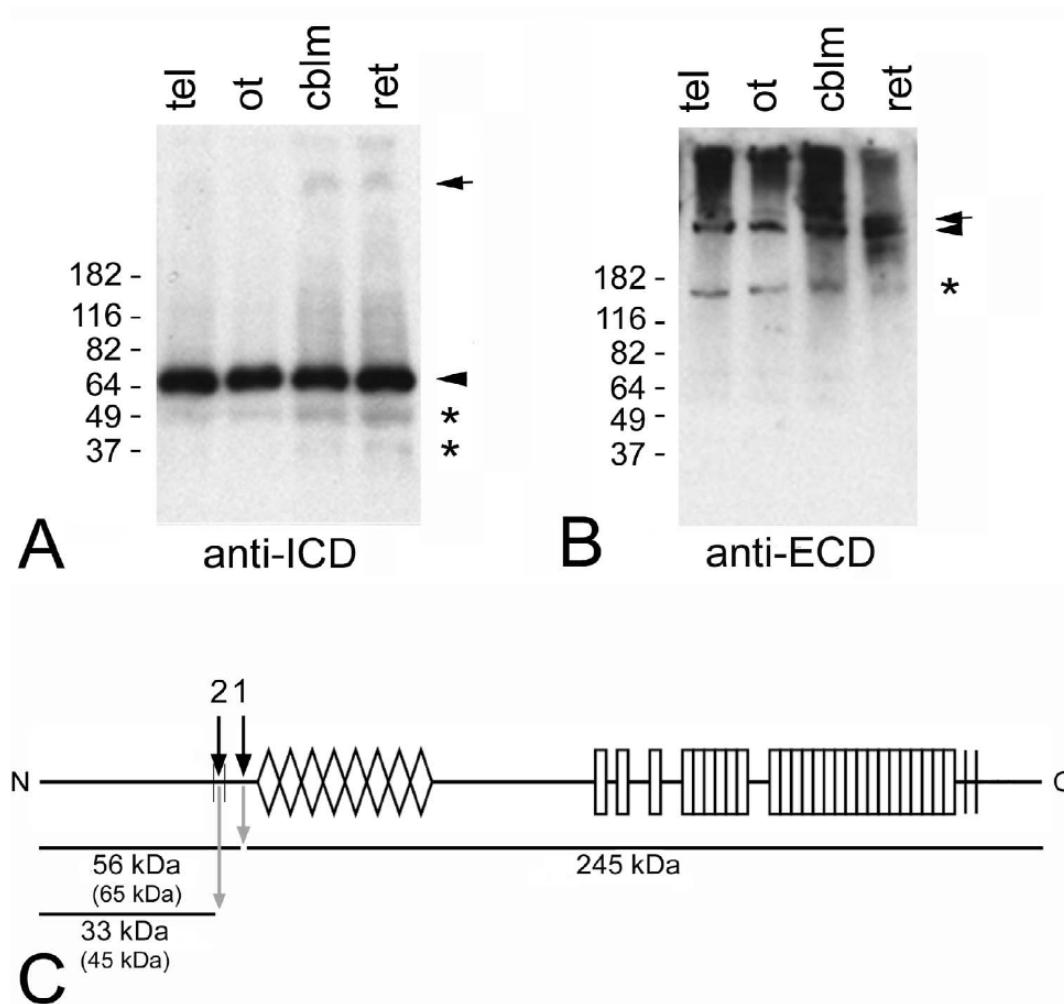


Figure 4
Teneurin-1 appears to be processed in the developing chicken brain. Western blot analysis of embryonic chicken brain lysates. Detection of endogenous teneurin-1 using anti-ICD (A) and anti-ECD antibodies (B). The numbers to the left indicate the positions of molecular weight standards. The anti-ICD detects a prominent N-terminal fragment at 65 kDa (arrowhead), which is much smaller than expected for the full-length protein (arrow), suggesting proteolytic processing. In contrast, using the anti-ECD antibody results in detection of the full-length protein (arrow) and a large C-terminal fragment (arrowhead). Asterisks label additional processing products (see text for details). Postulated cleavage sites and calculated molecular weights of processing products (C). Postulated cleavage sites: 1 = ectodomain shedding, 2 = intramembrane cleavage releasing the ICD. The sizes indicated are predicted from the amino acid sequence; known apparent molecular weights are shown in parentheses (see text for details). The calculated molecular weights are approximate, as the exact cleavage sites are not known.

suggest that proteolytic processing of the full-length protein takes place *in vivo*, resulting in N-terminal fragments. When the same extracts were analyzed using an antibody detecting the ECD (Fig. 4B), a faint band > 250 kDa (arrow) and a stronger band around 250 kDa (arrow-head) are observed. Since the predicted molecular weight of full-length teneurins is more than 300 kDa, the upper band may represent the full-length protein, and the lower band could correspond to the ECD after shedding, which has a predicted molecular weight of 245 kDa (Fig. 4C). The smear above these bands can be explained by glycosylation of the extracellular part of the protein [7]. The band at 150 kDa (Fig. 4B, asterisk) could be a further cleaved extracellular fragment of teneurin-1. In Figure 4C the postulated cleavage sites and the resulting fragments are summarized. Note that the molecular weights are either calculated based on the amino sequences or based on observations (shown in parentheses). The ICD has a higher apparent molecular weight than predicted, therefore we expect the same to be the case for the 65 kDa N-terminal fragment, for which the predicted molecular weight would only be 56 kDa (Fig. 4C).

Identification of a nuclear localization signal

The ICD of teneurin-1 contains the amino acid sequence arginine-lysine-arginine-lysine at position 62 to 65 from the N-terminus. This resembles a classical nuclear localization signal (NLS), which directs the nuclear import of proteins. This putative NLS is conserved in chicken, mouse and human teneurin-1. To test whether it is functional, the four basic amino acids were replaced by alanines in the construct named NLS-mut (Fig. 5A). COS-7 cells were transfected either with a construct encoding the ICD of teneurin-1 (ICD-wt) or the NLS-mut construct. Western blot analysis of cytoplasmic and nuclear extracts of the transfected cells showed decreased nuclear accumulation of the NLS-mut construct compared to the ICD-wt construct (Fig. 5B). Quantification of the nuclear-to-cytoplasmic ratio showed that ICD-wt accumulates in the nucleus, which is not the case for NLS-mut (Fig. 5C). The ICD-wt protein is detected in the nucleus by immunofluorescence (Fig. 5D, E). However, nuclear localization of the ICD was abolished if the NLS is mutated (Fig. 5F, G). More than 80% of the cells expressing the wt-construct exhibited nuclear staining, whereas this was only observed in 20% of the cells expressing the NLS-mut version (Fig. 5H). In addition to the strongly decreased nuclear localization, these cells also exhibited a more pronounced localization of the teneurin-1 ICD to the cell membrane and cell processes.

Discussion

In this work we analyzed the expression of teneurin-1 in the chicken embryo by *in situ* hybridization and immunohistochemistry, focusing on the developing nervous

system. Using an antibody recognizing the N-terminus of teneurin-1 we demonstrated for the first time the nuclear localization of a teneurin ICD in a developing vertebrate. This finding was supported by western-blot analysis of endogenous teneurin-1 and can be explained by the fact that the ICD contains a functional NLS. Thus, teneurin-1 is a transmembrane protein that can be processed to deliver a signal to the nucleus with the potential to alter gene expression.

Teneurin-1 expression suggests a role in the establishment of neuronal connectivity

Teneurin-1 has a distinctive temporal-spatial expression pattern in the developing nervous system that includes interconnected regions in the brain. For example, in the tectofugal pathway of the avian visual system, retinal ganglion cells project to neurons in the stratum griseum centrale of the optic tectum, which in turn, project to the nucleus rotundus. Teneurin-1 is expressed prominently by each component of this pathway. However, teneurin-1 expression is not limited to the visual system, but is also present in other parts of the brain. In the olfactory pathway, teneurin-1 is expressed both in the olfactory bulb and the piriform cortex, which receives input from mitral/tufted cells of the olfactory bulb and is involved in processing of odor information. Teneurin-1 mRNA and immunostaining were also present in nuclei processing auditory information such as the nucleus laminaris and the nucleus magnocellularis. In previous studies of teneurin-1 expression, which relied on low resolution *in situ* hybridization techniques, the expression of teneurin-1 outside the avian visual system was not observed [7,8]. The broader expression reported here is in line with studies in mice, where teneurin-1 has been reported to be expressed in specific parts of the cortex [13] as well as the hippocampus and cerebellum [22,12]. In both mouse and chicken, a common feature is the expression of teneurin-1 by interconnected neurons (see review [5]).

One of the most interesting features of teneurins is the complementarity of their expression patterns. A previous study [16] reported the presence of teneurin-2 in the thalamofugal visual pathway; here we confirmed the expression of teneurin-1 in the tectofugal visual pathway. This complementarity is again not limited to the visual system, but appears also in the olfactory bulb and in the nucleus laminaris and nucleus magnocellularis. The most intriguing complementary pattern was found in the inner plexiform layer in the retina, which is subdivided in five laminae. There, axons of the amacrine and bipolar cells meet the dendrites of retinal ganglion cells. Because most of these nerve terminals are confined to distinct laminae, it is thought that lamination is a major determinant of synaptic specificity in the retina. Teneurin-1 and teneurin-2 were found in distinct, non-overlapping laminae, sug-

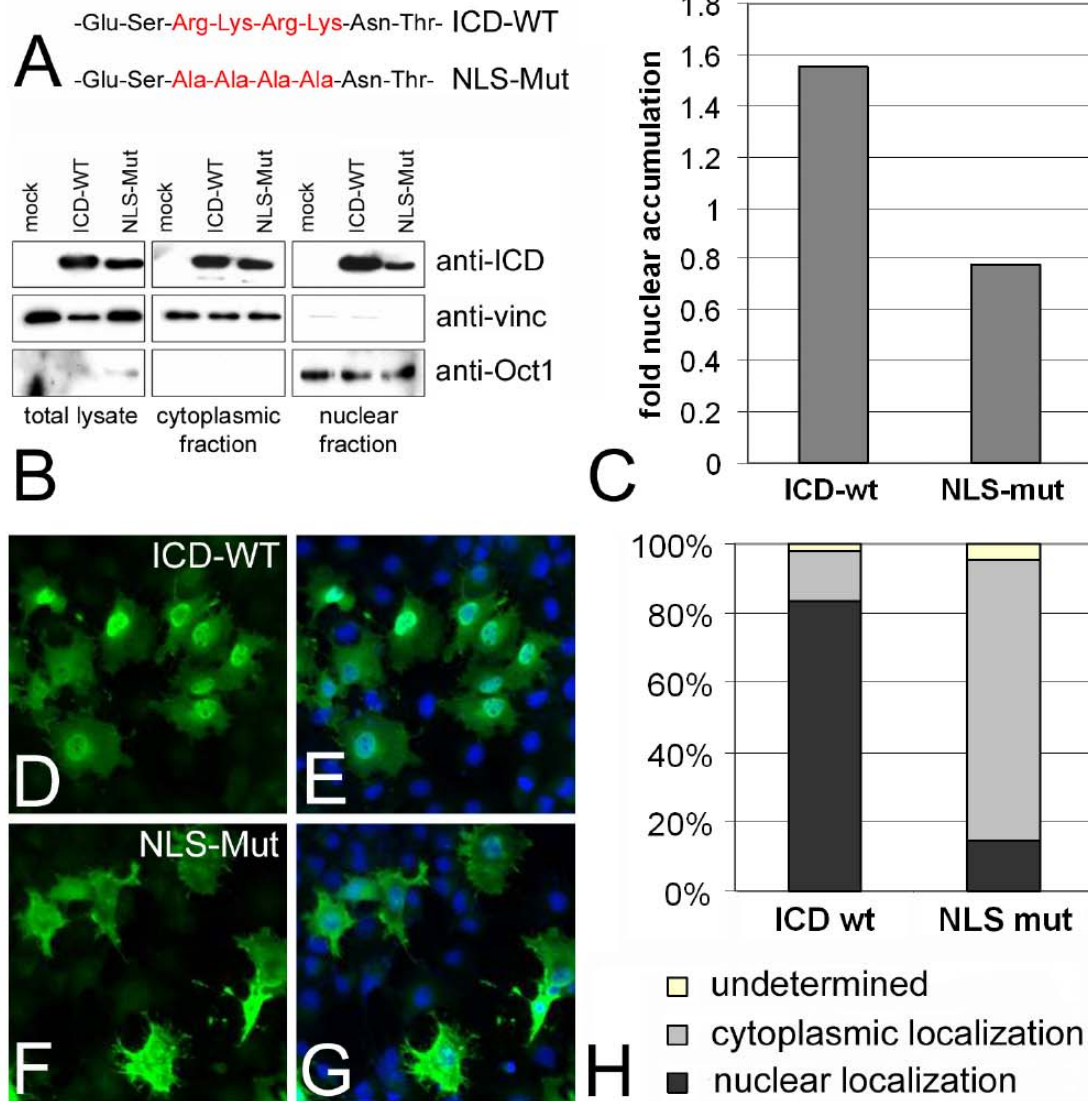


Figure 5
The teneurin-1 intracellular domain contains a nuclear localization signal. The amino acid sequence representing a putative nuclear localization signal (NLS) which was mutagenized to alanines (A). Western blot analysis of total lysates, cytoplasmic and nuclear fractions of COS-7 cells mock transfected, transfected with wild type ICD (ICD-WT) or transfected with the mutated NLS (NLS-Mut) constructs (B). Blots were probed with the anti-ICD, an antibody to the cytoplasmic protein vinculin, or an antibody to the nuclear protein Oct-1. Western blot quantification and calculation of the nuclear-to-cytoplasmic ICD ratio (C). Immunofluorescence staining of transfected COS-7 cells (D-G) and quantification of nuclear localization by cell counting (H). Both western blot analysis and immunofluorescence show that the overexpressed wild-type ICD is localized in the nucleus, whereas the NLS-Mut construct is predominantly found in the cytoplasm.

gesting that they are expressed by distinctive subpopulations of neurons. Other examples of molecules present in distinct sublaminae of the retina were reported by Yamagata et al., including the adhesive proteins sidekick-1 and -2 [23]. Retinal ganglion cells expressing sidekick-1 or -2 preferentially arborize in sidekick-1 or -2 positive sublaminae, and ectopic expression of each sidekick directs dendrites to sublaminae where the corresponding sidekick is present [24]. These observations suggest roles for each of the teneurins in the development of different neuronal pathways. The current study also provides evidence that a given neuron may switch teneurin expression as development proceeds. In the cerebellum, for example, teneurin-1 immunoreactivity is seen in the axons of granule cells adjacent to the external granular layer, whereas teneurin-2 immunoreactivity is seen in the axons of the older granule cells near the perikarya of Purkinje cells.

Based on its expression pattern we suggest a role for teneurins in the establishment of appropriate connectivity in the developing brain. This task is preformed in several steps, including the generation of appropriate neuronal cell types, migration of neurons to specific nuclei or laminae, growth of axons to target areas, and the formation and maintenance of synapses within the target [25-27]. Recent evidence suggests that the same molecules can be involved in several of these steps [28]. Currently there is no knowledge about a possible role of teneurins in defining neuronal precursor subpopulations, but there are some data indicating that teneurins are involved in the outgrowth and migration of axons. For example, teneurins promote neurite outgrowth *in vitro*, and recently published *in vivo* data show that the cell bodies of neurons expressing teneurin-3 (*tenm_3*) tend to cluster, their processes are intertwined, and have increased neurite outgrowth [18].

In 1963, Roger Sperry formulated his chemoaffinity hypothesis, according to which growing axons carry biochemical "tags" which allow them to find their appropriate target region [29]. In the meantime, many molecules that act in such a manner have been discovered; the best known example is the cadherin superfamily. Cadherins not only act as cell adhesion molecules through homophilic interactions mediated by their ECD, but are also involved in signal transduction through their ICDs. Many cadherins are also expressed in very restricted regions in the brain indicating a role in establishment of neuronal connections [30,31]. The observation that teneurins can mediate homophilic and heterophilic interactions suggests that they might function in a similar way to cadherins [19].

Regarding the complexity of the vertebrate brain, it is unlikely that only a few molecules govern compartmen-

talization and wiring in the developing brain. More probably, concerted action of many different genes is required, and it will be a challenge to define the exact role of teneurins within this genetic network. To date, very little is known about the factors which regulate teneurin expression and how the teneurins function. For further analysis of the role of teneurins in brain development, it will be crucial to manipulate the expression or function of teneurins *in vivo*.

Teneurins appear to be processed *in vivo*, possibly by regulated intramembrane proteolysis

At specific sites we observed nuclear staining with the antibody to the ICD of teneurin-1. These sites, both neuronal and non-neuronal, were subsets of the regions where teneurin-1 was expressed. This was confirmed with *in situ* hybridization and with antibodies to the ECD of teneurin-1. Western blot analysis confirmed the presence of N-terminal fragments of teneurin-1. Additionally, the ICD was found to contain a conserved NLS, which we demonstrated was functional in cultured cells.

Regulated intramembrane proteolysis (RIP) may provide an explanation for the detection of a transmembrane protein like teneurin-1 in the nucleus. There is only a limited set of known intramembrane proteases, all of which exhibit specificity for either Type-I (presenilin, rhomboid) or Type-II (site-2 protease, signal peptide peptidase) transmembrane proteins. Therefore, only the latter two are possible candidates for teneurin processing, including the recently identified SPP-like proteases [32]. Site-2 protease was the first intramembrane protease discovered, releasing the transcription factor SREBP from the ER-membrane in response to sterol depletion [33]. In addition, it has been shown to cleave ATF6, another transcription factor, in response to ER stress [34]. The expression pattern of SPP studied in adult mice partially overlaps with teneurin expression in distinct brain regions [35]. No data are available of SPP-like proteases in vertebrates, but a study in *C. elegans* suggests an important role in development [36]. Presenilin is the most studied intramembrane protease, responsible for the cleavage of Notch [37-39], APP [40,41] and other substrates, including some cadherins and ephrins. Most C-terminal fragments resulting from presenilin processing exhibit signaling activity and many of them localize to the nucleus, where they regulate transcription [42]. However, since presenilin only cuts type-I transmembrane proteins, it is not a candidate protease for teneurin processing.

Western blot analysis showed a prominent band at about 65 kDa using the ICD-antibody, which is larger than the predicted size of the ICD. A common feature of RIP is that a cleavage on the extracellular side has to occur first, resulting in the release of the ECD, before the remainder

of the protein can be a substrate for intramembrane cleavage. Therefore, this band most likely represents teneurin-1 after ectodomain shedding, which then, depending on the cellular context, is further processed to result in a soluble ICD (i.e., the faint smaller bands observed on the immunoblot). This fits with the observation that the 65 kDa band is very abundant in brain lysates, but nuclear ICD is observed in only few cells.

Based on the presence of nuclear ICD in mesenchyme as well as in a restricted subset of neurons, we can not draw a conclusion regarding a general biological function of teneurin processing during development. The occurrence of the nuclear ICD in such different cells and tissues implies a cell-type- or tissue-specific role for teneurin-1 intracellular signalling. This was particularly striking in the retina where we observed retinal ganglion cells negative for teneurin-1 and teneurin-1-positive cells with and without the nuclear ICD next to each other. One example of how to further address the biological relevance of these observations is provided by the elegant studies of Notch processing in genetically engineered mice. Replacement of the Notch ICD with Cre recombinase permitted the identification of cells in which Notch is cleaved, since the released Cre induces β -gal expression and labels specifically these cells [43].

Future work will have to be dedicated to finding the proteases responsible for teneurin processing and the elucidation of the function of the teneurin-1 ICD in the nucleus. Since this cleavage occurs only in subsets of cells at specific time points during development, it will be interesting to know if homophilic interactions or interactions with a yet to be identified ligand triggers the cleavage of the ICD.

Conclusion

In this study we show that teneurin-1 is expressed in interconnected regions of the developing chick brain, and its expression pattern is complementary to teneurin-2. We present the first evidence of teneurin processing in vertebrates and demonstrate that the ICD of teneurin-1 contains a functional NLS. Our results provide support for the hypothesis that teneurins can be proteolytically processed to generate a soluble ICD that translocates to the nucleus (Fig. 6).

Methods

In situ hybridization

Chicken embryos were sacrificed at different developmental stages and fixed in cold 4% paraformaldehyde in phosphate buffered saline (PBS) for a few hours or overnight, depending on the age. For E17, brain and eyes were dissected out, otherwise whole embryos or heads were used. Tissues were cryoprotected in 25% sucrose overnight before embedding in OCT Tissue-Tek (Sakura). Horizon-

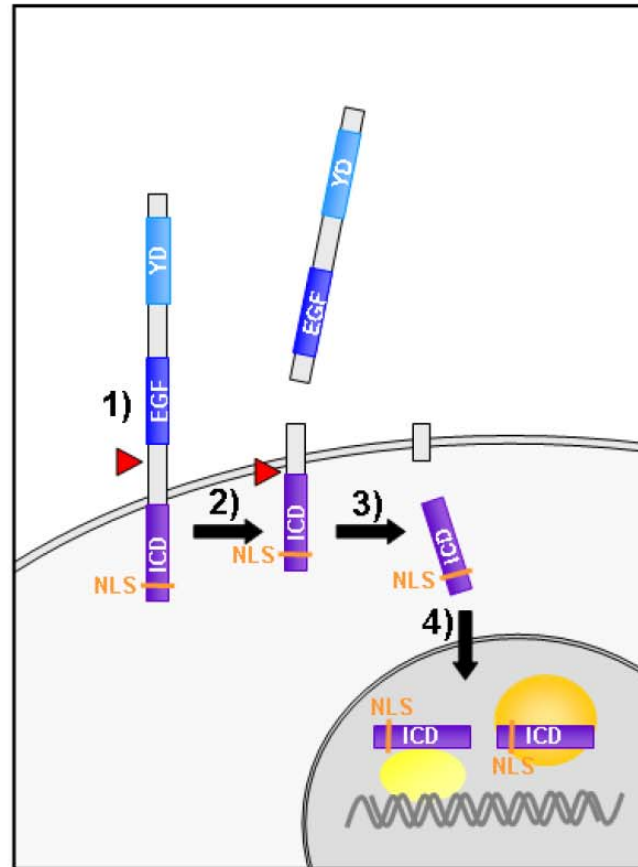
tal, sagittal and transversal sections were cut on a Microm cryostat, mounted on Superfrost slides (Menzel-Gläser), dried and stored at -80°C . The probe was synthesized by *in vitro* transcription of a chicken teneurin-1 EcoRI-XbaI fragment corresponding to 628 bp within the ICD cloned into pSPT18 using the Roche DIG RNA labeling kit. *In situ* hybridization was performed on a Ventana automatic staining module and the Ventana RiboMap and BlueMap kits. The *in situ* hybridization protocol included pre-fixation, cell conditioning and protease pretreatment. Probe was allowed to hybridize for 6 h at 65°C followed by three washes with increasing stringency ($1 \times \text{SSC}$, $0.5 \times \text{SSC}$ and $0.1 \times \text{SSC}$ at 65°C , respectively). After post-fixation, the probe was detected with anti-DIG (Roche) for 32 min and the slides were incubated with AP-substrate for 6 h. Antisense and sense controls were always performed in parallel.

Immunohistochemistry

Cryosections of chicken embryos at various embryonic stages were prepared as outlined above. Sections were hydrated in PBS, blocked with 0.5% BSA and incubated overnight in appropriately diluted primary antibody. Primary antibodies included rabbit polyclonal antisera raised against recombinant proteins corresponding to: 1) the 160 N-terminal amino acids of the ICD of chicken teneurin-1 (anti-ICD, [21]); the 300 C-terminal amino acids of the extracellular domain of chicken teneurin-1 (anti-ECD, [21]); 3) a fusion of the N-terminus of tenascin-C (for protein purification purposes) and the 8 EGF-like domains of chicken teneurin-1 (anti-EGF; see Fig. 3A for a summary of the teneurin-1 antisera). The latter antiserum was preabsorbed against purified tenascin-C prior to use to eliminate background. A previously described antiserum to chicken teneurin-2 [8] and a commercially available neuronal marker (the mouse monoclonal antibody TuJ1; Sigma) were also used. After incubation overnight in primary antibody the sections were rinsed in PBS, blocked again in PBS/BSA, and incubated for 2 hr in Alexa-tagged anti-rabbit or anti-mouse secondary antibodies (Invitrogen). For controls, adjacent sections were incubated in either diluted preimmune serum, with secondary antibody alone or the primary antibody blocked with the antigenic peptide. In all cases the control sections were unstained. Sections were viewed using Nikon Optiphot and a Zeiss Axiophot photomicroscopes with epi-illumination.

Cloning of constructs, cell culture and transfection

The teneurin-1 ICD missing the NLS was produced by two-step PCR from pCEP-ten1 ICD. Primers containing codons for alanines instead of arginines and lysines were used to introduce the mutation. The second PCR product was cloned into pCEP using NotI and XbaI. Primers used for mutagenesis were pCEP fw:

**Figure 6**

Model of teneurin signalling. This model describes how an intracellular domain (ICD) could be generated from a transmembrane protein and transported to the nucleus. This process takes place only in specific cells and tissues where the anti-ICD labeled nuclei. 1) A first protease sheds the extracellular domain (ECD) of teneurins. 2) The remainder of teneurin-1 can now become a substrate for an intramembrane protease. 3) The ICD is released. 4) The soluble ICD translocates to the nucleus via nuclear localization signal (NLS). *EGF*, *EGF-like repeats*; *YD*, *YD-repeats*. Red arrows indicate postulated cleavage sites and the yellow spheres proteins interacting with teneurin-1 ICD in the nucleus.

5'AGAGCTCGTTT'AGTGAACCT3', Ten1 NLS fw:
 5'TACAACAGTCAAAGCGCGGCGGCGGAATACTGA
 CCAATCC3', Ten1 NLS rev:
 5'GGATTGGTCACTATTCGCCGCGCGCGCTTTGACT'
 GTTGTAA3' and EBV rev: 5'GTGGTTTGTCCAAACTCATC3'.

To generate a fusion protein containing the tenascin-C N-terminus for secretion and the teneurin-1 EGF-like repeats for antibody-generation, two step PCR was performed using the following primers: KS:5' CGAGTCCGACGGTATCG3', TNC/EGF fw

5'AAAGGCCCCACCTGCCTTGTITGGTTTAACTGG3'
 , TNC/EGF rev:
 5'CCAGGTAAACCAAACAAGGAGCAGTTGGGGCCCTT'
 3' and EGF-His-Xho-rev:
 5'ACTACTCGAGTTAGTGGTGGTGGTGGTGCATTTT
 CATGACAACGTT3'. The PCR fragment was cloned using HindIII and XhoI into pCEP. This recombinant protein was expressed in 293T EBNA-cells and purified using the C-terminal HIS-tag to immunize rabbits. To remove tenascin-C immunoreactivity of the resulting antiserum, it was purified on a tenascin-C column.

COS-7 cells were maintained in DMEM containing 10% FCS. For transfection, the FUGENE reagent (Roche) was used according to the manufacturer's protocol. The cells were harvested 24 h after transfection for analysis.

Immunocytochemistry following transfection

24 h after transfection, the cells were fixed for 10 min with 4% paraformaldehyde, permeabilized with 1% Triton-X, blocked with BSA for 15 min, and stained with anti-ICD (1:300) or anti-Flag (1:1000). Secondary antibodies coupled with FITC from Alexa were used, and the nuclei were counterstained with Hoechst dye. Images were acquired on a Z1 fluorescence microscope. The 40× objective was used to obtain images showing the localization of the teneurin-1 ICD in detail. Low-magnification pictures were used for quantification by counting cells and classifying them as nuclear, cytoplasmic or undetermined localization of the ICD. The experiment was repeated three times, capturing five random images per transfection each time. All transfected cells on the images were counted: 492 for the ICD- wt construct and 420 for the NLS-mut construct. Nuclear staining was classified when the staining intensity was higher in the nucleus than in the cytoplasm, otherwise the cells were scored as cytoplasmic. The scoring was performed by an independent person who was not aware of which images were from ICD-wt or NLS-mut transfections. Cells were classified as undetermined if they were dividing, or if the staining intensity was too bright to determine if it is nuclear or cytoplasmic.

Western blot analysis

The specificity of the teneurin-1 and -2 antibodies was confirmed by detection of teneurin-1 and -2 in transfected cells. Chicken embryos at E17 were sacrificed and tissues were dissected out and frozen in liquid nitrogen. After grinding with a mortar and pestle, the powder was dissolved in RIPA buffer. Sample buffer containing β -mercaptoethanol was added and the lysate was heated at 95°C before loading on a 4–12% gradient gel (BioRad) for SDS-PAGE. The Benchmark prestained protein ladder and HiMark prestained protein standards (both from Invitrogen) were used to determine the size of the bands. Transfer to an immobilon membrane was performed at 45 V per gel for 2 h. For detection, both rabbit polyclonal antibodies anti-ICD and anti-ECD were used at a dilution of 1:1000.

To analyze COS-7 cell lysates, culture medium was removed and the cells were washed with PBS. For the total lysate, cells were lysed in sample buffer containing β -mercaptoethanol directly. The cytoplasmic and nuclear extract was prepared using the NuCLEAR kit from Sigma following the manufacturer's instructions. SDS-PAGE was performed on 12.5% gels, and the proteins transferred for 1 h at 45 V per gel. The transfected ICD was detected with an

anti-ICD or anti-Flag antibody diluted 1:1000. Anti-vinculin (hvin1, Sigma, 1:1000) served as a cytoplasmic marker and oct-1 (Santa Cruz, 1:1000) as a nuclear marker. SuperSignal (Pierce) was used for detection of horseradish-peroxidase coupled secondary antibody, which was used at 1:10,000. Chemiluminescence detection films were exposed and developed, and the results were scanned for image processing. Quantification of the western blot was performed using ImageJ 1.33 [44]. The intensity of the entire bands was measured, and the background was subtracted. The nuclear-to-cytoplasmic ratio was calculated by dividing the nuclear intensity by the cytoplasmic intensity, which indicates nuclear accumulation of the ICD.

Authors' contributions

DK carried out the in situ hybridization, western blot analysis and cell culture experiments and prepared the first draft of the manuscript. RC participated in planning and discussing the experiments and helped to write the manuscript. NL and RPT performed the immunohistochemistry, and RPT participated in writing the manuscript and preparing the figures. All authors read and approved the final manuscript.

Acknowledgements

This work was supported by the Novartis Research Foundation, the National Science Foundation (0235711) and the National Institutes of Health (NCRR C06 RR-12088-01). We thank Marianne Brown-Luedi for her help with the production of the EGF-antibody.

References

- Baumgartner S, Chiquet-Ehrismann R: **Tena**, a *Drosophila* gene related to tenascin, shows selective transcript localization. *Mechanisms of development* 1993, **40**(3):165-176.
- Baumgartner S, Martin D, Hagios C, Chiquet-Ehrismann R: **Tenm**, a *Drosophila* gene related to tenascin, is a new pair-rule gene. *Embo J* 1994, **13**(16):3728-3740.
- Levine A, Bashan-Ahrend A, Budai-Hadrian O, Gartenberg D, Menasherov S, Wides R: **Odd Oz**: a novel *Drosophila* pair rule gene. *Cell* 1994, **77**(4):587-598.
- Tucker RP, Kenzelmann D, Trzebiatowska A, Chiquet-Ehrismann R: **Teneurins: transmembrane proteins with fundamental roles in development**. *The international journal of biochemistry & cell biology* 2007, **39**(2):292-297.
- Tucker RP, Chiquet-Ehrismann R: **Teneurins: a conserved family of transmembrane proteins involved in intercellular signaling during development**. *Developmental biology* 2006, **290**(2):237-245.
- Minet AD, Chiquet-Ehrismann R: **Phylogenetic analysis of teneurin genes and comparison to the rearrangement hot spot elements of E. coli**. *Gene* 2000, **257**(1):87-97.
- Minet AD, Rubin BP, Tucker RP, Baumgartner S, Chiquet-Ehrismann R: **Teneurin-1, a vertebrate homologue of the Drosophila pair-rule gene ten-m, is a neuronal protein with a novel type of heparin-binding domain**. *Journal of cell science* 1999, **112** (Pt 12):2019-2032.
- Rubin BP, Tucker RP, Martin D, Chiquet-Ehrismann R: **Teneurins: a novel family of neuronal cell surface proteins in vertebrates, homologous to the Drosophila pair-rule gene product Tenm**. *Developmental biology* 1999, **216**(1):195-209.
- Otaki JM, Firestein S: **Neurestin: putative transmembrane molecule implicated in neuronal development**. *Developmental biology* 1999, **212**(1):165-181.

10. Otaki JM, Firestein S: **Segregated expression of neurestin in the developing olfactory bulb.** *Neuroreport* 1999, **10**(12):2677-2680.
11. Ben-Zur T, Feige E, Motro B, Wides R: **The mammalian Odz gene family: homologs of a Drosophila pair-rule gene with expression implying distinct yet overlapping developmental roles.** *Developmental biology* 2000, **217**(1):107-120.
12. Zhou XH, Brandau O, Feng K, Oohashi T, Ninomiya Y, Rauch U, Fassler R: **The murine Ten-m/Odz genes show distinct but overlapping expression patterns during development and in adult brain.** *Gene Expr Patterns* 2003, **3**(4):397-405.
13. Li H, Bishop KM, O'Leary DD: **Potential target genes of EMX2 include Odz/Ten-M and other gene families with implications for cortical patterning.** *Molecular and cellular neurosciences* 2006, **33**(2):136-149.
14. Tucker RP, Martin D, Kos R, Chiquet-Ehrismann R: **The expression of teneurin-4 in the avian embryo.** *Mechanisms of development* 2000, **98**(1-2):187-191.
15. Tucker RP, Chiquet-Ehrismann R, Chevrion MP, Martin D, Hall RJ, Rubin BP: **Teneurin-2 is expressed in tissues that regulate limb and somite pattern formation and is induced in vitro and in situ by FGF8.** *Dev Dyn* 2001, **220**(1):27-39.
16. Rubin BP, Tucker RP, Brown-Luedi M, Martin D, Chiquet-Ehrismann R: **Teneurin 2 is expressed by the neurons of the thalamofugal visual system in situ and promotes homophilic cell-cell adhesion in vitro.** *Development (Cambridge, England)* 2002, **129**(20):4697-4705.
17. Al Chawaf A, St Amant K, Belsham D, Lovejoy DA: **Regulation of neurite growth in immortalized mouse hypothalamic neurons and rat hippocampal primary cultures by teneurin C-terminal-associated peptide-1.** *Neuroscience* 2007, **144**(4):1241-1254.
18. Leamey CA, Glendinning KA, Kreiman G, Kang ND, Wang KH, Fassler R, Sawatari A, Tonegawa S, Sur M: **Differential Gene Expression between Sensory Neocortical Areas: Potential Roles for Ten_m3 and Bcl6 in Patterning Visual and Somatosensory Pathways.** *Cereb Cortex* 2007.
19. Feng K, Zhou XH, Oohashi T, Morgelin M, Lustig A, Hirakawa S, Ninomiya Y, Engel J, Rauch U, Fassler R: **All four members of the Ten-m/Odz family of transmembrane proteins form dimers.** *The Journal of biological chemistry* 2002, **277**(29):26128-26135.
20. Bagutti C, Forro G, Ferralli J, Rubin B, Chiquet-Ehrismann R: **The intracellular domain of teneurin-2 has a nuclear function and represses zic-1-mediated transcription.** *Journal of cell science* 2003, **116**(Pt 14):2957-2966.
21. Nunes SM, Ferralli J, Choi K, Brown-Luedi M, Minet AD, Chiquet-Ehrismann R: **The intracellular domain of teneurin-1 interacts with MBD1 and CAP/ponsin resulting in subcellular codistribution and translocation to the nuclear matrix.** *Experimental cell research* 2005, **305**(1):122-132.
22. Oohashi T, Zhou XH, Feng K, Richter B, Morgelin M, Perez MT, Su WD, Chiquet-Ehrismann R, Rauch U, Fassler R: **Mouse ten-m/Odz is a new family of dimeric type II transmembrane proteins expressed in many tissues.** *The Journal of cell biology* 1999, **145**(3):563-577.
23. Yamagata M, Weiner JA, Dulac C, Roth KA, Sanes JR: **Labeled lines in the retinotectal system: markers for retinorecipient sublaminae and the retinal ganglion cell subsets that innervate them.** *Molecular and cellular neurosciences* 2006, **33**(3):296-310.
24. Yamagata M, Weiner JA, Sanes JR: **Sidekicks: synaptic adhesion molecules that promote lamina-specific connectivity in the retina.** *Cell* 2002, **110**(5):649-660.
25. McLaughlin T, O'Leary DD: **Molecular gradients and development of retinotopic maps.** *Annual review of neuroscience* 2005, **28**:327-355.
26. Harada T, Harada C, Parada LF: **Molecular regulation of visual system development: more than meets the eye.** *Genes & development* 2007, **21**(4):367-378.
27. Sur M, Rubenstein JL: **Patterning and plasticity of the cerebral cortex.** *Science* 2005, **310**(5749):805-810.
28. Charron F, Tessier-Lavigne M: **Novel brain wiring functions for classical morphogens: a role as graded positional cues in axon guidance.** *Development (Cambridge, England)* 2005, **132**(10):2251-2262.
29. Sperry RW: **Chemoaffinity in the Orderly Growth of Nerve Fiber Patterns and Connections.** *Proceedings of the National Academy of Sciences of the United States of America* 1963, **50**:703-710.
30. Tepass U, Truong K, Godt D, Ikura M, Peifer M: **Cadherins in embryonic and neural morphogenesis.** *Nature reviews* 2000, **1**(2):91-100.
31. Takeichi M: **The cadherin superfamily in neuronal connections and interactions.** *Nature reviews* 2007, **8**(1):11-20.
32. Grigorenko AP, Moliaka YK, Korovaitseva GI, Rogaev EI: **Novel class of polytopic proteins with domains associated with putative protease activity.** *Biochemistry* 2002, **67**(7):826-835.
33. Brown MS, Goldstein JL: **The SREBP pathway: regulation of cholesterol metabolism by proteolysis of a membrane-bound transcription factor.** *Cell* 1997, **89**(3):331-340.
34. Ye J, Rawson RB, Komuro R, Chen X, Dave UP, Prywes R, Brown MS, Goldstein JL: **ER stress induces cleavage of membrane-bound ATF6 by the same proteases that process SREBPs.** *Molecular cell* 2000, **6**(6):1355-1364.
35. Urry J, Hermans-Borgmeyer I, Gercken G, Schaller HC: **Expression of the presenilin-like signal peptide peptidase (SPP) in mouse adult brain and during development.** *Gene Expr Patterns* 2003, **3**(5):685-691.
36. Grigorenko AP, Moliaka YK, Soto MC, Mello CC, Rogaev EI: **The Caenorhabditis elegans IMPAS gene, imp-2, is essential for development and is functionally distinct from related presenilins.** *Proceedings of the National Academy of Sciences of the United States of America* 2004, **101**(41):14955-14960.
37. Chan YM, Jan YN: **Roles for proteolysis and trafficking in notch maturation and signal transduction.** *Cell* 1998, **94**(4):423-426.
38. Struhl G, Adachi A: **Nuclear access and action of notch in vivo.** *Cell* 1998, **93**(4):649-660.
39. De Strooper B, Annaert W, Cupers P, Saftig P, Craessaerts K, Mumm JS, Schroeter EH, Schrijvers V, Wolfe MS, Ray WJ, Goate A, Kopan R: **A presenilin-1-dependent gamma-secretase-like protease mediates release of Notch intracellular domain.** *Nature* 1999, **398**(6727):518-522.
40. Haass C, De Strooper B: **The presenilins in Alzheimer's disease-proteolysis holds the key.** *Science* 1999, **286**(5441):916-919.
41. Ebinu JO, Yankner BA: **A RIP tide in neuronal signal transduction.** *Neuron* 2002, **34**(4):499-502.
42. Parks AL, Curtis D: **Presenilin diversifies its portfolio.** *Trends Genet* 2007, **23**(3):140-150.
43. Vooijs M, Ong CT, Hadland B, Huppert S, Liu Z, Korving J, van den Born M, Stappenbeck T, Wu Y, Clevers H, Kopan R: **Mapping the consequence of Notch1 proteolysis in vivo with NIP-CRE.** *Development (Cambridge, England)* 2007, **134**(3):535-544.
44. **Image J software** [<http://rsb.info.nih.gov/ij/>]

Publish with **BioMed Central** and every scientist can read your work free of charge

"BioMed Central will be the most significant development for disseminating the results of biomedical research in our lifetime."

Sir Paul Nurse, Cancer Research UK

Your research papers will be:

- available free of charge to the entire biomedical community
- peer reviewed and published immediately upon acceptance
- cited in PubMed and archived on PubMed Central
- yours — you keep the copyright

Submit your manuscript here:
http://www.biomedcentral.com/info/publishing_adv.asp



5.2 Expression of Teneurin-4 in the developing chick embryo

5.2.1 Expression of teneurin-4 in the visual system

As it is the case for the other teneurins examined so far, teneurin-4 was prominently expressed in the developing visual system. At E4, strong staining of primary fibers of the lens was observed, particularly towards the posterior side (Figure 12 A). The expression of teneurin-4 in the lens was transient and weaker in the lens of older embryos (Figure 12 B). At E7 teneurin-4 immunolabeling was found in the ciliary body and ciliary marginal zone of the retina (Figure 12 B). As it is known for teneurin-1 and -2, teneurin-4 was present along the retinotectal pathway: In the E12 retina, teneurin-4 was found in the IPL where synaptic connections between amacrine cells, bipolar cells and RGC's are formed, and in the OFL where the RGC axons travel to the optic nerve (Figure 12 C). Teneurin-4 was present in the optic nerve, particularly after crossing the optic chiasm (Figure 12 D) where strongly labeled axon tracts running along the dorsal thalamus to the OT were observed (Figure 12 E). In the OT, the stratum opticum in which the RGC axons run on the surface of the OT until they reach the appropriate target region was strongly stained. In addition, the stratum griseum et fibrosum superficiale (SGFS) of the OT was teneurin-4 positive (Figure 12 F). At E17, teneurin-4 expression in the visual system remained similar, but the RGC axons in the retina were much more strongly stained (Figure 12 G). Additionally, the ICD antibody revealed staining of neurons in the INL. In the optic tectum neurons strongly expressed teneurin-4 (Figure 12 H).

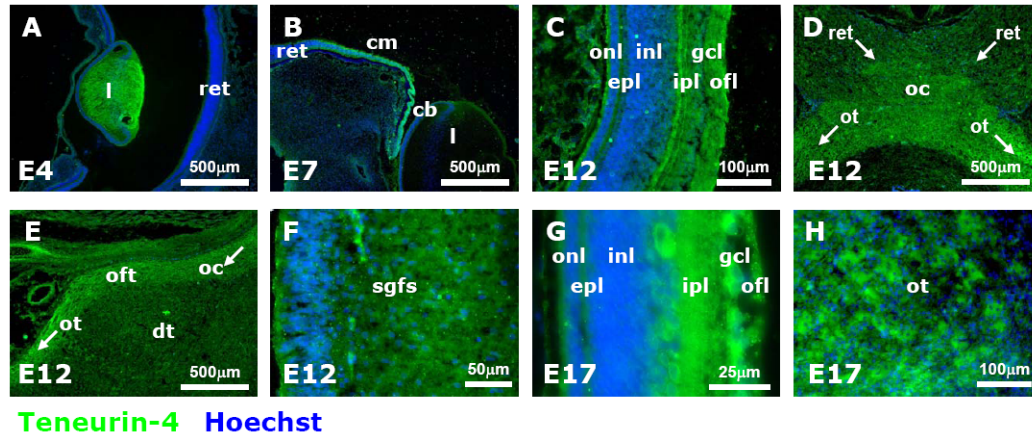


Figure 12: Teneurin-4 expression in the visual system.

A: E4 lens and retina (ICD); B: E7 lens and retina (ICD); C: E12 retina (ECD); D: E12 optic chiasm (ECD); E: E12 optic fiber tract running along dorsal thalamus (ECD); F: E12 optic tectum (ECD); G: E17 retina (ICD); H: E17 neurons in the optic tectum (ECD). The domain of teneurin-4 recognized by the antibody is indicated in parentheses. Legend: cb = ciliary body, cm = ciliary margin, dt = dorsal thalamus, epl = external plexiform layer, gcl = ganglion cell layer, inl = inner nuclear layer, ipl = inner plexiform layer, l = lens, oc = optic chiasm, ofl = optic fiber layer, oft = optic fiber tract, onl = outer nuclear layer, ot = optic tectum, ret = retina, sgfsf = stratum griseum et fibrosum superficiale.

5.2.2 Expression of teneurin-4 in the central nervous system (outside of visual system)

In E4 chick embryos, both antibodies detected teneurin-4 in the ventral horn of the spinal cord (Figure 13 A), and staining was also observed in the efferent motor axons exiting the ventral root (Figure 13 B). In the E12 olfactory system, Teneurin-4 was present in the olfactory epithelium (Figure 13 C), in mitral cells of the olfactory bulb (Figure 13 D) and in the piriform cortex which receives input from the mitral cells (Figure 13 E-H). In the piriform cortex, it was particularly evident that the ICD antibody stained the cell bodies (Figure 13 E, G), whereas the ECD antibody labeled the ECM surrounding the cells (Figure 13 F, H). The distribution of the teneurin-4 ECD staining around cells rather than on the cell surface may be explained by ECD shedding which releases the ECD from the cell membrane. At high magnification, the ICD antibody staining showed that only a subset of neurons in the piriform cortex expressed teneurin-4, whereas others did not (Figure 13 G).

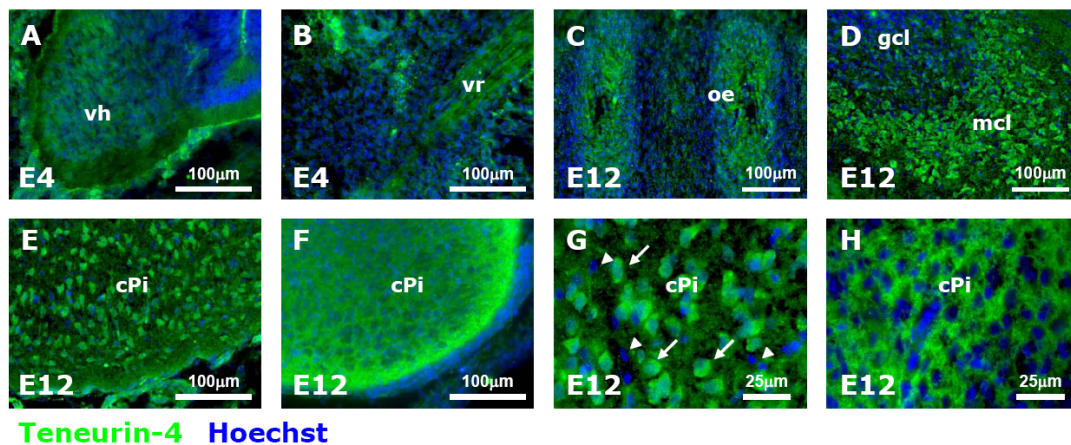


Figure 13: Teneurin-4 expression in the the CNS (outside of visual system).

A: E4 spinal cord (ECD); B: E4 ventral root nerves (ECD); C: olfactory epithelium (ECD), D: E12 olfactory bulb (ICD); F: E12 piriform cortex (ICD); F: E12 piriform cortex (ECD); G: piriform cortex (ICD); H: E17 near habenular nuclei (ECD). The domain of teneurin-4 recognized by the antibody is indicated in parentheses. Legend: cPi = cortex piriformis, gcl = granule cell layer, mcl = mitral cell layer, oe = olfactory epithelium, vh = ventral horn, vr = ventral root. Arrows = teneurin-4 positive cells in the cPi, arrowheads = teneurin-4 negative cells in the cPi.

5.2.3 Expression of teneurin-4 in non-neuronal tissues

Expression of teneurin-4 in non-neuronal tissues was particularly evident in young embryos. At E4, strong staining was observed in the mesenchyme around the lung primordium with both ICD and ECD antibodies (Figure 14 A). Teneurin-4 was also expressed in other developing organs, such as in tubules of the mesonephros (Figure 14 A, B) and in the gut epithelium as well as in the surrounding mesenchyme (Figure 14 C). At E7, no staining in these organs was detected anymore, suggesting that the expression of teneurin-4 in the developing lung, kidney and gut is transient. Other sites of teneurin-4 expression included the mesenchyme at various sites, for example in the pharyngeal arches, where teneurin-4 was present in the mesenchyme and in the ectoderm as previously found by whole-mount in-situ hybridization¹³³.

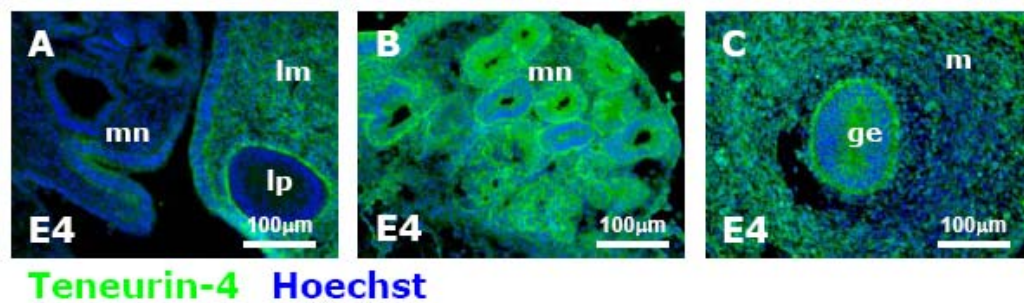


Figure 14: Teneurin-4 expression in non-neuronal tissues.

A: E4 lung and kidney (ECD); B: E4 kidney (ICD); C: E4 gut (ICD). The domain of teneurin-4 recognized by the antibody is indicated in parentheses. Legend: ge = gut epithelium, m = mesenchyme, lm = lung mesenchyme, lp = lung primordium, mn = mesonephros.

5.2.4 Expression of teneurin-4 in the limb

Outside the CNS, the most intriguing teneurin expression patterns were found in the developing limb. They suggest an important role in pattern formation, and as in the developing brain, the pattern for each teneurin in the limb is distinct and complementary. Teneurin-4 was present in the two most important signaling centers of the developing limb, in the AER, which regulates distal outgrowth, and in the ZPA, which regulates anterior-posterior patterning (Figure 15 A). Staining of the AER and adjacent ectoderm was observed at E4 (Figure 15 B) and E5 (Figure 15 G). However, expression of teneurin-4 at the tip of the limb appeared to be dynamic and involve both the AER as well as the underlying mesenchyme (Figure 15 C, I). Potentially, teneurin-4 is expressed by the AER and the ECD is shed and distributes to the underlying mesenchyme. Teneurin-4 expression at the tip of the limb persists to E6 (Figure 15 I). Particularly with the ICD antibody, teneurin-4 was detected in the ectoderm enveloping the mesenchyme of the limb (Figure 15 D, F). As with the ECD antibody, the ectoderm was stained and the staining extended to the underlying mesenchyme in regions between mesenchyme undergoing chondrogenic differentiation (Figure 15 K). The strongest teneurin-4 expression was detected in the ZPA, as described previously with *in situ* hybridization¹³³. This signal persisted from E4 (Figure 15 E) to E5 (Figure 15 H) and E6 (Figure 15 J). In older limbs (E7) some residual teneurin-4 expression in the ectoderm and underlying mesenchyme was observed (Figure 15 L) but the strong staining in the AER and ZPA was gone, indicating that teneurin-4 expression is transient and dynamic during limb development. In comparison, teneurin-1 is expressed in the dorsal ectoderm and ventral mesoderm (unpublished observation) and teneurin-2 is highly expressed exclusively in the AER¹¹⁷. Thus, teneurin-4 is unique in that it is expressed in both crucial signaling centers of the developing limb, which is not the case for any other teneurin.

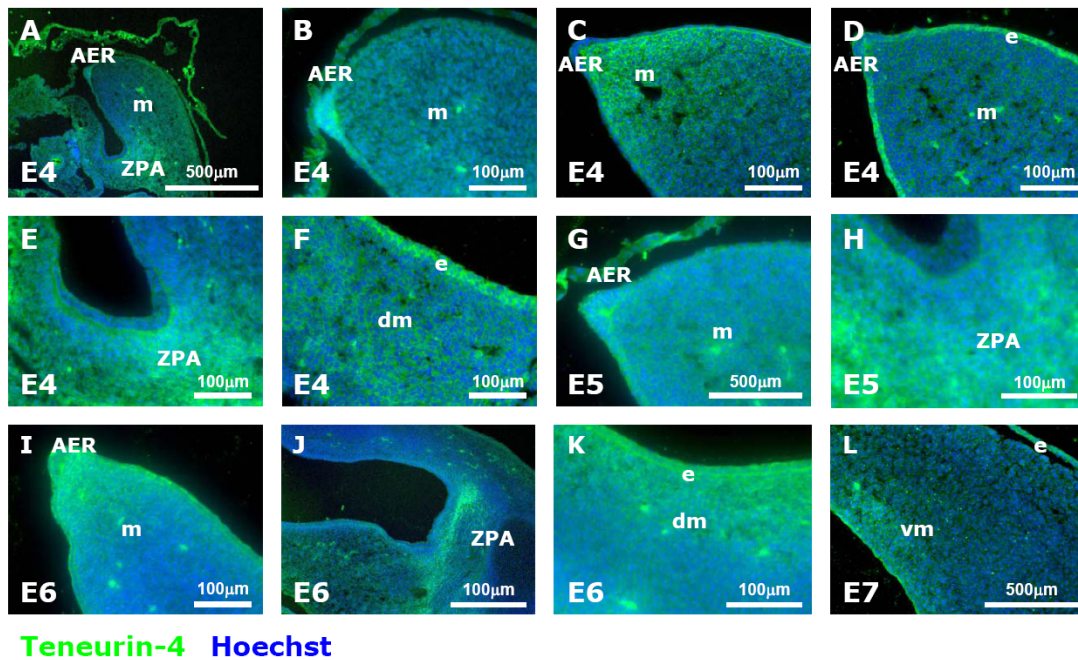


Figure 15: Teneurin-4 expression in the developing limb.

A: E4 limb primordium (ECD); B: E4 limb tip showing labeling in the AER (ECD); C: E4 limb tip showing immunostaining in the mesenchyme underlying the AER (ECD); D: E4 limb tip (ICD); E: E4 limb ZPA (ECD); F: E4 limb dorsal mesenchyme (ICD); G: E5 limb (ECD); H: E5 limb ZPA (ECD); I: E5 limb tip (ECD); J: E6 limb ZPA (ECD); K: E6 limb (ECD); L: E7 limb (ECD). The domain of teneurin-4 recognized by the antibody is indicated in parentheses. Legend: AER = apical ectodermal ridge, dm = dorsal mesenchyme, e = epithelium, m = mesenchyme, vm = ventral mesenchyme, ZPA = zone of polarizing activity.

5.2.5 WB analysis of teneurin-4 expression during chick development

Protein lysates of limb buds and different regions of the brain were collected at specific developmental stages and analyzed by WB using both ICD and ECD antibodies (Figure 16). Whereas full-length teneurin-4 was detected with both antibodies, N-terminal processing products were observed with the ICD antibody suggesting that teneurin-4 is processed by ECD shedding, possibly followed by RIP. Teneurin-4 expression was particularly strong in the retina, where a distinct pattern of N-terminal processing products was observed. The

same was observed before for teneurin-1 (unpublished observations) and indicates that teneurins are differentially processed in the retina compared to other tissues. Both antibodies showed stronger expression in young embryos (E4 and E7), which decreased in the E12 brain and was very weak in the E17 brain. In the early embryo, teneurin-4 expression in the limb bud is as strong as in the retina and the brain. In E12 and E17 brains, teneurin-4 was more highly expressed in the forebrain and the retina and only at low levels in the optic tectum and the cerebellum.

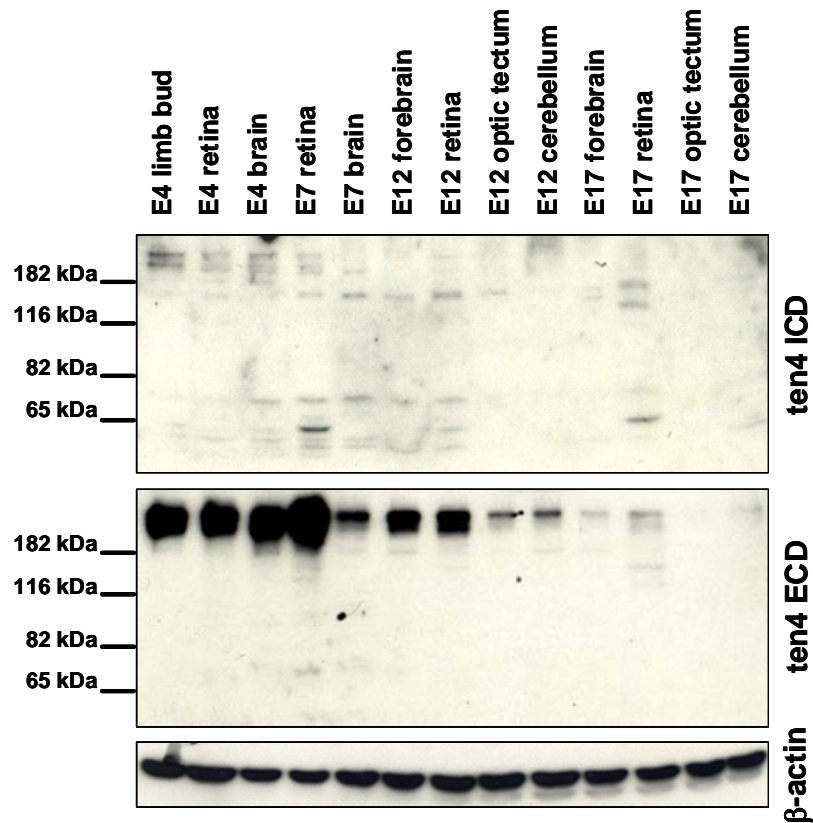


Figure 16: WB analysis of teneurin-4 expression during chick development.

Protein lysates from different tissues and developmental stages were analyzed using the ICD and ECD antibody. Full-length teneurin-4 was observed using both antibodies, and N-terminal processing products with the ICD antibody only. Teneurin-4 was more strongly expressed in younger embryos (E4 and E7), and expression decreases in the brain of older embryos (E12, E17). β -actin was used as a loading control.

Part II – Teneurins in Disease

5.3 Teneurin-1 as an XLMR candidate gene

5.3.1 Analysis of the human teneurin-1 genomic locus

The human teneurin-1 gene (called *odz-1*, gi:110347399) was analyzed using the UCSC browser. The exons to be sequenced were defined based on the transcript NM_014253. A list of the 31 sequenced exons including the sizes of the exons and preceding introns is provided in Table 4.

exon	exon size	intron size	5'flanking	5'end	3'end	3'flanking
exon 1	281		tcccttctctccag	gactgcttcattaaa	aaaaatctactcaag	gtagtctttatgga
exon 2	261	67295	ctttgttctctcag	agatggaattctgtga	tctgatggggaaaatg	gtaataaactacttga
exon 3	57	1628	atgttactgttacag	gtttcaaattctctcc	gctgggtctactcaag	gcaagtgtttcaaat
exon 4	241	157097	ctctctctctttag	atgtgcagagcagccc	taccattggagaccag	gtacttgagcttatt
exon 5	239	31705	tgttctttttcacag	gcatttcctgttcaaa	ctagcctatgtgattg	gtaagtcctttgtc
exon 6	153	33177	gctgttctcttcag	cagtgcattgttcgg	aaatcagagaaaaaag	gtacagtgatcaaaa
exon 7	206	17899	ctacctttaaactag	tgtttcagaaggac	acatactcaggattt	gatattataggtatt
exon 8	211	1453	tttgattgttccag	tttgattgttaaac	ttaactacagcaattg	gtaagctgttgcct
exon 9	102	5103	ttctctgtattactag	aaataatggatgactg	cctgactgtgtagag	gtaaigtgtctctt
exon 10	195	1271	aattgccaacctcag	attcctgccctgtgct	gaaatatgaggaag	gtcagaatccatttt
exon 11	201	3151	ttttgtgccttcag	aggactgcctagacc	tctgactgctcaacag	gtgtatggagtaaat
exon 12	186	76230	tttgaattccccacag	agctgtgtaccatgga	gaccactgcacaattg	gtaagtaccaccatac
exon 13	25	1601	ttcccccccttta	gctcactacttagatg	ttagatgctgtccgag	gtaagalttttccac
exon 14	147	1931	tctgatgtctttcag	atggctgccagggt	ttggacaatgatggag	gtgagtcattataaa
exon 15	217	14580	tgggtttatttcag	atgggttaaccgactg	tgcatittgacagcag	gtacatatgtattat
exon 16	120	16890	tggtctgtgttcag	gcgtgctgtgtgatt	gccggcaagatggaag	gtagtcaatgttgt
exon 17	262	6238	gtttttctcttag	ctttgacctgtgccc	gtttctgagctgcag	gtgagtatattggcct
exon 18	268	2579	tttttttatttcag	gttgacagaggaaa	ctggcagaggctttgg	gtagttgaactaatt
exon 19	144	16813	aaactctgttttcag	tatctgtgggataga	ttgaatcctcaaatg	gtaagtagcttttaa
exon 20	250	6294	tttccttgaatcag	gaatcatacataaag	gtattttggaattaag	gtaagctctctaata
exon 21	233	15051	ctttctctcttag	cacaagtcctgctcac	ctgaatagccctcgag	gtaaaaaataaaaaa
exon 22	155	28240	tgctctttccaacag	gcatcacagttgatag	aatggacatcactcag	gtaggcacactggtt
exon 23	367	30698	tctgttctttcacag	gtgagtagatgggc	gtgactgttttcag	gtagcacttttagc
exon 24	511	1450	agtccttctccaacag	gtgatgggtctatgc	ggacaaccgtttatga	gtaagttctaattct
exon 25	173	13821	tggttacattctcag	gtatgaccccagggga	tatattttaaaacaag	gtaagattttccaa
exon 26	236	1050	gctctctgtctacag	aaaatactcaaagtac	tgaaggaggctgagg	gtaaggcttgacttta
exon 27	297	12682	tatctcttctcatag	gcccaacaagaaacc	tacctactagaaaaa	gtaagtagatagggga
exon 28	388	5987	ctttgtctgtttcag	ctgtgatgctctcc	agatacaggcaaacag	gittgtgtgaaagag
exon 29	1221	822	gttttgttctctcag	gaccttattggacg	gcaaagtataccacag	glatttaaactattta
exon 30	143	821	atattgtgtctacag	acatcagaagttggt	gtgggatcctgaaag	gtagtaaaagtttta
exon 31	3319	1378	ctctcttctctagact	atctgggcattcagt	actactaatcagtagt	aaatcgaagagaaaca

Table 4: Exons to be sequenced.

The human *odz1*/teneurin-1 gene contains 31 exons which were sequenced. The size of the exon, the size of the preceding exon and the 5' and 3' splice junctions are listed. The coding sequence is written in bold, the adjacent noncoding sequence in normal script.

5.3.2 Summary of SNPs in the analyzed sequence

In the entire genomic locus of the teneurin-1 gene spanning more than 600kb, 1929 single nucleotide polymorphisms (SNPs) are present according to the Entrez SNP database which displays SNPs based on the dbSNP build 129. To know which alterations can be expected after sequencing of patient DNAs, a list of SNPs found in the teneurin-1 coding sequence including the exon flanking, 5' upstream and 3' untranslated regions that were included in my study was composed (Table 5). In the genomic region to be sequenced, 38 known SNPs are present: 27 SNPs are located in non-coding regions (5' upstream, exon flanking, 3' untranslated), and 11 in the coding sequence, of which 6 are synonymous and 5 result in amino acid exchanges. SNP rs36065191 results in the exchange of a tyrosine with a histidine in exon 1, SNP rs2213591 in an exchange of a methionine with a threonine in exon 6, and two SNPs in exon 11 lead to the replacement of a methionine with a valine (rs16999334) and a lysine with a glycine (rs6649271), respectively. One polymorphism in exon 23 (rs35405207) inserts a G nucleotide and thus results in a frameshift, however it is lacking validation by the HapMap project, multiple and independent submissions or frequency and genotype data. However, of these SNPs affecting the teneurin-1 amino acid sequence, only the one in exon 6 (SNP rs2213591) was found in my patients and controls, which included 24 individuals in total.

SNP	sequence	location	aa change
rs5956718	ttgcttgcccttgaaggtatcca[C/G]aatccaaccagatctctcaattc	5'upstream	
rs58984127	TATGAACATATACATATATATATATAT[C/T]ACACACACCAATGATTTCAACAACAA	5'upstream	
rs3834690	CTGATTTTTTAAAAAGGCTTACACA[-/CA]TTTGACTGATATATGTTTTAAATGG	5'upstream	
rs5956717	cgcccggccTATGTAGGCTGATTTTT[A/T]AAAAAAGGCTTACACATTTGACTGA	5'upstream	
rs5956716	gttagccaggatgtctcgatctcc[C/G]acctcgtgatccaccgccctcggcc	5'upstream	
rs11310365	TGTAGGCTGATTTTTATTGATCAAT[-/T]GATTGATTGATTGATTGATTGATT	5'upstream	
rs11284309	GATGTAGGCTGATTTTTATTGATCAA[-/T]TTGATTGATTGATTGATTGATTGAT	5'upstream	
rs10284039	TTTCATTCCTTACATTATTTTGTCA[C/T]JACCAATTTCACTCCACTGTTGCAACT	5'upstream	
rs34734884	AAATAGAGGACAACGTTGTTCTATGG[-/G]TGTGTGCGTGTTTTAATGTTAAAA	5'upstream	
rs57545535	GGAGAGAAGTAAAAGACAACACTAGAT[A/G]ACATGAAGCTAGCCGGAGGCAATAA	5'upstream	
rs5958635	AGATTCACAATTGGTCTGATAATAC[C/T]ATCAAAGGAGAGAAGTAAAAGACAA	5'upstream	
rs36065191	AAGATGGAAGAAAACCAAGACAGTCA[C/T]JACAACCTCCAGGGAGACCTGCACGA	exon 1 coding	TAC (Y) g CAC (H)
rs5958616	TCTAGCTGGTAGCCATGCCGAGAAAC[A/G]CTGTGCATGTCTGTTGGTAGCCAG	exon 2 coding	AGC (S) → AGT (S)
rs34981391	CTAGAGATGGGATCTGATGTGGACAC[A/G]GAGACAGAAGGTGCTGCCCTACCTG	exon 2 coding	ACA (T) → ACG (T)
rs16994522	GGAAACACAAGTTGGGCTATAAAAA[C/G]CAAAGCCAGTTGCTACAAAAACACA	exon 5 5' flanking	
rs2213591	CAAAGGGAACAGGGGACCGAGTCCA[C/T]GGACACTACTTACTCTCCAATTGGA	exon 6 coding	ATG (M) g ACG (T)
rs34322253	CCCACCACACAGCAGGGCAGGAAT[C/T]TGAAGGTTGGCAAATGAACTTGTA	exon 10 5'flanking	
rs60027201	GTGAACAGGTATGGCCAACATACCTT[A/G]GTATGATGAAACGGAGATTACATTG	exon 11 5'flanking	
rs16999334	TACACAGATGCCATGGTTGGAACACA[C/T]TGGGCTAGGCAGTCCCTCTGAAGGC	exon 11 coding	ATG (M) g GTG (V)
rs6649271	GCCAGTAGAACAGTGACATCTCTCT[C/T]TACACAGATGCCATGGTTGGAACAC	exon 11 coding	AAA (K) g GAA (G)
rs7882953	ATTCGATCAAAAAAGTCTTGAAGT[A/G]TGCTGAGAGAAGAGAGTTTGGCTTT	exon 15 coding	AGC (S) → AGT (S)
rs5958502	ACCCAAGGGTatatatatatatat[A/T]tatttattatTTTTACCTCGAGG	exon 21 3'flanking	
rs61310498	ACCCAAGGGTATATATATATATATAT[-/ATATA]TTATTTTATTTTACCTCGAG	exon 21 3'flanking	
rs34974707	TCTTTAGATGACCCAAGGGTATATAT[-/TATATA]JATATATATATTTATTTATTTT	exon 21 3'flanking	
rs10673684	ATCTTTAGATGACCCAAGGGTatata[-/TATATA]tatatatatttatttattt	exon 21 3'flanking	
rs10656532	AATAAAATCTTTAGATGACCCAAGGG[-/TATATA]tatatatatatatatatttattt	exon 21 3'flanking	
rs35405207	AATTGTCCATAGGATTACTGCAAGG[-/G]TCTGTTGGCCACTCTAATCGCACCT	exon 23 coding	GAC (H) → frameshift!
rs12013090	GCTAAGGAGGAAGGGCTTTCATCTT[C/T]GCATCTTTGGCATAGCCACCATCAC	exon 24 coding	GCA (A) → GCG (A)
rs960869	ACCTCTCCAGTGGGAAACGTTGCATT[G/T]GTCAGGTGCCCTCGGGGTCATACC	exon 25 coding	ACC (T) → ACA (T)
rs59812568	GGAAGGGAAGAGCAGGAAGCAGAAAA[C/G]JAGACAGTTTGTATTTAGGAGGCAC	exon 26 5'flanking	
rs34194370	ACAACAACAACAACAACAACAACAAC[-/AAAC]JAAAACACCTATAAAAAGTTCTATATC	exon 26 3'flanking	
rs2076165	TGAATAAACGTCACCAATCCCGAAGG[C/T]GAATATGTGATGTTCACTTCATTAT	exon 27 coding	TCA (S) → TCG (S)
rs41312759	ACAGTTAAGGATGAAACTGCTTCTCA[C/T]JAATAGAGATAGAGAACCTTGGGTTT	3'untranslated	
rs6648597	TATTGCACCACCTATTCAAATAGCC[C/A/G]TAAGTTCTGCCAACAGTTAAGGATG	3'untranslated	
rs59761033	AGTTTCAGATACTATTGCACCACCTA[A/G]JACAGTTAAGGATGAAACTGCTTCTC	3'untranslated	
rs41310478	TTTGGTATCATGTACACACGAGCAA[C/T]JAGCGGCTATACAGTCTGGTTACCAC	3'untranslated	
rs5958477	GTTCAATACAGAATTGTACATTTGAA[A/G]GATAAATCTAAGTGGGCTGAAACAA	3'untranslated	
rs5958476	CGATTAATAAAGATAAATGGGTAAG[G/T]JACGGAGAACGAAAATAACTAAGTGT	3'untranslated	

Table 5: List of SNPs in the odz coding and exon flanking region.

The names and sequences of all SNPs present in the analyzed regions of the *teneurin-1* locus are listed, indicating whether they are located in a coding or non-coding region of the gene. The last column lists the consequences of SNPs located in the coding regions on the amino acid sequence of the *teneurin-1* protein. Sequence in lower case is used for sequence identified by RepeatMasker as low-complexity or repetitive elements.

SNPs in the coding region are bold, and non-synonymous SNPs are marked in red.

5.3.2 Summary of XLMR patient sequencing results

The coding, exon flanking, 5' upstream and 3' untranslated regions of the human teneurin-1 gene were sequenced in 21 XLMR patients linked to Xq25 and compared to the reference sequence. The results are summarized in Table 6. In total, 27 alterations were identified, 21 SNPs in the non-coding regions (5' upstream, exon flanking, 3' untranslated), and 6 in the coding sequence. 16 of these alterations were known SNPs, and 11 were novel and may represent novel SNPs or spontaneous mutations. In particular the nucleotide changes in the flanking region of exon 18, exon 20 and exon 26 may constitute novel SNPs, since they were found in several patients.

Generally, the 50 intronic nucleotides adjacent to the splice site are thought to be important for the regulation of splicing, therefore it is difficult to predict if a nucleotide alteration in the exon flanking region has an effect on splicing. Only the nucleotides immediately adjacent to the splice site are highly conserved, and none of the alterations I have found interferes with these splicing recognition sites. Of the 6 alterations found in the exons, 5 were synonymous, and only one located in exon 6 resulted in an amino acid sequence change. However, since this alteration corresponded to a known SNP (rs2213591) and was found in two different XLMR patients, it is very unlikely to be the cause for the disease. One alteration found in exon 29 was novel, but it is a synonymous mutation and therefore not likely to affect the function of the teneurin-1 protein.

SNP (if known)	patients	region	nucleotide	amino acid change
rs5956718	p	5' upstream	C → G	
? (near rs58984127)	p	5' upstream	Δ TA	
rs5956717	TW, MD, GL, a, b, f, g, m, n, o, p	5' upstream	A → T	
?	p	5' upstream	C → T	
rs5956716	n	5' upstream	G → C	
?	n	5' upstream	A → T	
rs11284309, rs11310365	n, p	5' upstream	TCA insert	
rs10284039	p	5' upstream	G → A	
rs5958635	n, p	5' upstream	G → A	
rs5958616	n	exon 2 coding	C → T	AGC (S) → AGT (S)
rs16994522	g	exon 5 flanking 5'	C → G	
rs2213591	g, p	exon 6 coding	T → C	ATG (M) → ACG (T)
?	MD, m, n, s	exon 18 flanking 5'	Δ T	
?	j, q, r, t, v, w	exon 20 flanking 3'	G → T	
rs5958502, rs61310498	l	exon 21 flanking 3'	A → T	
rs34974707, rs10673684, rs10656532	MD, a,b,c,d,h,l,j,k,l,m,n,o,p,q,r,s,t, v	exon 21 flanking 3'	TA insert	
?	n	exon 23 flanking 5'	C → A	
rs12013090	a, h, r	exon 24 coding	A → G	GCA (A) → GCG (A)
?	u	exon 24 flanking 3'	A → G	
?	d	exon 24 flanking 3'	G → A	
rs960869	TW, c, f, l, j, k, n, q	exon 25 coding	C → A	ACC (T) → ACA (T)
? (near rs34194370)	MD, g, l, o, p, t	exon 26 flanking 3'	Δ/insert GTT	
rs2076165	c, f, j	exon 27 coding	A → G	TCA (S) → TCG (S)
?	w	exon 29 flanking 5'	T → G	
?	c	exon 29 coding	T → G	GTT (V) → GTG (V)
rs41312759	w	3'untranslated	C → T	
?	MD	3'untranslated	A → C	
rs6648597	b, c, j, k, t, w	3'untranslated	C → T	
rs5958476	ref, g, v, w	3'untranslated	C → A	

Table 6: List of SNPs and unknown alterations found in XLMR patients.

All alterations found in 23 XLMR patients and 3 controls are listed, indicating whether they correspond to a known SNP (black) or if they do not represent known SNPs (red). The location of the alteration within the gene, nucleotides exchanged, and consequences on the amino acid sequence are indicated. The last column lists the patients for which the alteration was found.

5.3.3 SNPs in the 5' upstream region

Remarkably, patient p was found to have several alterations in the 5' upstream region, where the promoter of teneurin-1 may be located. 5 of these alterations corresponded to known polymorphisms, and 2 were novel. Whereas it is unlikely that one SNP in the 5' upstream region of teneurin-1 causes a XLMR phenotype, possibly the accumulation of several SNPs may result in XLMR caused by altered teneurin-1 expression. Therefore, two additional samples of affected brothers of the same XLMR families were obtained to test whether they also exhibit the same SNPs. The results are summarized in Table 7. It can be ruled out that the accumulation of SNPs in the 5'upstream region is responsible for the XLMR phenotype of patient p, because 6 of the 7 SNPs were not shared by patient p and his affected brothers. The remaining SNP that both patient p and the brothers carry is very common and was found in most patients and the healthy controls, and is thus unlikely to result in XLMR.

rs5956718	
reference	agatctggttgatt c tgatacctttcaaa
patient_p	agatctggttgatt g tgatacctttcaaa
p_brother1	agatctggttgatt c tgatacctttcaaa
p_brother2	agatctggttgatt c tgatacctttcaaa
? (near rs58984127)	
reference	gtgtatatatatata ta gtatatgttcatat
patient_p	gtgtatatatatata-- tg tatatgttcatat
p_brother1	gtgtatatatatata ta gtatatgttcatat
p_brother2	gtgtatatatatata ta gtatatgttcatat
rs5956717	
reference	tgtaagccttttt a aaaaatcagcctacat
patient_p	tgtaagccttttt t aaaaatcagcctacat
p_brother1	tgtaagccttttt t aaaaatcagcctacat
p_brother2	tgtaagccttttt t aaaaatcagcctacat
?	
reference	tttgggaggccgagg c gggtggatcacgagg
patient_p	tttgggaggccgagg t gggtggatcacgagg
p_brother1	tttgggaggccgagg c gggtggatcacgagg
p_brother2	tttgggaggccgagg c gggtggatcacgagg
rs11284309, rs11310365	
reference	tcaatcaatcaatca---aattgatcaataaaa
patient_p	tcaatcaatcaatca tca aattgatcaataaaa
p_brother1	tcaatcaatcaatca---aattgatcaataaaa
p_brother2	tcaatcaatcaatca---aattgatcaataaaa
rs10284039	
reference	gtggactgaaatggt g atgacaaaataatgt
patient_p	gtggactgaaatggt a atgacaaaataatgt
p_brother1	gtggactgaaatggt g atgacaaaataatgt
p_brother2	gtggactgaaatggt g atgacaaaataatgt
rs5958635	
reference	cttctctccttgat g gtattatcaggacca
patient_p	cttctctccttgat a gtattatcaggacca
p_brother1	cttctctccttgat g gtattatcaggacca
p_brother2	cttctctccttgat g gtattatcaggacca

Table 7: 5' upstream polymorphisms in patient p.

The SNPs (black) and unknown alterations (red) found in patient p are listed, and the sequence of the reference is compared with patient p and two affected brothers in patient p. The altered nucleotide was shown in bold and red.

5.4 Teneurin-4 overexpression in brain tumors

5.4.1 Microarray data of brain tumors

From a microarray analysis performed in the Hemmings lab, teneurin expression data of normal adult human brain and a panel of different types of brain tumors, including astrocytoma, oligodendroglioma, glioblastoma and secondary glioblastoma were obtained. Teneurin-2 (215993_at, 231867_at) and teneurin-3 (219523_s_at) did not show any difference in expression levels between normal brain and brain tumors, and the values of teneurin-1 expression were too low to be considered. In contrast, teneurin-4 (213273_at) was strongly and consistently upregulated in all types of brain tumors, 13.7-fold in astrocytoma, 6.3-fold in oligodendroglioma, 8.7-fold in glioblastoma and 6.4-fold in secondary glioblastoma (Figure 17).

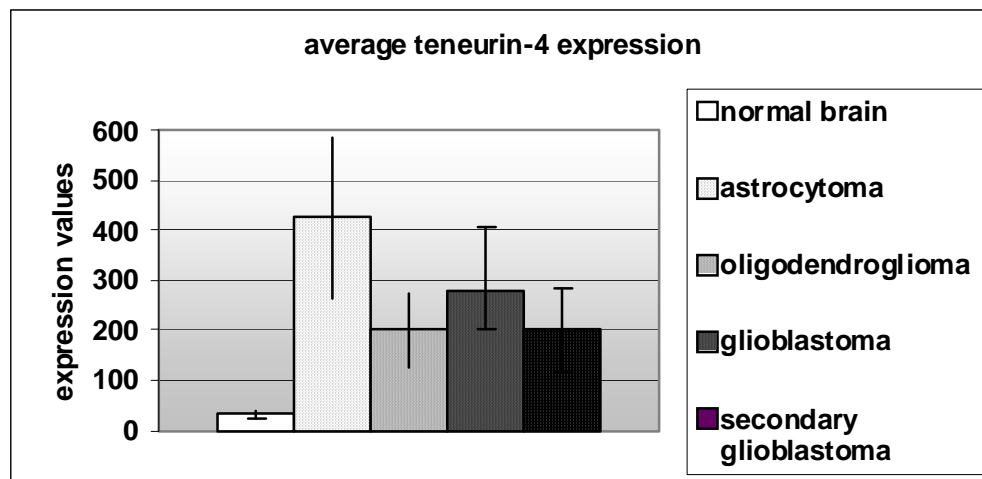


Figure 17: Teneurin-4 expression in normal brain and brain tumors.

The average expression levels of teneurin-4 in human normal brain ($n = 2$), astrocytoma ($n = 8$), oligodendroglioma ($n = 7$), glioblastoma ($n = 13$) and secondary glioblastoma ($n = 3$) including error bars indicating the standard deviation.

Figure 18 depicts the expression values of the individual samples, which show that the upregulation of teneurin-4 was very consistent in all tumor samples, with a two-fold upregulation even present in brain tumors with low teneurin-4 expression. The highest expression values were observed in astrocytomas, some of which had up to 18.8-fold upregulation of teneurin-4. Astrocytomas had two-fold higher teneurin-4 expression levels than oligodendrogliomas, while glioblastomas ranged in between. The sample number of secondary glioblastoma ($n = 3$) was too small to conclude that teneurin-4 expression is lower in secondary glioblastoma than glioblastoma. The expression values of all samples are depicted in Figure 18 and listed in Table 8.

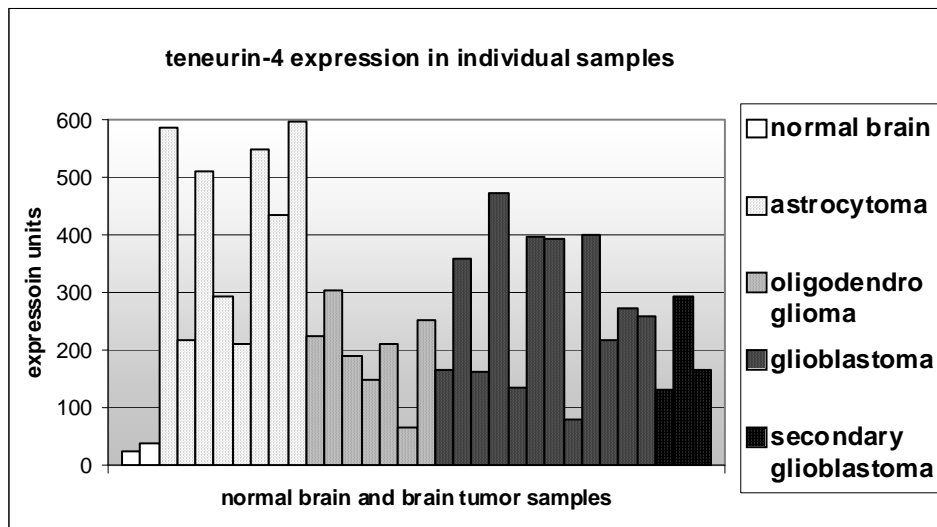


Figure 18: Teneurin-4 expression in individual normal brain and tumor samples. The expression levels of teneurin-4 in human normal brain ($n = 2$), astrocytoma ($n = 8$), oligodendroglioma ($n = 7$), glioblastoma ($n = 13$) and secondary glioblastoma ($n = 3$).

brain (n = 2) average: 31.08 SD: 9.17	16 67.68 17 253.94
1 24.59 2 37.57	glioblastoma (n = 12) average: 277.56 SD: 126.76
astrocytoma (n = 8) average: 425.66 SD: 162.57	18 167.47 19 360.73 20 164.78 21 474.24 22 134.24 23 397.96 24 394.07 25 82.38 26 402.95 27 218.22 28 275.25 29 258.46
oligodendroglioma (n = 7) average: 200.12 SD: 76.29	secondary glioblastoma (n =3) average: 197.71 SD: 86.86
11 223.98 12 305.32 13 190.22 14 148.79 15 210.88	30 131.28 31 296.01 32 165.84

Table 8: List of teneurin-4 expression values.

The expression values of each individual normal brain and brain tumor sample are listed. Samples of 2 normal brains, 8 astrocytomas, 7 oligodendrogliomas, 12 glioblastomas and 3 secondary glioblastomas were analyzed. For each group, the average and standard deviation (SD) was calculated.

5.4.2 WB analysis of brain tumors

To be able to analyze teneurin-4 expression on protein level, antibodies against human teneurin-4 were produced. It was attempted to obtain antibodies against both the ICD and ECD to be able to confirm results with several independent antibodies and to study teneurin processing and signaling. Both antigens were used for the production of polyclonal as well as monoclonal antibodies. Polyclonal antibodies were successfully obtained in both rabbits A and B for the ECD antigen, but none of the rabbits for the ICD antibodies generated antibodies, probably because the size of the antigen was too small to be immunogenic (<10 kDa). Screening of monoclonal antibodies resulted in two clones that recognized the ECD (32f, 67b), but unfortunately they reacted only the recombinant protein and not with endogenous teneurin-4 in cell and tumor lysates. Currently, monoclonal antibodies against the ICD are being screened and hopefully will work in WB analysis and in IHC, which can then be used to confirm the results I describe below.

Thus, all the results so far were obtained with the polyclonal ECD antibodies. The antibodies were first tested on recombinant protein, and subsequently on cell and tumor lysates. In brain tumors, a main band of about 200 kDa was observed, which was not present in the controls including the ECD antibodies preabsorbed with the antigen and the preimmune serum (Figure 19). For a full-length teneurin-4, a molecular weight of >300 kDa is expected, therefore the observed band may correspond to a shed ECD. Subsequently, three samples of normal brain (total brain, cortex, and cerebellum) were compared to three tumors with varying expression levels of teneurin-4, which was found to be nearly absent in normal brain. In cerebellum and cortex, faint bands with lower molecular weights than the bands present in the tumor samples were observed at >120 kDa (Figure 19).

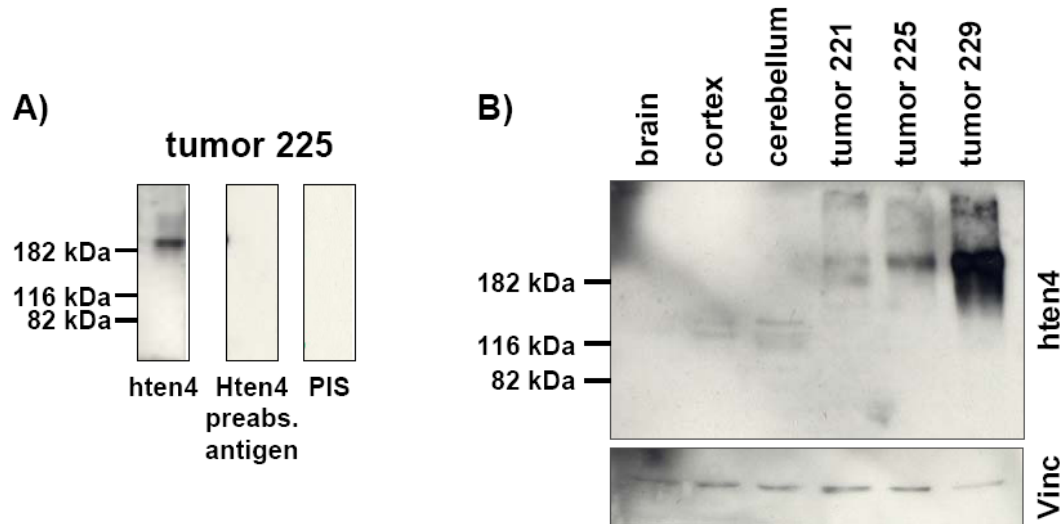


Figure 19: Characterization of antibodies and comparison normal brain with tumors.

A) Testing the specificity of the ECDA polyclonal antibody on brain tumor lysate: Left lane ECDA 1:1000, middle lane ECDA preabsorbed with antigen 1:1000, right lane preimmune serum 1:1000. B) Comparison of teneurin-4 expression in three samples of normal brain (brain, cortex, cerebellum), and three brain tumors with different teneurin-4 expression levels (221, 225, 299).

Finally, three different panels of brain tumors were analyzed by western blotting using the ECDA antibody. Two panels of brain tumors included different types of tumors, astrocytoma, oligodendroglioma and glioblastoma (Figure 20). Teneurin-4 was found to be overexpressed in all types, particularly in glioblastoma (e.g. BS 117T, BS 229, 116, 117). The astrocytomas present in the two panels showed lower expression of teneurin-4 (BS 177T, BS 246T, A96, A103, A127). The presence of teneurin-4 in oligodendroglioma appeared to be intermediate (BS 189, BS 271, 220G, 920G). In general, teneurin-4 expression varied between individual tumor samples. A third panel of brain tumors consisting of 15 glioma samples was analyzed, where almost all tumors expressed teneurin-4, some at very high levels (Figure 21). In most samples, a band or a smear was observed on top of the lane in addition to the 200 kDa band, which may represent glycosylated and/or dimerized teneurin-4.

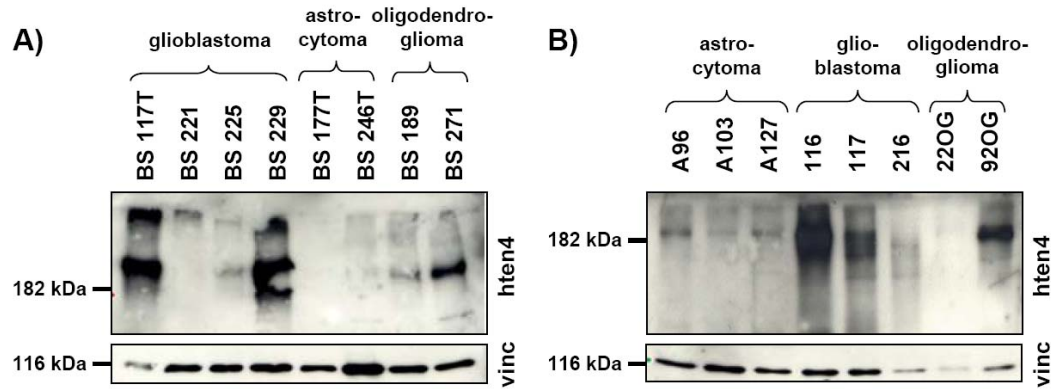


Figure 20: WB analysis of two panels of different brain tumors.

A) Four glioblastoma (BS 117T, BS 221, BS 225, BS 229), two astrocytoma (BS177T, BS 246T) and two oligodendroglioma (BS 189, BS 271) were analyzed for teneurin-4 expression. B) A second panel of brain tumors included three astrocytomas (A96, A103, A127), three glioblastoma (116, 117, 216) and two oligodendroglioma (220G, 920G). Vinculin serves as a loading control.

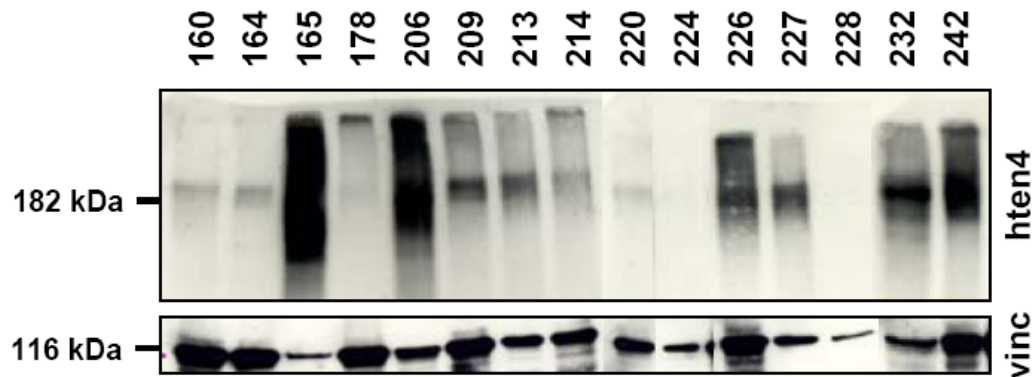


Figure 21: WB analysis of a panel of glioblastomas.

A third panel of brain tumors was analyzed for teneurin-4 expression, all 15 samples are derived from glioblastomas patients. Vinculin serves as a loading control.

5.4.3 IHC of brain tumors

Frozen sections of brain tumors were obtained, which were stained with the EGFA antibody to find out if the tumor cells themselves expressed teneurin-4, or if it was rather derived from stromal cells. Since the number of tissue slides was very limited, standard staining conditions were used and it was not possible to optimize the staining protocol. Several tumors exhibited a very strong staining of tumor cells and blood vessels, which is also weakly present in the preimmune control. However, these tumors consisted of large regions of necrosis (labeled N in the H&E staining picture) characteristic of progressing glioblastomas, which were strongly but unspecifically stained. In other tumors, the teneurin-4 staining was restricted to the blood vessels while the tumor cells themselves were not positive for teneurin-4 (Figure 22). However, the integrity of the frozen tissue sections was far from optimal and the morphology of the tumors is poorly preserved. Therefore, it is difficult to draw conclusions based on these tissue sections.

Several tumors exhibited staining of blood vessels (tumor 103A, tumor 96A, tumor 92OG, tumor 271, tumor 221, tumor 225), suggesting a role for teneurin-4 in angiogenesis (Figure 23). It appeared that not only the endothelial cells were stained, but the entire blood vessel wall, suggesting that the teneurin-4 ECD may be shed and incorporated into the basal membrane surrounding the blood vessels. It will be interesting in the future to confirm the specificity of this staining and to determine if the teneurin-4 present around the blood vessels is derived from tumor cells or from endothelial cells.

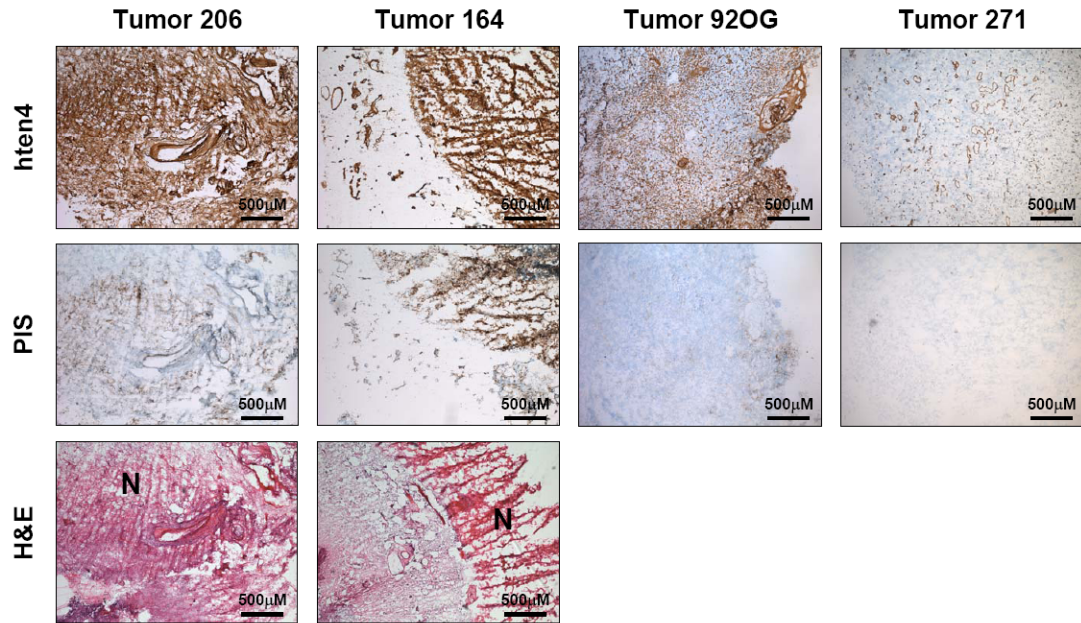


Figure 22: Teneurin-4 IHC in brain tumors.

Certain tumors were strongly positive for teneurin-4 (e.g. tumor 206, tumor 164); however they exhibited large regions of necrosis (labeled N in the H&E staining picture) that are stained. Other tumors were less positive for teneurin-4, and staining was more restricted to blood vessels (tumor 92OG, tumor 271). The teneurin-4 staining appears brown and the cell nuclei are counterstained with blue dye. H&E staining is depicted where available.

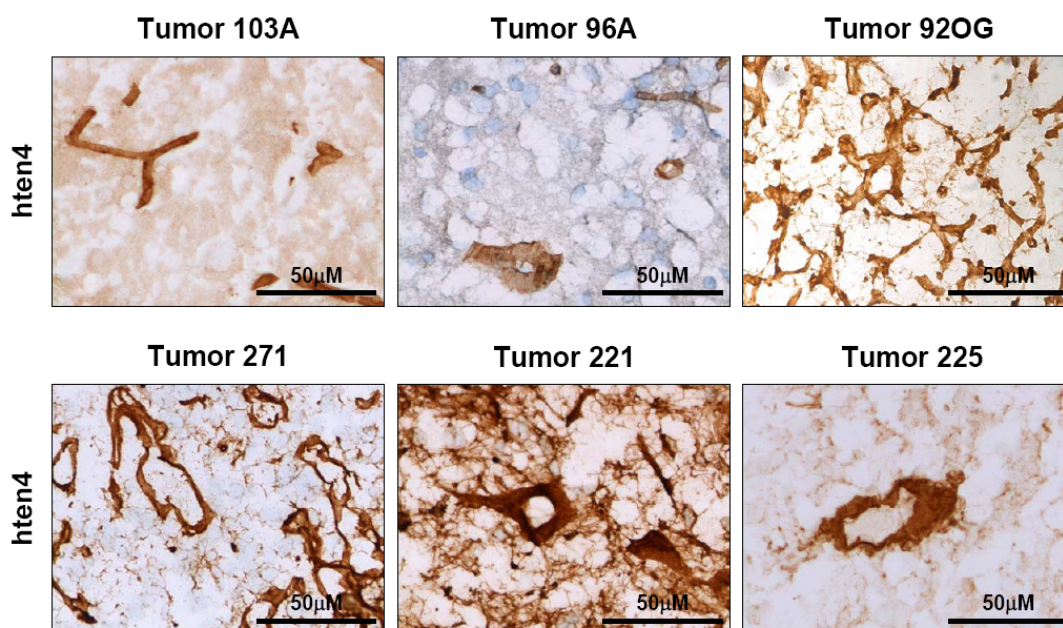


Figure 23: Teneurin-4 staining is present on blood vessels.

Blood vessels were stained in all tumors (e.g. tumor 221), and in most tumors teneurin-4 was restricted to blood vessels (tumor 103A, tumor 96A, tumor 92OG, tumor 271, tumor 225). This staining was observed in all types of tumors, astrocytomas (tumor 103A, tumor 96A) oligodendrogliomas (tumor 92 OG, tumor 271) and glioblastomas (tumor 221, tumor 225).

5.4.4 Comparison between WB analysis and IHC

The staining intensities on WBs and on tissue sections were compared relative and scored as absent (-), very low (-/+), medium (+), strong (++) and very strong (+++). Overall, there was a good correlation between WB analysis and IHC staining (Table 9). Higher levels of teneurin-4 protein was detected in glioblastoma by both methods, however this might be due to the large regions of necrosis which are certainly also present in protein lysates. The necrotic areas might also explain why on protein level as detected with the ECD antibody, seemingly more teneurin-4 was detected than in the microarray analysis.

Brain tumor	tumor type	WB	IHC staining
116	GBM	+++	++
117	GBM	++	++
164	GBM	+	+++
206	GBM	+++	+++
221	GBM	-/+	+++
225	GBM	+	++
226	GBM	+++	+++
229	GBM	+++	++
232	GBM	++	+++
242	GBM	+++	+++
103A	AII	-/+	+
177	AII	-	-/+
246	AII	-/+	+
96A	AIII	+	+
127	AIII	+	+
220G	OG	-	+
920G	OG	++	++
189	OGIII	+	+
271	OGIII	++	++

Table 9: Comparison between WB analysis and IHC of teneurin-4 expression.

The intensities of staining on immunoblots and tissue section were scored relative to the other tumor samples as absent (-), very low (-/+), medium (+), strong (++) and very strong (+++).

6. DISCUSSION

The potential role of teneurins in neuronal development and the establishment of appropriate synaptic connections as well as our teneurin signaling hypothesis are already discussed in my publication "Teneurin-1 is expressed in interconnected regions of the developing brain and is processed in vivo"¹²⁷ and my review "Teneurins, a transmembrane protein family involved in cell communication during neuronal development"¹¹⁵. Thus, the discussion of these two aspects is covered by my paper and my review, and only as short section discussing the unpublished results of teneurin-4 expression is added. This is followed by two sections discussing in detail the unpublished parts of teneurin-1 as a candidate gene for XLMR and teneurin-4 as a marker for brain tumors.

6.1 Teneurins in neuronal development and our teneurin signaling hypothesis

Visions & Reflections Minireview:

"Teneurins, a transmembrane protein family involved in cell communication during neuronal development."

Visions & Reflections (Minireview)

Teneurins, a transmembrane protein family involved in cell communication during neuronal development

D. Kenzelmann^{a,*}, R. Chiquet-Ehrismann^a and R. P. Tucker^b

^aFriedrich Miescher Institute, Maulbeerstr. 66, 4057 Basel (Switzerland), Fax: +41 61 697 39 76,
e-mail: daniela.kenzelmann@fmi.ch

^bSchool of Medicine, 1 Shields Avenue, University of California at Davis, Davis, California 956168643 (USA)

Received 28 February 2007; received after revision 28 March 2007; accepted 17 April 2007
Online First 14 May 2007

Abstract. Teneurins are a unique family of transmembrane proteins conserved from *Caenorhabditis elegans* and *Drosophila melanogaster* to vertebrates, in which four paralogs exist. In vertebrates, teneurin expression is most prominent in the developing brain. Based on their distinct, complementary expression patterns, we suggest a possible function in the establishment of proper connectivity in the brain. Functional studies show that teneurins can stimulate neurite outgrowth, but they might also play a role in axon guidance as well as in target recognition and

synaptogenesis, possibly mediated by homophilic interactions. Though teneurins are transmembrane proteins, there is evidence that the intracellular domain has a nuclear function, since it can interact with nuclear proteins and influence transcription. Therefore, we speculate that teneurins might be processed by proteolytic cleavage (possibly regulated intramembrane proteolysis), which is triggered by homophilic interactions or, alternatively, by the binding of a still unknown ligand.

Keywords. Neural circuit, regulated intramembrane proteolysis, brain, nervous system, odz, ten-m.

Teneurins – an emerging family of transmembrane proteins

The goals of this article are to introduce the teneurin family of transmembrane proteins and to discuss possible functions based on gene expression patterns and cell culture studies. Additionally, we will summarize evidence indicating that teneurins could be a novel substrate for regulated intramembrane proteolysis (RIP).

Originally discovered in *Drosophila* (*ten-m* and *ten-a*), the teneurin protein family is conserved from *Caenorhabditis elegans* (*ten-1*) to vertebrates, in which four

paralogs exist (teneurin-1 to -4 or odz-1 to -4). Their distinct domain architecture is highly conserved between invertebrate and vertebrate teneurins, particularly in the extracellular part [1, for reviews see refs. 2, 3]). The large C-terminal extracellular domain is composed of eight tenascin-type, epidermal growth factor (EGF)-like repeats, a region of conserved cysteines and 26 YD-repeats, which are not present in any other eukaryotic protein. The N-terminal intracellular domain of vertebrate teneurins contains two EF-hand-like calcium-binding motifs and two polyproline domains involved in protein-protein interactions, followed by a single-span transmembrane domain (Fig. 1a).

* Corresponding author.

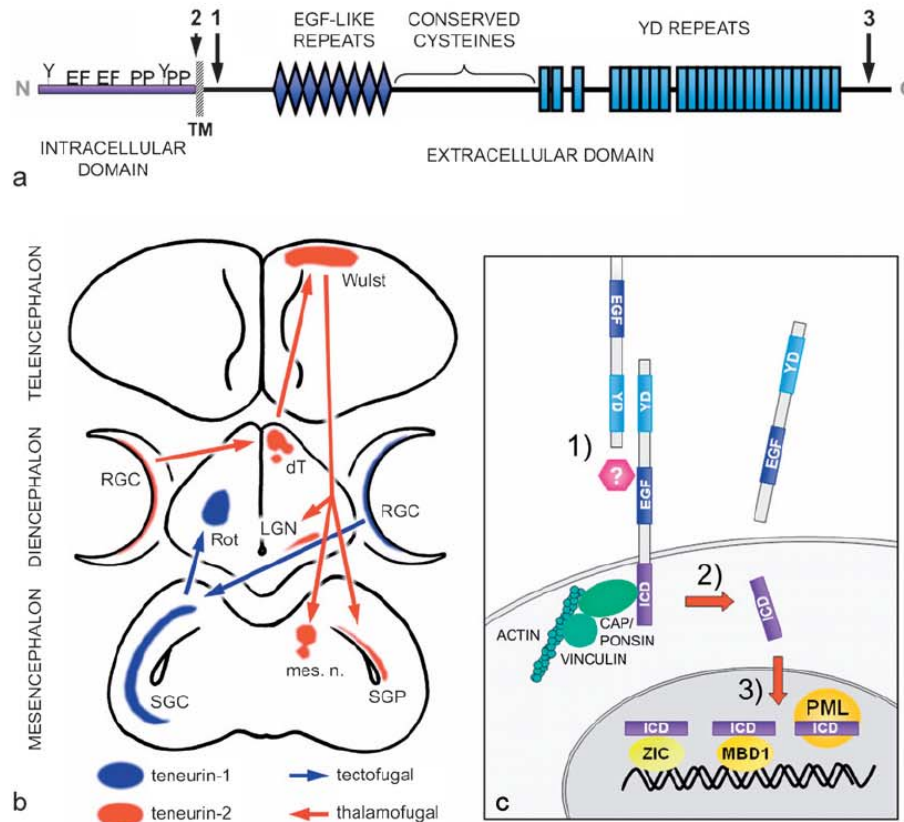


Figure 1. (a) Domain organization of teneurins. Teneurins have an N-terminal intracellular domain, a single transmembrane domain (TM) and a large extracellular domain. The intracellular domain contains two EF-hand-like motifs (EF), two polyproline motifs (PP) and several conserved tyrosines (Y) that are predicted phosphorylation sites. The extracellular domain consists of eight tenascin-type EGF-like repeats, a region of conserved cysteines and the YD-repeats. Arrows with numbers indicate postulated cleavage sites: 1) cleavage site for ectodomain shedding (a prerequisite for intramembrane proteolysis), 2) transmembrane cleavage site resulting in the release of the intracellular domain, and 3) an additional cleavage site releasing a teneurin C-terminus associated peptide, which is proposed to have neuromodulatory activity. (b) Expression pattern and neuronal connectivity. Teneurin-1 is expressed at key sites along the tectofugal visual pathway, including retinal ganglion cells (RGC), the stratum griseum centrale (SGC) of the optic tectum, and the rotund nucleus (Rot) in the diencephalon. In contrast, teneurin-2 is present in the thalamofugal pathway: RGCs connect to nuclei in the contralateral dorsal thalamus (dT) and further to the Wulst, which in turn projects back to the lateral geniculate nucleus (LGN), various mesencephalic nuclei (mes. n.) and the stratum griseum periventriculare (SGP) of the optic tectum. (c) Teneurin signaling hypothesis. 1) A signal, which can be either a homophilic interaction or binding of a yet unknown ligand, triggers the mechanism. 2) After shedding the extracellular domain, the remaining teneurin part becomes a substrate for intramembrane proteolysis, resulting in the release of the intracellular domain. 3) Nuclear translocation of the intracellular domain, where it associates with PML bodies and nuclear proteins such as MBD-1, a methyl-CpG-binding protein, and Zic, a transcription factor family implied in neuronal development. Additionally, CAP/Ponsin can bind to the intracellular domain, which could represent a link to the actin cytoskeleton which is important for neurite outgrowth.

RIP was discovered in studies of the sterol response, where SREBP, a transcription factor residing in the endoplasmic reticulum (ER) membrane, is cleaved by the intramembrane protease Site-2 and thereby released to translocate to the nucleus [19]. Four families of intramembrane proteases and dozens of substrates have since been identified [reviewed in refs. 20–22]; the best known substrates are Notch and APP, both of which are cleaved by presenilin.

Transmembrane proteases exhibit specificity for the orientation of the substrate in the membrane. Presenilin cleaves type I transmembrane proteins, whereas Site-2 protease and signal peptide peptidase (SPP) and SPP-like proteases cleave type II transmembrane proteins and are therefore candidate proteases for teneurin processing. In addition, cleavage by Rhomboid was recently found not to be restricted to type I transmembrane proteins [23]. A

common feature of the RIP mechanism is that a cleavage on the extracellular side has to occur prior to the intramembrane cleavage. Indeed, teneurin-2 can be processed at a furin site between the transmembrane domain and the EGF-like repeats, resulting in shedding of the ectodomain [9]. This furin cleavage site seems to be conserved in teneurin-3 and -4, but probably not in teneurin-1.

Outlook

More work will be needed to prove that RIP and nuclear localization of the intracellular domain take place, and to identify the proteases responsible for the cleavage. It is conceivable that such a cleavage is tightly regulated during development and takes place only in response to a specific stimulus, e.g., by the recognition of a guidance cue or target region by an outgrowing axon. Another possibility to obtain a soluble intracellular domain could be alternative splicing resulting in a teneurin variant that ends before the transmembrane domain.

Their distinctive localization in the developing brain suggests that expression of each teneurin must be intricately regulated by a complex network of transcription factors that govern patterning. Therefore, it will be interesting to identify and investigate the factors that regulate teneurin expression and which genes are, in turn, regulated by teneurins. Teneurins were found to be differentially expressed in the caudal and rostral cortex by microarray analysis together with many other genes, most of which belong to two groups: transcription factors and extracellular signaling molecules [24]. The teneurins might combine both of these functions in a single molecule.

To prove that teneurins are indeed required for proper connectivity and regionalization in the brain and to investigate a potential role in neuronal regeneration, more sophisticated neurobiological studies will be required. Furthermore, analysis of the teneurin-1 gene in X-linked mental retardation patients would reveal if mutations in this gene are responsible for the disease and confirm a role for teneurins in brain development and axonal connectivity.

- 1 Minet, A. D. and Chiquet-Ehrismann, R. (2000) Phylogenetic analysis of teneurin genes and comparison to the rearrangement hot spot elements of *E. coli*. *Gene* 257, 87 – 97.
- 2 Tucker, R. P. and Chiquet-Ehrismann, R. (2006) Teneurins: a conserved family of transmembrane proteins involved in intercellular signaling during development. *Dev Biol* 290, 237 – 245.
- 3 Tucker, R. P., Kenzelmann, D., Trzebiatowska, A. and Chiquet-Ehrismann, R. (2007) Teneurins: transmembrane proteins with fundamental roles in development. *Int. J. Biochem. Cell. Biol.* 39, 292 – 297.
- 4 Ben-Zur, T., Feige, E., Motro, B. and Wides, R. (2000) The mammalian Odz gene family: homologs of a *Drosophila* pair-rule gene with expression implying distinct yet overlapping developmental roles. *Dev. Biol.* 217, 107 – 120.
- 5 Li, H., Bishop, K. M. and O'Leary, D. D. (2006) Potential target genes of EMX2 include Odz/Ten-M and other gene families with implications for cortical patterning. *Mol. Cell. Neurosci.* 33, 136 – 149.
- 6 Minet, A. D., Rubin, B. P., Tucker, R. P., Baumgartner, S. and Chiquet-Ehrismann, R. (1999) Teneurin-1, a vertebrate homologue of the *Drosophila* pair-rule gene *ten-m*, is a neuronal protein with a novel type of heparin-binding domain. *J. Cell. Sci.* 112, 2019 – 2032.
- 7 Otaki, J. M. and Firestein, S. (1999) Neurestin: putative transmembrane molecule implicated in neuronal development. *Dev. Biol.* 212, 165 – 181.
- 8 Rubin, B. P., Tucker, R. P., Brown-Luedi, M., Martin, D. and Chiquet-Ehrismann, R. (2002) Teneurin 2 is expressed by the neurons of the thalamofugal visual system in situ and promotes homophilic cell-cell adhesion in vitro. *Development* 129, 4697 – 4705.
- 9 Rubin, B. P., Tucker, R. P., Martin, D. and Chiquet-Ehrismann, R. (1999) Teneurins: a novel family of neuronal cell surface proteins in vertebrates, homologous to the *Drosophila* pair-rule gene product *Ten-m*. *Dev Biol* 216, 195 – 209.
- 10 Tucker, R. P., Martin, D., Kos, R. and Chiquet-Ehrismann, R. (2000) The expression of teneurin-4 in the avian embryo. *Mech. Dev.* 98, 187 – 191.
- 11 Zhou, X. H., Brandau, O., Feng, K., Oohashi, T., Ninomiya, Y., Rauch, U. and Fassler, R. (2003) The murine *Ten-m/Odz* genes show distinct but overlapping expression patterns during development and in adult brain. *Gene Expr. Patt.* 3, 397 – 405.
- 12 Oohashi, T., Zhou, X. H., Feng, K., Richter, B., Morgelin, M., Perez, M. T., Su, W. D., Chiquet-Ehrismann, R., Rauch, U. and Fassler, R. (1999) Mouse *ten-m/Odz* is a new family of dimeric type II transmembrane proteins expressed in many tissues. *J. Cell. Biol.* 145, 563 – 577.
- 13 Mieda, M., Kikuchi, Y., Hirate, Y., Aoki, M. and Okamoto, H. (1999) Compartmentalized expression of zebrafish *ten-m3* and *ten-m4*, homologues of the *Drosophila ten(m)/Odz* gene, in the central nervous system. *Mech. Dev.* 87, 223 – 227.
- 14 Al Chawaf, A., St Amant, K., Belsham, D. and Lovejoy, D. A. (2007) Regulation of neurite growth in immortalized mouse hypothalamic neurons and rat hippocampal primary cultures by teneurin C-terminal-associated peptide-1. *Neuroscience* 144, 1241 – 1254.
- 15 Nunes, S. M., Ferralli, J., Choi, K., Brown-Luedi, M., Minet, A. D. and Chiquet-Ehrismann, R. (2005) The intracellular domain of teneurin-1 interacts with MBD1 and CAP/ponsin resulting in subcellular codistribution and translocation to the nuclear matrix. *Exp. Cell Res.* 305, 122 – 132.
- 16 Drabikowski, K., Trzebiatowska, A. and Chiquet-Ehrismann, R. (2005) *ten-1*, an essential gene for germ cell development, epidermal morphogenesis, gonad migration, and neuronal pathfinding in *Caenorhabditis elegans*. *Dev Biol* 282, 27 – 38.
- 17 Feng, K., Zhou, X. H., Oohashi, T., Morgelin, M., Lustig, A., Hirakawa, S., Ninomiya, Y., Engel, J., Rauch, U. and Fassler, R. (2002) All four members of the *Ten-m/Odz* family of transmembrane proteins form dimers. *J. Biol. Chem.* 277, 26128 – 26135.
- 18 Bagutti, C., Forro, G., Ferralli, J., Rubin, B. and Chiquet-Ehrismann, R. (2003) The intracellular domain of teneurin-2 has a nuclear function and represses *zic-1*-mediated transcription. *J. Cell Sci.* 116, 2957 – 2966.
- 19 Brown, M. S. and Goldstein, J. L. (1997) The SREBP pathway: regulation of cholesterol metabolism by proteolysis of a membrane-bound transcription factor. *Cell* 89, 331 – 340.

- 20 Hoppe, T., Rape, M. and Jentsch, S. (2001) Membrane-bound transcription factors: regulated release by RIP or RUP. *Curr. Opin. Cell Biol.* 13, 344 – 348.
- 21 Urban, S. and Freeman, M. (2002) Intramembrane proteolysis controls diverse signalling pathways throughout evolution. *Curr. Opin. Genet. Dev.* 12, 512 – 518.
- 22 Wolfe, M. S. and Kopan, R. (2004) Intramembrane proteolysis: theme and variations. *Science* 305, 1119 – 1123.
- 23 Tsruya, R., Wojtalla, A., Carmon, S., Yogev, S., Reich, A., Bibi, E., Merdes, G., Schejter, E. and Shilo, B. Z. (2007) RhoGDI cleaves Star to regulate the levels of secreted Spitz. *EMBO J.* 26, 1211 – 1220.
- 24 Sansom, S. N., Hebert, J. M., Thamrongkol, U., Smith, J., Nisbet, G., Surani, M. A., McConnell, S. K. and Livesey, F. J. (2005) Genomic characterisation of a Fgf-regulated gradient-based neocortical protomap. *Development* 132, 3947 – 3961.

To access this journal online:
<http://www.birkhauser.ch/CMLS>

6.2 Teneurin-4 in chick CNS and limb development

The domain architecture and amino acid sequence of the four vertebrate teneurin paralogs is highly conserved and teneurin-4 is expressed at similar sites as the other teneurins. Teneurin-4 is expressed strongly in specific parts of the CNS and in non-neuronal sites of pattern formation such as the limb bud, as it has been previously described for other teneurins. Furthermore, by using teneurin-4 ICD antibodies, I could detect N-terminal processing products, as it was already observed for teneurin-1¹²⁷ and teneurin-2 (unpublished observation). This suggests that the proposed signaling mechanism including processing by RIP is conserved among the four vertebrate teneurin paralogs.

Since the expression patterns of teneurins in the brain have already been discussed in detail, I will focus this section on the discussion of teneurin expression patterns in the developing limb. Teneurin-4 exhibited a particularly interesting expression pattern in the developing limb. It was present in both crucial signaling centers: the AER at the tip of the limb bud and in the ZPA near the base of the developing limb. FGFs expressed by the AER induce the proliferation of underlying mesenchymal cells and distal outgrowth of the limb bud; and cells of the ZPA secrete Shh to determine anterior-posterior patterning. Previously, teneurin-2 was shown to be expressed in the AER¹¹⁷ and induced by FGF8 in limb bud cultures, suggesting that teneurin-2 is induced by FGFs expressed in the limb bud in vivo. Thus, teneurin-4 expression may be regulated by FGF signaling as well. During AER formation, teneurin-2 and -4 may function as adhesion molecules facilitating the migration of induced AER precursors to the future AER site or their subsequent compaction. In the ZPA, the expression of teneurin-4 may be induced by Shh, as it is suggested to be the case in the *Drosophila* eye imaginal disc. The expression of ten-m in the morphogenetic furrow is strongly reduced in a mutant carrying a hypomorphic Hedgehog allele, implying that ten-m is downstream of hedgehog signaling¹⁴². As a putative adhesion molecule, teneurin-4 may function to promote adhesion of Shh-expressing cells in the ZPA to maintain the integrity of this signaling center. Thus, teneurin-4 appears to be important in signaling centers in the limb bud regulating proximo-distal as well as anterior-posterior axis specification.

6.3 Is teneurin-1 a candidate gene for XLMR?

When this project was started in 2005, several XLMR families with unknown cause linked to Xq25 existed, and none of the 45 XLMR genes known at that time was located in Xq25 except *OCRL1* causing the Lowe-Syndrome⁷⁰. In the meantime, the number of known XLMR genes has almost doubled, and three new genes in Xq25 have been identified: *GRIA3*⁷², *ZDHHC9*⁷¹ and *UPF3B*¹⁴³. At the end of 2007, the genetic cause was still unknown for 133 XLMR families⁵⁹. We hypothesized that teneurin-1 located at Xq25 is a promising candidate gene because of its suggested function in synaptic connectivity. Defects in neuronal connectivity are thought to underlie mental retardation, particularly when gross brain abnormalities are absent⁶⁹. In addition, several genes that have been shown to interact with teneurin-1 are implicated as XLMR genes, such as *Syn1*⁷³ and *MBD1*⁷⁵, both of which bind to the teneurin-1 ICD⁷⁶ (and unpublished observation). Moreover, several factors that are thought to regulate teneurin expression are crucial for brain development, such as *EMX2*, *ZIC* and *FGFs*⁶⁸.

Unfortunately, no obvious disease causing mutation was found in the analysis of the coding and exon-flanking sequence of teneurin-1 in 21 XLMR patients linked to Xq25. Of 27 alterations found, 21 were located in non-coding regions and 6 within the exon-coding sequence. While 16 corresponded to known SNPs, 11 may represent novel SNPs, particularly those which were found in several patients (flanking regions of exon 18, exon 20 and exon 26). There were 5 synonymous nucleotide exchanges in the coding region, one in exon 29 being novel, and one non-synonymous resulting in the exchange of a methionine with a threonine in exon 6 (SNP rs2213591). No alteration was detected in the splice consensus sequence, and most nucleotide exchanges found in the 5'upstream and 3'untranslated region corresponded to known SNPs. One patient (p) exhibited an accumulation of SNPs in the 5'upstream region, which were however not present in two affected brothers and therefore can be ruled out as the cause for XLMR in this family.

The fact that no mutations likely to cause XLMR were found in the coding sequence of the patients analyzed does not exclude that a mutation in a regulatory sequence causes misexpression of the teneurin-1 gene. However this is difficult to predict, particularly since the promoter of teneurin-1 has not yet been characterized. Preliminary experiments show that the teneurin-1 gene contains an untranslated first exon that is located about 250kb upstream of the first translated exon in a region containing CpG islands (unpublished observation). Therefore, it is likely that the promoter of teneurin-1 is located far more upstream than assumed for my patient sequence analysis, or that alternative promoters exist. Since regulatory sequences are often located in the first intron, it will be very difficult to identify regions that are important for teneurin gene regulation. Furthermore, alternative splicing could result in the transcription of additional coding exons that were not included in my analysis. The alignment of the predicted human teneurin-1 to -4 paralogs which are highly conserved in their amino acid sequence suggests the existence of additional exons that were not part of the reference sequence used for this analysis, e.g. between exon 3 and exon 4 and between exon 20 and exon 21. Thus, a mutation located on one of those exons would have escaped my analysis. In addition, although only the nucleotides directly at the exon-intron boundaries are highly conserved, those further away from the splice site may also affect regulation of splicing, and it is difficult to predict whether such a mutation would affect splicing of teneurin-1. Both the levels of teneurin-1 expression and regulation of (alternative) splicing can be studied using immortalized lymphocytes from XLMR patients by RT-PCR or Q-PCR. These methods have already been successful in the identification of XLMR splice site mutations in the past, e.g. in the case of *HADH2*¹⁴⁴. However none of the alterations I have identified seemed promising enough to undertake such experiments. Besides, since gene expression and splicing is often regulated in a tissue-specific manner there are potentially differences between lymphocytes and brain. Finally, ncRNAs or miRNAs that are present in the teneurin-1 locus that regulate the expression of teneurin-1 or exert other biological functions may be affected by a mutation. Such an ncRNA has been identified in an intronic region of the teneurin-3 gene¹⁴⁵, and several ncRNAs are predicted in the *odz1* locus (e.g. AK086544).

The SNPs that are present in the teneurin-1 coding region and result in amino acid exchanges (rs2213591 in exon 6, rs16999334 and rs6649271 in exon 11 and rs35405207 in exon 23) could potentially affect teneurin-1 function in individuals carrying these SNPs. If teneurin-1 is important for the development of appropriate neuronal connectivity, these SNPs may affect brain function in humans. An additional SNP is located in exon 23 (rs35405207) and inserts a G nucleotide, this results in a frame shift and truncation of the teneurin-1 protein in the ECD. Since no validation or frequency data is available for this SNP, it would be interesting to confirm its occurrence in the human population and test whether it is associated with any phenotype of altered brain function. In addition even a silent SNP may alter protein function, as it has been shown in the case of *MDR1* gene. In such a case, the of an alternative codon altered the speed of translation and protein folding which finally affected protein function¹⁴⁶.

X-linked lymphoproliferative disease (XLP) is characterized by extreme sensitivity to the Epstein-Barr virus (EBV) resulting in a complex phenotype involving severe infections and malignant lymphoma caused by mutations in the *SH2D1A/SAP* or *XIAP/BIRC4* genes^{147,148}. Recently, a family with XLP and chronic active inflammatory gastric lesions was described, which carries a 3 Mb deletion comprising *SH2D1A*, the adjacent teneurin-1 gene and two other predicted genes¹⁴⁹. Thus, if these patients do not have mental retardation in addition of these symptoms, it is very unlikely that teneurin-1 is involved in XLMR except in the case that a mutated teneurin-1 would exhibit a gain-of-function phenotype causing XLMR. However, it is also possible that these patients do have subtle defects in brain function, as it was described for the teneurin-3 knockout mice, which show an impairment of binocular vision¹²⁹. Such a minor phenotype may not be diagnosed, particularly in XLP patients that suffer from a severe and fatal disease.

6.4 Is teneurin-4 a marker for cancer?

The data of a microarray study analyzing brain tumor samples performed in the Hemmings lab showed high and consistent upregulation of teneurin-4 and prompted us to generate the tools to investigate the expression of human teneurin-4 in brain tumors and possibly other types of cancers. Teneurin-4 was the only teneurin that was upregulated in this study while teneurin-2 and teneurin-3 levels in contrast were the same for normal brain and tumors. For teneurin-1 no conclusion is possible because the probe on the microarray did not detect any significant expression and thus no data was available. Therefore, we focused on teneurin-4 as a potential brain tumor marker.

The microarray data are a good indication, but it was important to confirm the overexpression of teneurin-4 on protein levels. Therefore, I generated recombinant proteins for the production of polyclonal and monoclonal antibodies recognizing the ICD and ECD of teneurin-4. The goal was not only to develop the tools to test teneurin-4 expression on protein level, but also to be able to study teneurin processing as it is suggested by our teneurin signaling hypothesis. To date, only polyclonal antibodies recognizing the ECD were successfully obtained, and potentially useful monoclonal antibodies recognizing the ICD are being evaluated. By using the polyclonal ECD antibodies, I could confirm a strong overexpression of teneurin-4 in all types of brain tumors, including astrocytoma, oligodendroglioma and glioblastoma, compared to three samples of normal brain both by WB analysis and IHC of brain tumor sections. However, several things need to be considered: First, more samples of normal brain would be needed to make a statistically significant statement, especially since expression of teneurin-4 in the adult brain may vary strongly depending on the exact anatomical location, as suggested by the very specific teneurin-4 expression during brain development in chick and mouse. Second, it is very important to confirm the results using a different antibody, as it is difficult to prove the specificity of the band detected by the polyclonal ECD antibody. Hopefully, the monoclonal ICD antibodies will soon be available to confirm

teneurin-4 overexpression independently. Moreover, on tissue sections the ECD antibody stains non-specifically large regions of necrosis, which certainly are also present in the protein lysates. Indeed, the correlation between the WB analysis and IHC of glioblastoma may be derived from the extent of necrosis in the individual tumors rather than from specific teneurin-4 expression. This may also be the reason why on WB and IHC, glioblastomas show higher teneurin-4 expression than astrocytomas, whereas the opposite is true for the microarray data. Third, the quality of the frozen brain tumor sections is not sufficient, because in addition of the large areas of necrosis, there are regions with freezing and thawing artifacts. Necrosis is an intrinsic characteristic of progressing glioblastomas and thus cannot be avoided, whereas the brain tumor tissue will certainly be better preserved on paraffine sections. Therefore, it is important to test the polyclonal ECD and monoclonal ICD antibodies on paraffine sections and establish a reliable staining protocol. For this purpose, normal human fetal brain may be useful, as teneurin-4 is certainly expressed in some regions of the brain. Fourth, whereas blood vessels were stained in all tumors analyzed by IHC, some tumors exhibited also staining of tumor cells themselves. It will be important to confirm the specificity of the blood vessel staining and to determine if teneurin-4 is expressed by the tumor itself, or by endothelial cells, for example by in-situ hybridization. Even the teneurin-4 that is found around blood vessels may be produced by tumor cells and subsequently processed resulting in the release of the ECD, which then incorporates into the basal membrane that is present around the blood vessels. The furin cleavage site that was shown to mediate ECD shedding in chick teneurin-2¹¹⁶ is also conserved in human teneurin-4. In *C.elegans*, genetic interactions between teneurin and components of the BM as well as BM receptors on the cell surface have been described, and the BM integrity is affected by BM mutants¹¹⁴. In developing chick embryos, teneurin-2 was found to colocalize with laminin, suggesting that it is incorporated into the BM⁸¹. Depending on the cell type expressing teneurin-4, different sets of experiments have to be performed to analyze the function of teneurin-4 in brain tumors. Fifth, it appears that teneurins are described to be mainly expressed in neurons and not in glial cells, whereas astrocytomas, oligodendrogliomas and glioblastomas are all of glial origin. However, co-staining of a glial cell marker and teneurin has not yet been performed to exclude that teneurins are expressed also in glial cells during

development. Conversely, it will be interesting to test the expression of teneurin-4 in brain tumors of neuronal origin, e.g. neuroblastoma.

After the overexpression of teneurin-4 in brain tumors has been confirmed, it will be interesting to determine whether teneurin-4 has a function in cancer development and progression. To this aim, it will be necessary to clone the full-length teneurin-4. It would be interesting to determine if the conserved furin cleavage site on the ECD is functional and if this cleavage resulting in ECD shedding occurs is regulated or occurs constitutively. This implies that teneurin-4 activity would not be restricted to the cell membrane, but that it would act as a soluble molecule like e.g. the tenascins. Depending on which cells are assumed to be affected by the presence of teneurin-4, the cancer cells or the endothelial cells, different sets of experiments should be performed. Possibly, teneurin-4 may also affect both cell types. If teneurin-4 is suspected to be implicated in angiogenesis, HUVEC cells can be used for experiments to perform angiogenesis assays, such as the spheroid sprouting assay and the matrigel tubule formation assay. Other possible assays for testing the effect of soluble teneurin-4 on angiogenesis include the aortic ring assay, chicken chorioallantoic membrane assay and matrigel plug assay. If teneurin-4 is expressed in HUVEC cells, it would be interesting to see the effects of an RNAi or shRNA knockdown on the tube formation capacity of these cells after stimulation with angiogenetic factors, such as VEGF. To test the effects of teneurin-4 on tumor cells, a glioma or neuroblastoma cell line overexpressing the full length protein can be established and used to perform several assays, such as proliferation assay, adhesion assay, aggregation assay, migration assay, scratch assay and invasion assay. Conversely, if a cell line that normally expresses high levels of teneurin-4 is identified, the same assays could be performed using siRNA treated cells or a stable shRNA knockdown cell line. Finally, it is also conceivable to test the function of teneurin-4 in cancer growth in an in-vivo xenograft model by injection of cells that overexpress teneurin-4 or are depleted of teneurin-4 by shRNA.

Cancer type	compared to	name of study
upregulated in cancer		
Glioblastoma	normal brain	Shai_Brain
B-cell leukemia	normal bone marrow	Andersson_Leukemia
Carcinoid lung	normal lung	Battarchajee_Lung
Seminoma	normal testis	Korkola_Seminoma
Clear cell carcinoma of kidney	normal kidney	Cutcliffe_Renal
downregulated in cancer		
Ovarian endothelial adenocarcinoma	normal ovary	Hendrix_Ovarian
Ovarian clear cell carcinoma	normal ovary	Hendrix_Ovarian
Ovarian cancer	normal cervix	Pyeon_Multi_Cancer
upregulated in cancer type		
Acute lymphoblastic leukemia	Acute myelogenous leukemia	Andersson_Leukemia
Acute lymphoblastic leukemia	Myelomonocytic leukemia	Armstrong_Leukemia
Gastrointestinal stromal tumor	other soft tissue tumors	Nielsen_Multi_Cancer
Synovial sarcoma	other sarcomas	Nakayama_Sarcoma
Ovarian carcinoma	other carcinomas	Bittner_Multi_Cancer
Serous papillary ovarian adenocarcinoma	other carcinomas	Sh_Multi_Cancer
downregulated in cancer type		
Lung adenocarcinoma	Small cell lung cancer	Bild_Lung
Lung adenocarcinoma	Small cell lung cancer	Kim_Lung
Ewing sarcoma	other sarcomas	Baird_Sarcoma
Colon Carcinoma	other carcinomas	Bittner Multi_cancer
Renal Carcinoma	other carcinomas	Bittner Multi_cancer
Prostate Carcinoma	other carcinomas	Bittner Multi_cancer
T-cell leukemias	B-cell leukemias	Schmidt_Leukemia
upregulated with molecular alterations		
Leukemia with E2A-PBX1	other leukemias	Yeoh_Leukemia
Leukemia with E2A-PBX1	other leukemias	Ross_Leukemia
Leukemia with TCF3-PBX1	other leukemias	Andersson_Leukemia
Leukemia with TEL-AML	other leukemias	Yeoh_Leukemia
upregulated in metastatic cancer		
Metastatic lung cancer	primary cancer	Battarchajee_Lung
downregulated in metastatic cancer		
Metastatic melanoma	primary cancer	Xu_Melanoma

Table 10: Summary of entries for teneurin-4 (od4) in the oncomine database.

The results are grouped into comparisons between cancer and normal tissue or cancer with other cancer types, and up- or downregulation of teneurin-4, respectively. Listed are the type of cancer, the comparison group and the name of the micorarray study. All the results listed are statistically significant with a p value of > 0.0001.

In the oncomine database, several studies suggest that teneurin-4 is overexpressed in a variety of cancers, as summarized in Table 10. Most studies use the probes 213273_at or 36078_at, both of which are located in the same region and comprise the two last exons of teneurin-4. Several studies report overexpression of teneurin-4 in the following cancers compared to normal tissues: Glioblastoma, B-cell leukemia, lung carcinoma, seminoma and kidney clear cell carcinoma. In contrast, teneurin-4 appears to be downregulated in several types of ovarian cancer. Compared to other cancers, teneurin-4 was upregulated in acute lymphoblastic leukemia, ovarian carcinoma, serous papillary ovarian carcinomas, gastrointestinal tumors and synovial carcinoma. In contrast, teneurin-4 appears to be downregulated in B-cell leukemia, lung adenocarcinoma, Ewing Sarcoma, and in carcinomas of the colon, kidney and prostate. Very striking is the upregulation of teneurin-4 in leukemias carrying the E2A-PBX1, TCF3-PBX1 and TEL-AML translocation. This suggests that teneurin-4 may be regulated by PBX1, which acts as a cofactor to regulate Hox-dependent gene expression during development, particularly since the hox genes as well as the teneurins are expressed at sites of pattern formation. Regarding teneurin-4 expression in metastatic versus primary cancer, two contradictory studies are found, one stating that teneurin-4 is overexpressed in metastatic lung cancer, and one that it is downregulated in metastatic melanoma. Thus, there is no clear indication so far that teneurin-4 may be implicated in cancer progression. Because several studies in the oncomine database suggest that teneurin-4 may be overexpressed in a variety of cancers, it will be worthwhile to investigate the expression of teneurin-4 in other cancers and normal tissues, this can be done by the staining of a tissue-microarray as soon as a reliable antibody and staining protocol are available.

Only teneurin-4 appears to be upregulated in cancer and not the other teneurins, as indicated by the brain tumor microarray data and oncomine entries. Therefore, it is an interesting question if teneurin-4 may have an additional function that is missing in the other teneurins that could promote cancer development, for example in the maintenance or proliferation of stem cells. The SVZ of the lateral ventricles and the subgranular zone (SGZ) of the dentate gyrus are two regions in the rodent brain where adult neurogenesis

occurs¹⁵⁰. Indeed, teneurin-4 is strongly expressed in both of these regions during mouse brain development up to postnatal day 7, whereas the other teneurins are only weakly expressed or absent⁷⁷. Moreover, during development, the cortical progenitor cells are generated in the ventricular and subventricular zone, coinciding spatially and temporally with teneurin-4 expression⁷⁷. In the developing chick, strong teneurin-4 expression was detected in the ciliary margin of the retina (Figure 12), where the retinal progenitor cells which continue proliferation until adulthood reside¹⁵¹.

In addition to study the role of teneurin-4 in cancer, a cell line expressing teneurin-4 may also be useful as a model to study teneurin signaling. Such a model was missing so far as most of our teneurin studies were performed with chicken proteins and only very few chicken cell lines exist. To be able to study teneurin-4 signaling, it will be important to have specific antibodies for both the ICD and the ECD that can be used in WBs and immunofluorescence. Possibly shed teneurin-4 ECD could be detected in the medium of teneurin-4 expressing cells. Additionally, a wild-type and furin-cleavage site mutated teneurin-4 construct can be transfected into cells to verify proteolytic processing of the ECD. The cells can be fractionated to detect cleaved ICD in the cytoplasmic or nuclear fractions, possibly this may be only the case after stimulation with an appropriate signal and/or the treatment with proteasome inhibitors, if the ICD is very unstable as it is the case for Notch ICD¹⁵². To study teneurin signaling, it will be crucial to find extracellular ligands for teneurin that may activate the teneurins in addition to homophilic interaction, which appears to promote teneurin cleavage. This could be done by purification of a recombinant secreted protein, e.g. the ECD fragment that results after furin cleavage, which then can be used to generate a teneurin-4 ECD column for affinity purification of interacting proteins from brain protein lysate. In case it is difficult to express the entire teneurin-4 ECD, it may also be possible to perform the same experiments with recombinant proteins comprising single domains of the ECD, e.g. EGF-like repeats or YD-repeats. Such recombinant proteins can also be used to test if these domains modulate cell adhesion, cell migration or neurite outgrowth. Especially if the overexpression of teneurin-4 in brain tumors and possibly other

cancers is confirmed, it will be interesting to elucidate the biological function of teneurin-4 and to determine in which signaling pathways it is involved.

6.5 Final conclusions

In the first part of my PhD work, I intended to shed light on the potential function and signaling mechanism of the teneurins. A detailed analysis of teneurin-1 expression in the brain showed expression in distinct and interconnected regions in the brain, suggesting that teneurins may play a role in the establishment of appropriate synaptic connectivity. For the first time, teneurin processing was studied in-vivo using N-terminal antibodies. By WB analysis and IHC of developing chick embryos, N-terminal processing products and nuclear ICD of teneurin-1 in developing chick embryos were found. Additionally, the ICD was shown to localize to the nucleus in an NLS-dependent manner in cultured cells. Data obtained for teneurin-4 also show specific expression in interconnected regions in the brain and N-terminal processing products, suggesting that the function and signaling mechanism of the four vertebrate teneurin paralogs is conserved.

In the second part, I investigated the involvement of teneurins in human disease. Although teneurin-1 is a promising candidate gene for XLMR, no disease causing mutation was identified. Since in the meantime a patient with a deletion of the teneurin-1 gene was published in XLP patients, it is unlikely that teneurin-1 causes a severe XLMR phenotype. Based on microarray analysis that showed upregulation of teneurin-4 in brain tumors, antibodies were produced and the overexpression of teneurin-4 was confirmed on protein level. In an ongoing project, these findings are being validated with an ICD antibody and the function of teneurin-4 in cancer is been investigated in cell culture.

7. APPENDIX

7.1 Abbreviations

AER	Apical ectodermal ridge (limb bud)
APC	Adenomatous polyposis coli
Array-CGH	Comparative genome hybridization technology
BM	Basement membrane
BMP	Bone morphogenetic protein
CAM	Cell adhesion molecule
CNS	Central nervous system
CSPG	Chondroitin sulphate proteoglycan
dLGN	Dorsal lateral geniculate nucleus
ECD	Extracellular domain
ECM	Extracellular matrix
EGF	Epidermal growth factor
EGL	External germinal layer (cerebellum)
En1	Engrailed-1
FAK	Focal adhesion kinase
FGF	Fibroblast growth factor
FISH	Fluorescence in-situ hybridization
FMR1	Fragile X mental retardation 1
GAP-43	Growth-associated protein 43
GBM	Glioblastoma multiforme
GCL	Ganglion cell layer (retina)
GCP	Granule cell precursor (cerebellum)
HSPG	Heparin sulphate proteoglycan
ICAM	Intercellular adhesion molecule
ICD	Intracellular domain
Ig-CAM	Immunoglobulin-like cell adhesion molecule
IHC	Immunohistochemistry
INL	Inner nuclear layer (retina)
IPL	Innater plexiform layer (retina)
MB	Medulloblastoma
miRNA	microRNA
MR	Mental retardation

ncRNA	noncoding RNA
odz1 to -4	Alternative name for teneurin-1 to -4
OFL	Optic fiber layer (retina)
ONL	Outer nuclear layer (retina)
OPL	Outer plexiform layer (retina)
OT	Optic tectum
PDGF	Platelet derived growth factor
PNS	Peripheral nervous system
POFUT1	Protein-O-fucosyltransferase-1
RGC	Retinal ganglion cell
RIP	Regulated intramembrane proteolysis
S2P	Site-2 protease
SC	Superior colliculus
SGFS	Stratum griseum et fibrosum superficiale (OT)
SHH	Sonic hedgehog
SNP	Single nucleotide polymorphism
SPP	Signal peptide peptidase
SPPL	Signal peptide peptidase-like
SVZ	Subventricular zone
TCAP	Teneurin-associated C-terminal peptide
Ten-1L	<i>C.elegans</i> teneurin homolog, long isoform
Ten-1S	<i>C.elegans</i> teneurin homolog, short isoform
Ten-a	<i>Drosophila</i> teneurin homolog
Ten-m/odz	<i>Drosophila</i> teneurin homolog
Ten_m1 to -4	Mouse teneurin-1 to-4
TNF	Tumor necrosis factor
TM	Transmembrane
VEGF	Vascular endothelial growth factor
VZ	Ventricular zone (cortex, cerebellum)
WB	Western blot
XLMR	X-linked mental retardation
XLP	X-linked lymphoproliferative disease
ZPA	Zone of polarizing activity (limb bud)

7.2 List of Figures and Tables

<i>Figure 1: Overview Cell-Cell and Cell-ECM adhesion.</i>	p7
<i>Figure 2: Signaling pathways in vertebrate limb development.</i>	p12
<i>Figure 3: Comparison of the progress zone and early specification model.</i>	p13
<i>Figure 4: Early development of the CNS.</i>	p16
<i>Figure 5: Key guidance cues acting in the mouse optic pathway.</i>	p21
<i>Figure 6: The four intramembrane protease families.</i>	p23
<i>Figure 7: Known XLMR genes to date (XLMR update 2007).</i>	p27
<i>Figure 8: Biological functions that underlie mental retardation.</i>	p30
<i>Figure 9: Developmental paths in the CNS and classification of CNS tumors.</i>	p32
<i>Figure 10: Genetic pathways in the development of primary and secondary GBM.</i>	p33
<i>Figure 11: Domain architecture of vertebrate teneurins.</i>	p40
<i>Figure 12: Teneurin-4 expression in the visual system.</i>	p72
<i>Figure 13: Teneurin-4 expression in the the CNS (outside of visual system).</i>	p73
<i>Figure 14: Teneurin-4 expression in non-neuronal tissues.</i>	p74
<i>Figure 15: Teneurin-4 expression in the developing limb.</i>	p76
<i>Figure 16: WB analysis of teneurin-4 expression during chick development.</i>	p77
<i>Figure 17: Teneurin-4 expression in normal brain and brain tumors.</i>	p85
<i>Figure 18: Teneurin-4 expression in individual normal brain and tumor samples.</i>	p86
<i>Figure 19: Characterization of antibodies and comparison normal brain with tumors.</i>	p89
<i>Figure 20: WB analysis of two panels of different brain tumors.</i>	p90
<i>Figure 21: WB analysis of a panel of glioblastomas.</i>	p90
<i>Figure 22: Teneurin-4 IHC in brain tumors.</i>	p92
<i>Figure 23: Teneurin-4 staining is present on blood vessels.</i>	p93
<i>Table 1: Summary teneurin expression in vertebrates.</i>	p42
<i>Table 2: List of samples from XLMR families.</i>	p50
<i>Table 3: List of PCR and sequencing primers to analyze the human teneurin-1 gene.</i>	p52
<i>Table 4: Exons to be sequenced.</i>	p78
<i>Table 5: List of SNPs in the odz coding and exon flanking region.</i>	p80
<i>Table 6: List of SNPs and unknown alterations found in XLMR patients.</i>	p82
<i>Table 7: 5' upstream polymorphisms in patient p.</i>	p84
<i>Table 8: List of teneurin-4 expression values.</i>	p87
<i>Table 9: Comparison between WB analysis and IHC of teneurin-4 expression.</i>	p94
<i>Table 10: Summary of entries for teneurin-4 (odz4) in the oncomine database.</i>	p10

7.3 References

- 1 Alberts, *Molecular Biology of the Cell, 4th edition*. (Garland Science, New York, 2002).
- 2 L. Niswander, C. Tickle, A. Vogel et al., *Cell* **75** (3), 579 (1993).
- 3 J. F. Fallon, A. Lopez, M. A. Ros et al., *Science* **264** (5155), 104 (1994).
- 4 R. D. Riddle, R. L. Johnson, E. Laufer et al., *Cell* **75** (7), 1401 (1993).
- 5 C. Chiang, Y. Litingtung, M. P. Harris et al., *Developmental biology* **236** (2), 421 (2001).
- 6 P. Kraus, D. Fraidenraich, and C. A. Loomis, *Mechanisms of development* **100** (1), 45 (2001).
- 7 J. A. MacCabe, J. Errick, and J. W. Saunders, Jr., *Developmental biology* **39** (1), 69 (1974).
- 8 H. Chen and R. L. Johnson, *The International journal of developmental biology* **46** (7), 937 (2002).
- 9 L. Niswander, *Nat Rev Genet* **4** (2), 133 (2003).
- 10 L. Niswander, S. Jeffrey, G. R. Martin et al., *Nature* **371** (6498), 609 (1994).
- 11 E. Laufer, C. E. Nelson, R. L. Johnson et al., *Cell* **79** (6), 993 (1994).
- 12 X. Sun, F. V. Mariani, and G. R. Martin, *Nature* **418** (6897), 501 (2002).
- 13 A. Zuniga, A. P. Haramis, A. P. McMahon et al., *Nature* **401** (6753), 598 (1999).
- 14 S. Pizette and L. Niswander, *Development (Cambridge, England)* **126** (5), 883 (1999).
- 15 B. A. Parr and A. P. McMahon, *Nature* **374** (6520), 350 (1995).
- 16 Y. Yang and L. Niswander, *Cell* **80** (6), 939 (1995).
- 17 C. E. Nelson, B. A. Morgan, A. C. Burke et al., *Development (Cambridge, England)* **122** (5), 1449 (1996).
- 18 A. P. Davis, D. P. Witte, H. M. Hsieh-Li et al., *Nature* **375** (6534), 791 (1995).
- 19 D. Duboule, *Current opinion in genetics & development* **5** (4), 525 (1995).
- 20 D. J. Goff and C. J. Tabin, *Development (Cambridge, England)* **124** (3), 627 (1997).
- 21 Gilbert, *Developmental Biology, 4th edition*. (Sinauer Associates, Inc, Sunderland, Massachusetts, 1994).
- 22 F. J. Livesey and C. L. Cepko, *Nat Rev Neurosci* **2** (2), 109 (2001).
- 23 B. J. Dickson, *Science* **298** (5600), 1959 (2002).
- 24 F. Charron and M. Tessier-Lavigne, *Development (Cambridge, England)* **132** (10), 2251 (2005).
- 25 A. Lilienbaum, A. A. Reszka, A. F. Horwitz et al., *Molecular and cellular neurosciences* **6** (2), 139 (1995).
- 26 R. Riehl, K. Johnson, R. Bradley et al., *Neuron* **17** (5), 837 (1996).
- 27 H. Stier and B. Schlosshauer, *Development (Cambridge, England)* **121** (5), 1443 (1995).
- 28 A. S. Plump, L. Erskine, C. Sabatier et al., *Neuron* **33** (2), 219 (2002).
- 29 P. A. Brittis, D. R. Canning, and J. Silver, *Science* **255** (5045), 733 (1992).
- 30 P. A. Brittis, V. Lemmon, U. Rutishauser et al., *Molecular and cellular neurosciences* **6** (5), 433 (1995).
- 31 H. Ott, M. Bastmeyer, and C. A. Stuermer, *J Neurosci* **18** (9), 3363 (1998).
- 32 J. A. Weiner, S. J. Koo, S. Nicolas et al., *Molecular and cellular neurosciences* **27** (1), 59 (2004).
- 33 P. Zelina, H. X. Avci, K. Thelen et al., *Development (Cambridge, England)* **132** (16), 3609 (2005).
- 34 A. Kolpak, J. Zhang, and Z. Z. Bao, *J Neurosci* **25** (13), 3432 (2005).
- 35 M. S. Deiner, T. E. Kennedy, A. Fazeli et al., *Neuron* **19** (3), 575 (1997).
- 36 E. Birgbauer, C. A. Cowan, D. W. Sretavan et al., *Development (Cambridge, England)* **127** (6), 1231 (2000).

- 37 E. Birgbauer, S. F. Oster, C. G. Severin et al., *Development (Cambridge, England)* **128** (15), 3041 (2001).
- 38 J. Liu, S. Wilson, and T. Reh, *Developmental biology* **256** (1), 34 (2003).
- 39 S. F. Oster, M. O. Bodeker, F. He et al., *Development (Cambridge, England)* **130** (4), 775 (2003).
- 40 F. Trousse, E. Marti, P. Gruss et al., *Development (Cambridge, England)* **128** (20), 3927 (2001).
- 41 E. Herrera, L. Brown, J. Aruga et al., *Cell* **114** (5), 545 (2003).
- 42 W. Pak, R. Hindges, Y. S. Lim et al., *Cell* **119** (4), 567 (2004).
- 43 J. A. Sakai and M. C. Halloran, *Development (Cambridge, England)* **133** (6), 1035 (2006).
- 44 S. McFarlane, E. Cornel, E. Amaya et al., *Neuron* **17** (2), 245 (1996).
- 45 R. W. Sperry, *Proceedings of the National Academy of Sciences of the United States of America* **50**, 703 (1963).
- 46 A. B. Huber, A. L. Kolodkin, D. D. Ginty et al., *Annual review of neuroscience* **26**, 509 (2003).
- 47 A. D. Huberman, K. D. Murray, D. K. Warland et al., *Nature neuroscience* **8** (8), 1013 (2005).
- 48 L. Erskine and E. Herrera, *Developmental biology* **308** (1), 1 (2007).
- 49 S. Urban and M. Freeman, *Current opinion in genetics & development* **12** (5), 512 (2002).
- 50 A. L. Parks and D. Curtis, *Trends Genet* **23** (3), 140 (2007).
- 51 G. Eissner, W. Kolch, and P. Scheurich, *Cytokine & growth factor reviews* **15** (5), 353 (2004).
- 52 E. Friedmann, E. Hauben, K. Maylandt et al., *Nature cell biology* **8** (8), 843 (2006).
- 53 J. Urny, I. Hermans-Borgmeyer, G. Gercken et al., *Gene Expr Patterns* **3** (5), 685 (2003).
- 54 R. Luckasson and A. Reeve, *Mental retardation* **39** (1), 47 (2001).
- 55 R. E. Stevenson, *American journal of medical genetics* **97** (3), 174 (2000).
- 56 R. M. Plenge, R. A. Stevenson, H. A. Lubs et al., *American journal of human genetics* **71** (1), 168 (2002).
- 57 H. H. Ropers and B. C. Hamel, *Nat Rev Genet* **6** (1), 46 (2005).
- 58 P. Chiurazzi, B. C. Hamel, and G. Neri, *Eur J Hum Genet* **9** (2), 71 (2001).
- 59 P. Chiurazzi, C. E. Schwartz, J. Gecz et al., *Eur J Hum Genet* **16** (4), 422 (2008).
- 60 F. Molinari, F. Foulquier, P. S. Tarpey et al., *American journal of human genetics* **82** (5), 1150 (2008).
- 61 L. M. Dibbens, P. S. Tarpey, K. Hynes et al., *Nature genetics* **40** (6), 776 (2008).
- 62 XLMR update, Available at <http://www.ggc.org/xlmr.htm>.
- 63 H. H. Ropers, *Current opinion in genetics & development* **16** (3), 260 (2006).
- 64 F. L. Raymond and P. Tarpey, *Human molecular genetics* **15 Spec No 2**, R110 (2006).
- 65 L. R. Jensen, S. Lenzner, B. Moser et al., *Eur J Hum Genet* **15** (1), 68 (2007).
- 66 B. B. de Vries, R. Pfundt, M. Leisink et al., *American journal of human genetics* **77** (4), 606 (2005).
- 67 L. Zhang, C. Jie, C. Obie et al., *Genome research* **17** (5), 641 (2007).
- 68 J. K. Inlow and L. L. Restifo, *Genetics* **166** (2), 835 (2004).
- 69 J. Chelly, M. Khelifaoui, F. Francis et al., *Eur J Hum Genet* **14** (6), 701 (2006).
- 70 O. Attree, I. M. Olivos, I. Okabe et al., *Nature* **358** (6383), 239 (1992).
- 71 F. L. Raymond, P. S. Tarpey, S. Edkins et al., *American journal of human genetics* **80** (5), 982 (2007).
- 72 T. Chiyonobu, S. Hayashi, K. Kobayashi et al., *Am J Med Genet A* **143A** (13), 1448 (2007).
- 73 C. C. Garcia, H. J. Blair, M. Seager et al., *Journal of medical genetics* **41** (3), 183 (2004).
- 74 R. E. Amir, I. B. Van den Veyver, M. Wan et al., *Nature genetics* **23** (2), 185 (1999).
- 75 H. Li, T. Yamagata, M. Mori et al., *Brain & development* **27** (5), 321 (2005).

- 76 S. M. Nunes, J. Ferralli, K. Choi et al., *Experimental cell research* **305** (1), 122
(2005).
- 77 H. Li, K. M. Bishop, and D. D. O'Leary, *Molecular and cellular neurosciences* **33** (2),
136 (2006).
- 78 T. Granata, L. Farina, A. Faiella et al., *Neurology* **48** (5), 1403 (1997).
- 79 A. Faiella, S. Brunelli, T. Granata et al., *Eur J Hum Genet* **5** (4), 186 (1997).
- 80 S. A. Brown, D. Warburton, L. Y. Brown et al., *Nature genetics* **20** (2), 180 (1998).
- 81 C. Bagutti, G. Forro, J. Ferralli et al., *Journal of cell science* **116** (Pt 14), 2957
(2003).
- 82 Y. Zhu and L. F. Parada, *Nat Rev Cancer* **2** (8), 616 (2002).
- 83 D. N. Louis, *Annual review of pathology* **1**, 97 (2006).
- 84 M. Marutani, H. Tonoki, M. Tada et al., *Cancer research* **59** (19), 4765 (1999).
- 85 E. A. Maher, C. Brennan, P. Y. Wen et al., *Cancer research* **66** (23), 11502 (2006).
- 86 E. C. Holland, J. Celestino, C. Dai et al., *Nature genetics* **25** (1), 55 (2000).
- 87 R. M. Bachoo, E. A. Maher, K. L. Ligon et al., *Cancer cell* **1** (3), 269 (2002).
- 88 S. K. Singh, I. D. Clarke, M. Terasaki et al., *Cancer research* **63** (18), 5821 (2003).
- 89 C. Dai, J. C. Celestino, Y. Okada et al., *Genes & development* **15** (15), 1913 (2001).
- 90 M. Wolter, J. Reifenberger, B. Blaschke et al., *Journal of neuropathology and
experimental neurology* **60** (12), 1170 (2001).
- 91 K. Ichimura, E. E. Schmidt, H. M. Goike et al., *Oncogene* **13** (5), 1065 (1996).
- 92 E. C. Holland, *Nat Rev Genet* **2** (2), 120 (2001).
- 93 J. S. Rao, *Nat Rev Cancer* **3** (7), 489 (2003).
- 94 J. H. Uhm, C. L. Gladson, and J. S. Rao, *Front Biosci* **4**, D188 (1999).
- 95 M. Natarajan, T. P. Hecker, and C. L. Gladson, *Cancer journal (Sudbury, Mass)* **9**
(2), 126 (2003).
- 96 Y. Okada, E. E. Hurwitz, J. M. Esposito et al., *Cancer research* **63** (2), 413 (2003).
- 97 M. Nagane, F. Coufal, H. Lin et al., *Cancer research* **56** (21), 5079 (1996).
- 98 T. G. Graeber, C. Osmanian, T. Jacks et al., *Nature* **379** (6560), 88 (1996).
- 99 K. H. Plate, G. Breier, H. A. Weich et al., *Nature* **359** (6398), 845 (1992).
- 100 P. Bailey and H. Cushing, *Proceedings of the National Academy of Sciences of the
United States of America* **11** (1), 82 (1925).
- 101 D. Ellison, *Neuropathology and applied neurobiology* **28** (4), 257 (2002).
- 102 S. Levanat, R. J. Gorlin, S. Fallet et al., *Nature genetics* **12** (1), 85 (1996).
- 103 L. V. Goodrich, L. Milenkovic, K. M. Higgins et al., *Science* **277** (5329), 1109 (1997).
- 104 R. J. Wechsler-Reya and M. P. Scott, *Neuron* **22** (1), 103 (1999).
- 105 K. Lai, B. K. Kaspar, F. H. Gage et al., *Nature neuroscience* **6** (1), 21 (2003).
- 106 J. Turcot, J. P. Despres, and F. St Pierre, *Diseases of the colon and rectum* **2**, 465
(1959).
- 107 A. Koch, A. Waha, J. C. Tonn et al., *International journal of cancer* **93** (3), 445
(2001).
- 108 A. P. McMahon and A. Bradley, *Cell* **62** (6), 1073 (1990).
- 109 S. Baumgartner, D. Martin, C. Hagios et al., *Embo J* **13** (16), 3728 (1994).
- 110 A. Levine, A. Bashan-Ahrend, O. Budai-Hadrian et al., *Cell* **77** (4), 587 (1994).
- 111 Y. Kinel-Tahan, H. Weiss, O. Dgany et al., *Dev Dyn* **236** (9), 2541 (2007).
- 112 N. Rakovitsky, Y. Buganim, T. Swissa et al., *Mechanisms of development* **124** (11-
12), 911 (2007).
- 113 K. Drabikowski, A. Trzebiatowska, and R. Chiquet-Ehrismann, *Developmental
biology* **282** (1), 27 (2005).
- 114 A. Trzebiatowska, U. Topf, U. Sauder et al., *Molecular biology of the cell* **19** (9),
3898 (2008).
- 115 D. Kenzelmann, R. Chiquet-Ehrismann, and R. P. Tucker, *Cell Mol Life Sci* **64** (12),
1452 (2007).
- 116 B. P. Rubin, R. P. Tucker, D. Martin et al., *Developmental biology* **216** (1), 195
(1999).
- 117 R. P. Tucker, R. Chiquet-Ehrismann, M. P. Chevron et al., *Dev Dyn* **220** (1), 27
(2001).

- 118 D. A. Lovejoy, A. Al Chawaf, and M. Z. Cadinouche, *General and comparative*
endocrinology **148** (3), 299 (2006).
- 119 G. Orend and R. Chiquet-Ehrismann, *Cancer letters* **244** (2), 143 (2006).
- 120 K. Feng, X. H. Zhou, T. Oohashi et al., *The Journal of biological chemistry* **277** (29),
26128 (2002).
- 121 D. J. Moloney, V. M. Panin, S. H. Johnston et al., *Nature* **406** (6794), 369 (2000).
- 122 K. Bruckner, L. Perez, H. Clausen et al., *Nature* **406** (6794), 411 (2000).
- 123 N. Haines and K. D. Irvine, *Nature reviews* **4** (10), 786 (2003).
- 124 R. Rampal, K. B. Luther, and R. S. Haltiwanger, *Current molecular medicine* **7** (4),
427 (2007).
- 125 A. D. Minet, B. P. Rubin, R. P. Tucker et al., *Journal of cell science* **112** (Pt 12),
2019 (1999).
- 126 T. Ben-Zur, E. Feige, B. Motro et al., *Developmental biology* **217** (1), 107 (2000).
- 127 D. Kenzelmann, R. Chiquet-Ehrismann, N. T. Leachman et al., *BMC developmental*
biology **8**, 30 (2008).
- 128 C. A. Leamey, K. A. Glendining, G. Kreiman et al., *Cereb Cortex* **18** (1), 53 (2008).
- 129 C. A. Leamey, S. Merlin, P. Lattouf et al., *PLoS biology* **5** (9), e241 (2007).
- 130 A. C. Lossie, H. Nakamura, S. E. Thomas et al., *Genetics* **169** (1), 285 (2005).
- 131 M. Mieda, Y. Kikuchi, Y. Hirate et al., *Mechanisms of development* **87** (1-2), 223
(1999).
- 132 T. Oohashi, X. H. Zhou, K. Feng et al., *The Journal of cell biology* **145** (3), 563
(1999).
- 133 R. P. Tucker, D. Martin, R. Kos et al., *Mechanisms of development* **98** (1-2), 187
(2000).
- 134 X. H. Zhou, O. Brandau, K. Feng et al., *Gene Expr Patterns* **3** (4), 397 (2003).
- 135 J. M. Otaki and S. Firestein, *Developmental biology* **212** (1), 165 (1999); J. M. Otaki
and S. Firestein, *Neuroreport* **10** (12), 2677 (1999).
- 136 T. V. Getchell, H. Liu, R. A. Vaishnav et al., *Journal of neuroscience research* **80**
(3), 309 (2005).
- 137 B. P. Rubin, R. P. Tucker, M. Brown-Luedi et al., *Development (Cambridge,*
England) **129** (20), 4697 (2002).
- 138 T. R. Young and C. A. Leamey, *The international journal of biochemistry & cell*
biology (2008).
- 139 D. D. Cilliers, R. Parveen, P. Clayton et al., *European journal of medical genetics* **50**
(3), 216 (2007).
- 140 L. I. Macedo-Souza, F. Kok, S. Santos et al., *Neurogenetics* **9** (3), 225 (2008).
- 141 ClustalW2, Available at <http://www.ebi.ac.uk/Tools/clustalw2/index.html>.
- 142 A. Levine, C. Weiss, and R. Wides, *Dev Dyn* **209** (1), 1 (1997).
- 143 P. S. Tarpey, F. L. Raymond, L. S. Nguyen et al., *Nature genetics* **39** (9), 1127
(2007).
- 144 C. Lenski, R. F. Kooy, E. Reyniers et al., *American journal of human genetics* **80**
(2), 372 (2007).
- 145 T. R. Mercer, M. E. Dinger, S. M. Sunkin et al., *Proceedings of the National*
Academy of Sciences of the United States of America **105** (2), 716 (2008).
- 146 C. Kimchi-Sarfaty, J. M. Oh, I. W. Kim et al., *Science* **315** (5811), 525 (2007).
- 147 A. J. Coffey, R. A. Brooksbank, O. Brandau et al., *Nature genetics* **20** (2), 129
(1998).
- 148 S. Rigaud, M. C. Fondaneche, N. Lambert et al., *Nature* **444** (7115), 110 (2006).
- 149 A. L. Rougemont, J. C. Fournet, S. R. Martin et al., *The American journal of surgical*
pathology **32** (2), 323 (2008).
- 150 C. Zhao, W. Deng, and F. H. Gage, *Cell* **132** (4), 645 (2008).
- 151 A. J. Fischer and T. A. Reh, *Developmental biology* **220** (2), 197 (2000).
- 152 E. H. Schroeter, J. A. Kisslinger, and R. Kopan, *Nature* **393** (6683), 382 (1998).

7.3 Acknowledgements

First of all, I would like to thank my supervisor Prof. Ruth Chiquet-Ehrismann for giving me the opportunity to work on this project. I am very grateful for her support and advice and that she always had time to discuss my project. Many thanks also to Prof. Markus Rüegg, my second reader, and to Prof. Nancy Hynes, my faculty representative for having agreed to join my thesis committee.

A particularly big thank you goes to Professor Richard P. Tucker, who has thought me how to prepare chick embryos to IHC, and with whom I also learned a lot about chick development and anatomy. Thanks also for reading my manuscripts and supporting me at all stages of my PhD thesis.

Thanks to those people in the lab who supported me during my PhD work and for the times when we had a laugh. I want to thank Florence for our German/French lunches and Elisa for the Spanish lunches, during which we not only practiced languages, but also became friends. I am particularly grateful for having met many friends through the WIN mentoring program, with whom I had many discussions about career and life.

I want to thank my parents Paul and Margrit Kenzelmann, as well as my brother Reto Kenzelmann for their continuous support and encouragement to be successful. I highly appreciate that my parents-in-law invited me to spend my last months in Switzerland after Petr's departure with them, thanks for welcoming me in your house.

Last but certainly not least, I want to thank my wonderful husband Petr Brož. Without you, my PhD would not have been possible and I would not have found my exciting post-doc position at Stanford University. I think we are a great team always encouraging each other and I hope it will remain like this in the future. I am looking forward very much to spend an exciting time with you in California!

7.4 Curriculum Vitae

CV Daniela Kenzelmann Brož

Personal Data

Name	Daniela Kenzelmann Brož
Address	Maienweg 10, 4310 Rheinfelden AG, Switzerland
Cell phone	+ 41 78 602 21 86
E-mail	daniela.kenzelmann@fmi.ch
Nationality	Swiss
Date of birth	1.2.1981
Civil status	married

Education

2000 – 2004	Master of Molecular Biology , grade 5.6 (6 = best, 1= worst) at the Biozentrum of the University of Basel Minor subject: Molecular Medicine
-------------	---

Work Experience

Jan 2005 to now	PhD thesis in Cell Biology at the Friedrich Miescher Institute, Basel Title: " <i>Function and Mechanism of Teneurin signaling</i> " Supervisor: Prof. Dr. Ruth Chiquet-Ehrismann Date of my defense: 11.12.2008
Oct 2003 – Oct 2004	Master thesis at the Medical Faculty, University of Basel Title: " <i>Design of a molecular diagnostic test for Gleevec-resistance in CML patients</i> " Supervisor: PD Dr. Thomas Klimkait
Jul 2003 – Sept 2003	IAESTE-Traineeship at the University of Michigan, Ann Arbor, USA Title: " <i>Cloning of a novel GTPase activating protein with a potential role in aggressive breast cancers</i> " Supervisor: Assistant Professor Dr. Kenneth Van Golen

Technical Skills

Molecular Biology	Purification and analysis of RNA and DNA, PCR, RT-PCR, Q-PCR, DNA sequencing, resequencing microarrays, cloning, site-directed mutagenesis, 5'RACE, 3'RACE
Cell Biology	Cell culture, transient transfection, stable transfection, viral transduction, protein expression, shRNA knockdown, cellular assays (proliferation, migration, adhesion, neurite outgrowth), immunofluorescence, fluorescence microscopy
Biochemistry	Protein extraction from cell and tissues, immunoblotting, immunoprecipitation, purification of His-tagged proteins from bacteria and mammalian cells, production and validation of polyclonal and monoclonal antibodies
Histology	Preparation of tissue sections, in-situ hybridization, immunohistochemistry

Other Skills

Computer Literacy	MS Office, Adobe Photoshop, Corel Draw, Vector NTI, ClustalW, UCSC Genome Browser
Languages	German (mother tongue), English (very good, oral and written), French (good), Spanish (good)
Other Skills	Presentation of scientific data, scientific writing

Additional Experience

Aug 2008	Participant of Novartis Biotechnology Leadership Camp 2008
Apr 2007 to Apr 2008	WIN-Mentee (Women into Industry): Introduction into drug development and the organization of a pharmaceutical company, organization of meetings and workshops as part of the mentee project group, networking at Novartis
Oct 2006 to Feb 2007	Teaching of a tutorial for first-semester biology students
Mar 2006 to Aug 2008	Science journalist in the Access Program: Communication of science to a lay audience, supervised by Dr. Robert Derham
Oct 2003 to Dec 2005	Member of IAESTE local committee Basel: Organization of events for exchange trainees, coordination of reception and accommodation

Publications and Scientific Contributions

Posters	ASCB Annual Meeting, Dec 1-5 2007, Washington DC, USA Cellular Signaling, May 26 to June 1 2006, Dubrovnik, Croatia International PhD Symposium, Dec 1-3 2005, Heidelberg, Germany FMI Annual Meetings, 2004 to 2008, Switzerland
Publications	Kenzelmann D. , Leachman N. T., Chiquet-Ehrismann R., and Tucker, R. P. (2008). Teneurin-1 is expressed in interconnected regions in the brain and is processed in vivo. <i>BMC Dev Biol. Mar 25; 8:30</i> Picture of the month, featured article Kenzelmann D. , Chiquet-Ehrismann R., and Tucker RP. (2007). Teneurins, a transmembrane protein family involved in cell communication during neuronal development. <i>Cell Mol Life Sci. Jun; 64(12):1452-6</i> Tucker R. P., Kenzelmann D. , Trzebiatowska A., and Chiquet-Ehrismann R. (2007). Teneurins: Transmembrane proteins with fundamental roles in development. <i>Intl J. Biochem Cell Biol 39(2): 292-7</i>